CRITICAL ROLES FOR THE CO-REPRESSOR, RCOR1, IN LINEAGE DETERMINATION

By

Huilan Yao

A DISSERTATION

Presented to the Department of Cell and Developmental Biology

and the Oregon Health & Science University

School of Medicine

in partial fulfillment of the requirements for the degree of

Doctor of Philosophy

July 2014

School of Medicine

Oregon Health & Science University

CERTIFICATE OF APPROVAL

This is to certify that the Ph.D. dissertation of

Huilan Yao

has been approved

_____

Gail Mandel, PhD; Mentor/Advisor

_____

Richard Goodman, MD, PhD; Chair

_____

William H. Fleming, MD, PhD; Member

_____

Jeffrey Tyner, PhD; Member

_____

John Adelman, PhD; Member

_____

Jacob Raber, PhD; Member

TABLE OF CONTENTS

List of Figures

List of Abbreviations

AML, Actue myeloid leukemia

BM, Bone marrow

BFU-E, Burst forming units-erythroid

CBC, Complete blood count

CFU-E, Colony forming unit-erythroid

CFU-G, Colony forming unit-granulocyte

CFU-GM, Colony forming unit-granulocyte, monocyte

CFU-GEMM, Colony forming unit-granulocyte, erythrocyte, monocyte, megakaryocyte

CFU-M, Colony forming unit-monoctye

CLP, Common lymphoid progenitor

CMP, Common myeloid progenitor

CSF, Colony stimulating factor

CSF2RB, Colony stimulating factor 2 receptor, beta

CSF2RB2, Colony stimulating factor 2 receptor, beta 2

EKLF, Krueppel-like factor

ELM2, EGL-27 and MTA1 homology 2

EPO, Erythropoietin

GATA, GATA-binding factor

GFAP, Glial Fibrillary Acidic Protein

Gfi, Growth factor independent

GMP, Granulocyte-macrophage progenitor

HAT, Histone acetyltransferase

HDAC, Histone deacetylase

Hox, Hemobox

HSC, Hematopoietic stem cell

IL, interleukin

JAK, Janus kinase

LSD1/KDM1A/Kdm1a, lysine-specific demethylase 1a

Ly6G, Lyphocyte antigen 6 complex, locus G

MDP, Monocyte/macrophage and dendritic cell progenitors

MDS, Myelodysplasia syndrome

MEP, Megakaryocyte erythroid progenitor

MK, Megakaryocyte

MPD, Myeloproliferative disorders

RBC, Red blood cell

RCOR1/Rcor1, REST corepressor 1

REST, RE1 silencing transcription factor

WBC, white blood cell

WT, Wild type

SANT, SW13/ADA2/NCoR/TFIIIB

STAT, Signal transducer and activator of transcription

SCF, Stem cell factor

ACKNOWLEDGEMENTS

I would like to thank my thesis advisor, Dr. Gail Mandel for her constant guidance and support. Without her trust and encouragement, it would have been impossible to finish a hematopoietic project in a neuroscience lab.

I am grateful to Dr. William Fleming, an expert in hematology, for his guidance on my project and his advice on my future career.

Thank you to Dr. Devorah Goldman, my best collaborator, for her dedication, countless hours spent in the lab, excellent experimental support, and encouragement. Much of the data was generated with her assistance. Without her help there would not be so much progress on this project.

Thank you to Dr. Guang Fan for using her clinic expertise to help me understand my project.

I want to thanks all the current and former members of the Mandel lab for being so kind and supportive to me. I enjoyed working with everyone in the lab every day. I am grateful to Dr. Tamilla Nechiporuk who put up with my many inquiries every day, and gave me so much experimental support and encouragement; I am grateful to Dr. Jon Oyer who taught me how to do CHIP, discussed experiments with me every day and edited almost every important email for me; I thank Glen Corson for being an incredible lab manager, who can answer almost every question I have; I want to thank the excellent mouse technician team, Andrea Ansari, Travis Polston, Jennifer Miller, Philip Micha, and Joseph Willson, for taking care of the mouse colony and other experimental support. I appreciate John Sinnamon for editing my thesis and sharing his passion for science with

me. Thank you Karin Mullendoff (now Dr. Karin Mullendoff) and Caitlin Monoghan for being great peer graduate students and our great movie time. Thanks to Dr. Ednund Nesti, Dr. Saurabh Garg, Dr. James McGann, and Dr. Dan Lioy for helpful discussions and feedback.

Thanks to Pamela Canaday, Dorian LaTocha and Mandy Boyd of the Flow Cytometry Core for their technical support.

Thank you to Dr. Richard Goodman for taking me as a rotation student and being my committee chair. I also want to thank the current and former members in Goodman lab for their feedback and technical support, especially Dr. Yinyu Zhang, Dr. Lulu Cambornne, Dr. Ngan Vo, Dr. Rongkun Shen and Dr. Stephen Magill.

I am grateful to Dr. John Adelman and Dr. Jacob Raber, my thesis advisory committee members, and to Dr. Jeffrey Tyner, the member of my dissertation committee, for their guidance, helpful recommendations, and time.

I am grateful to the Program in Molecular & Cellular Biosciences and the Cell & Developmental Biology Department and to my funding sources: American Heart Association.

I want to thank my parents and parents-in-law for their constant love and encouragement. I especially grateful that they all came and helped me take care of my daughter while I was busy with experiments and my dissertation. Finally, I have my biggest thanks to Weike Mo, my husband, for his love and support and the joyful time we have spent together.

ABSTRACT

The transcriptional co-repressor, Rcor1, is a critical component of gene expression regulatory machinery. It interacts with two important histone modification enzymes and couples their activities during gene expression regulation. Although many transcription factors have been shown to use Rcor1 as a cofactor to regulate gene expression, it was not clear what biological functions were dependent upon Rcor1. To study Rcor1 function *in vivo*, I characterized three Rcor1 knockout mouse models that lacked Rcor1 globally, in the nervous system, or in the hematopoietic system respectively.

Nervous system conditional Rcor1 knockout did not show an obvious phenotype during development, likely due to compensation from Rcor2, another Rcor family member. Therefore, the function of Rcor1 in adult brain remains to be tested using different genetic models that disallow compensation. In contrast, I observed profoundly anemic and late gestation lethality in mice deleted globally for Rcor1, indicating that Rcor1 plays an important role in hematopoiesis. Specifically, definitive erythroid cells from mutant mice arrest at the transition from proerythroblast to basophilic erythroblast. Remarkably, Rcor1 null erythroid progenitors cultured *in vitro* form myeloid colonies instead of erythroid colonies. The mutant proerythroblasts also aberrantly express genes of the myeloid lineage as well as genes typical of hematopoietic stem cell (HSC) / progenitor cells. I show that the Colony Stimulating Factor 2 Receptor Beta subunit (Csf2rb), which codes for a receptor implicated in myeloid cytokine signaling, is a direct target for both Rcor1 and the transcription repressor Gfi1b in erythroid cells. In the absence of Rcor1, the Csf2rb gene is highly induced, and *Rcor1*$^{-/-}$ progenitors exhibit CSF2-dependent

phospho-Stat5 hypersensitivity. Blocking this pathway can partially reduce myeloid colony formation by Rcor1 deficient erythroid progenitors. Thus, Rcor1 promotes erythropoiesis by repressing HSC/progenitor genes, as well as the genes and signaling pathways that lead to myeloid cell fate.

While the study with global Rcor1 knockout model demonstrates that the co-repressor Rcor1 is essential for maturation of definitive erythroid cells in the fetal liver, the embryonic lethality prevented me from studying other hematopoietic lineages. Because Rcor1 interacts with several transcription factors that are critically important for regulating multiple hematopoietic lineage differentiation, I also investigated Rcor1 function in adult hematopoiesis following its conditional deletion *in vivo*. Loss of Rcor1 expression in hematopoietic cells led to the rapid development of severe anemia due to a complete block of erythropoiesis downstream of committed erythroid progenitors. By contrast, production of megakaryocyte progenitors, megakaryocyte maturation and thrombopoiesis were maintained. In the myeloid lineage, neutrophil differentiation was completely abrogated in the absence of Rcor1 expression and monocytic cells were significantly expanded, resulting in a peripheral blood leukocytosis and a monocytic infiltration in the liver. Rcor1-deficient monocytic cells were less apoptotic and had cytokine-dependent progenitor activity. Together, these data demonstrate that Rcor1 is essential for both erythroid and myelomonocytic differentiation and that its loss of function gives rise to significant myelodysplasia. As indicated in the chapters, some of these studies were done in collaboration with Devorah Goldman and Harv Fleming at OHSU, experts in hematopoiesis.

CHAPTER 1: Introduction

1.1 Transcriptional regulation and lineage determination

During development, different cell types display distinct patterns of gene expression, which define cell identities. These specific gene expression patterns are controlled by combinatorial interactions of transcription factors. Early recognition of this idea came from overexpression of the myogenic family of transcription factors in fibroblasts, which turned non-muscle cells into muscle phenotype (Davis et al., 1987). The particular power of transcription factors in cell type determination has been highlighted more recently by the derivation of induced pluripotent cells through expression of pluripotency-associated transcription factors in differentiated cells (Takahashi and Yamanaka, 2006; Wilson et al., 2010). Although a wide variety of external stimuli, such as cytokines and growth factors, can influence and modulate lineage choices, these factors usually cooperate with internal transcription factors to change the cellular gene expression pattern. Therefore it is reasonable to conclude that understanding the functions of transcription factors and how they regulate gene expression is key to understanding how organism development is programmed.

1.1.1 Histone modifications and transcriptional regulation

Transcription factors are proteins that bind to specific DNA sequences and regulate the transcription of genes either positively or negatively (Latchman, 1997). However, eukaryotic genes do not exist as naked linear DNA molecules in the nucleus, or as DNA molecules bound only to transcription factors. Instead, DNA molecules are complexed with histone proteins to form a substance known as chromatin (Olins and Olins, 2003).

Therefore chromatin structures have to be regulated and coordinated with other parts of the transcriptional regulatory apparatus. The basic repeating unit of chromatin, the nucleosome, consists of DNA wrapped around a core of two copies of each of the histone proteins H2A, H2B, H3 and H4(Weaver, 2002). Higher-order chromatin structure involves nucleosome-nucleosome contacts, mediated in part by the N-terminal tails of histones. Accumulated evidence has shown that covalent modifications of histone tails can greatly influence chromatin structure and transcriptional activation or repression (Lee and Young, 2000).

Histone acetylation is one of the best understood histone modifications. Several lysine residues on the N-terminal tail of each of the core histones can be acetylated. It is generally accepted that histone acetylation is positively associated with transcriptional activation through two mechanisms. First, neutralizing the positively charged lysine by acetyl groups can disrupt the affinity of histone tails to DNA and the interaction of histone tails between two neighboring nucleosomes, which provides greater access to DNA sequences for the transcription apparatus and its regulators(Garcia-Ramirez et al., 1995; Lee and Young, 2000). Second, histone acetylation can actively recruit proteins, such as bromo-domain containing proteins, which can themselves influence transcription and other chromatin-template processes (Josling et al., 2012). Importantly, histone acetylation is a reversible process. Histone acetyltransferases (HATs) and histone deaceytlases (HDACs) are enzymes responsible for regulating this modification. Consistent with the above findings, hypoacetylated histones are enriched in regions that

are transcriptionally silent and histone deacetylation is viewed as a mechanism leading to gene repression (Josling et al., 2012; Lee and Young, 2000).

Another important histone modification is histone methylation; however, it is more complex than acetylation. Histones can be methylated on arginine and lysine residues. Several lysine residues on the tails of histone H3 and H4 can be mono-, di- or trimethylated. Their functions in transcriptional regulation depend on the position of the arginine or lysine and the exact state of methylation. So far, over 20 methyl marks on lysine and arginine residues have been identified. The five lysine residues on the histone tails that have garnered the most attention are shown in Figure 1.1. The first mark that has been characterized in detail is methylation of histone 3 lysine 4 (H3K4me) (Strahl et al., 1999). It is now appreciated that trimethylation of H3K4 is strongly associated with transcription activation at promoter regions, while H3K4me1 is associated with enhancer elements. In contrast, trimethylation at H3K9, H3K27, and H4K20 are generally considered as repressive modifications. It is important to note that repressive and active trimethyl-markers are not always mutually exclusive. The prime example of this is the presence of both H3K4me3 and H3K27me3, the so-called bivalent marks, in developmentally important gene loci in embryonic stem cells, signifying an epigenetic state primed for either activation or repression (Mosammaparast and Shi, 2010; Sanders et al., 2004).

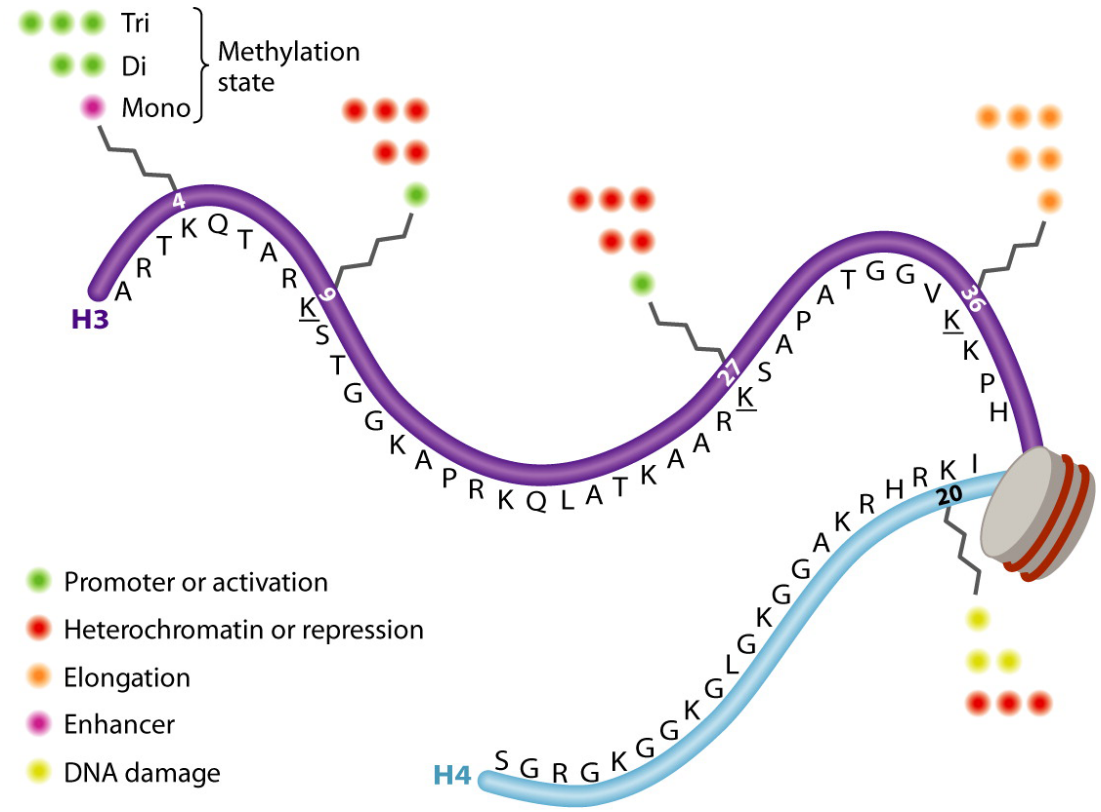

Mosammaparast N, Shi Y. 2010.
Annu. Rev. Biochem. 79:155–79

Figure 1.1. Major lysine methylation marks on the amino-termini of histones H3 and H4.

Unlike histone deacetylation, which involves simple hydrolysis of an amide bond, methylated histones were thought to be irreversible due to the more stable nature of the Carbon-Nitrogen bond. Experimental evidence of enzymatic demethylation was lacking for several decades until the discovery of lysine-specific demethylase 1 (Lsd1 or Kdm1a), which uses flavin adenine dinucleotide- dependent amine oxidase mechanism (Shi et al., 2004b). Another group of demethylase is the Jumonji C-terminal family proteins which use Fe^{2+} - and the 2-oxolglutarate- dependent dioxygenase mechanism (Whetstine et al., 2006). To date, many of the key methylated histone markers have a corresponding demethylase (Mosammaparast and Shi, 2010).

1.1.2 Transcriptional cofactors and the REST corepressor (Rcor1) complex

Transcription factors and histone modification enzymes are connected by transcriptional cofactor proteins. These proteins do not bind to specific DNA sequences themselves or directly modify chromatin; therefore, the importance of transcription cofactors is usually less appreciated, in part because they have been less easily studied. However, transcription cofactors play important roles in controlling gene expression and diversifying gene expression patterns through linking specific chromatin modifiers to specific transcription factors, and through their unique regulatory function in the complex.

Two major observations highlight the importance of transcription cofactors. First, from an evolutionary point of view, it is interesting to note that yeast only have one mediator, a multi-subunit co-activator complex, while metazoans contain at least five related complexes. Even a two fold increase in the number of potential cofactors would result in

a substantial increase in the combinatorial control of gene expression. Therefore, the diversification of transcription cofactors might reflect the increasing needs of establishment and maintenance of cell type specific gene expression pattern in higher organisms (Levine and Tjian, 2003). Second, transcription factors traditionally are designated as either activators or repressors. However increasing studies suggest that the function of many transcription factors is context dependent. Whether they promote or inhibit transcription depends on whether they interact with a coactivator complex or a corepressor complex at a specific promoter. In contrast, transcriptional cofactor complexes seem to have more restricted functions and can be viewed as functional units (Hayakawa and Nakayama, 2011). Therefore, to understand the transcriptional network that is required for establishing cell identities, we need to study both transcription factors and cofactors. The major work of this thesis is to study a prominent transcription cofactor in the cell, REST corepressor 1 (Rcor1).

Even though Rcor1 is now known as a general corepressor, it was first identified through its interaction with the C-terminal zinc finger motif of REST and was hypothesized to mediate repression by REST. In support of this idea, when Rcor1 was fused to a yeast Gal4 DNA-binding domain, it repressed reporter genes containing the Gal4 upstream activator sequence (Andres et al., 1999). The deduced primary sequence of human Rcor1 is 485 amino acids in length. It contains one ELM2 (EGL-27 and MTA1 homology 2) domain (103-189) and two SANT (SW13/ADA2/NCoR/TFIIIB) domains (190-241; 381-432) separated by 140 amino acid (predicted by ScanProsite). These domains are conserved between mouse and human Rcor1 proteins. Proteins with ELM2 domains are

known components of chromatin-regulatory complexes containing one or more histone deacetylases (HDACs). The SANT domain is proposed to function as a histone-interaction module that couples histone-tail binding to enzyme catalysis for the remodeling of nucleosomes (Boyer et al., 2004; Grune et al., 2003).

Consistent with the primary sequence analysis, pull down of Rcor1 from Hela cells revealed a novel HDAC1/2 containing complex, distinct from the previously identified mSin3 and NuRD complex (Humphrey et al., 2001; You et al., 2001). A 179 amino acid region (75-245) which contained the ELM2 domain and the N-terminal SANT domain of Rcor1 was required for interaction with HDAC1 (You et al., 2001). In the complex, there is another histone modification enzyme: Kdm1a, which removes mono- and dimethyl marks on H3K4 (Shi et al., 2004b) and H3K9 (Metzger et al., 2005). The demethylation of these residues leads to opposite transcriptional events: while demethylation of H3K4 is associated with gene repression, demethylation of H3K9 leads to gene activation. However, thus far only repressor function has been reported with the Rcor1/Kdm1a complex. Kdm1a binds to Rcor1 through a domain mapped between the two SANT domains (Shi et al., 2005). The interactions of these two enzymes are important to Rcor1 function. Interestingly, the binding regions of these two enzymes correlate to the two distinct repressor domains of Rcor1 that are each sufficient for repression. Repressor Domain 1 is between amino acids 102 and 195 in the N-terminal half of Rcor1, which is also important for HDAC/Rcor1 interaction. Repressor domain 2 is spanning amino acids 321–442, which is overlap with the LSD1 interaction region. However, the intact CoREST protein is a much more efficacious repressor than either of its repressor domains,

suggesting cooperativity of these enzymes in the repression mechanism (Ballas et al., 2001).

Although the co-repressor function of the Rcor1 complex seems to rely on the enzymatic function of HDAC1/2 and Kdm1a, Rcor1 protein has its own contributions to the complex. *In vitro* reconstitution of the Kdm1a/Rcor1 complex reveals an essential role for Rcor1 protein in stimulating demethylation on core histones (Lee et al., 2005). In addition to that, while recombinant Kdm1a is unable to demethylate H3K4 on nucleosomes, Kdm1a and Rcor1 together can readily demethylate nucleosomes. Furthermore, hyperacetylated nucleosomes are less susceptible to Rcor1/KDM1A-mediated demethylation, suggesting that hypoacetylated nucleosomes may be the preferred physiological substrates. By bringing HDAC1/2 and KDM1A close together, Rcor1 promotes the collaboration of these two enzymes to generate a repressive chromatin environment. Consistent with this model, TSA treatment results in derepression of Kdm1A target genes (Shi et al., 2005).

Other proteins in the Rcor1 complex that have been identified by several groups include Hmg20b (also called BRAF35) and phf21a (also call BHC80). The Hmg20b protein is a structural DNA binding protein with specificity for cruciform DNA. It can alter DNA conformation, allowing access to associated factors (Marmorstein et al., 2001). Single point mutation in the HMG domain of Hmg20b abrogated REST-mediated transcriptional repression. In addition, binding of Inhibitor of BRAF35 (iBRAF) to Hmg20b impaired its interaction with Kdm1A-Rcor1 complex and consequently impaired the function of Kdm1A/Rcor1 complex, suggesting the Hmg20b protein is a crucial part of the complex

(Ceballos-Chavez et al., 2012; Hall et al., 2005). Phf21a, a PHD finger containing protein that preferentially binds to unmethylated histone3 lysine 4, is proposed to prevent a futile cycle of H3K4 remethylation and promote the repressed state (Lan et al., 2007). Overall, every member serves a distinct but collaborative role.

While the Rcor1 complex has been established biochemically, its biological functions have been largely hypothetical based on the function of its interaction proteins. As mentioned earlier, the Rcor1 complex was originally found to mediate the repression function of REST (Andres et al., 1999). REST binds to and represses many essential neuronal genes, such as ion channels, synaptic transmission proteins, and adhesion/path-finding genes, in non-neuronal cells, including neural progenitors (Otto et al., 2007). The expression level of REST is high in embryonic stem cells (ESCs) but dramatically decreases during the differentiation of ESCs to neural progenitors (NPs) and decreases even further at terminal differentiation of neurons. These observations have led to the hypothesis that REST is a master transcriptional repressor of neural genes, which functions to maintain a non-neuronal status outside the nervous system and to time terminal differentiation in neural progenitors (Ballas et al., 2005). This hypothesis is supported by *in vitro* differentiation assay, where removal of REST led to precocious differentiation of neural progenitors (Gao et al., 2011) and *in vivo* where persistent expression impeded terminal differentiation (Mandel et al., 2011). While REST level is low in the neurons, Rcor1 level stays high during the whole process of differentiation (Ballas et al., 2005), leading to the question: what's the function of Rcor1 in mature neurons? Besides the functions mediated through the interaction with REST, Rcor1 may

have other roles due to interactions with other transcription factors. For example, Rcor1 interacts with NAC1 (Korutla et al., 2007), a brain POZ/BTB (Pox virus and zinc finger/bric-a-brac tramtrack broad complex) protein that can prevent cocaine-induced sensitization in the rat (Mackler et al., 2000), indicating this interaction may have important role in behavioral sensitization. Another repressor, TLX, an orphan nuclear receptor that plays an essential role in maintaining the undifferentiated state of adult neural stem cells in the mouse forebrain (Shi et al., 2004a), also interacts with Rcor1/Kdm1A (Yokoyama et al., 2008). Rcor1 complex also functions with Nurr1, another orphan nuclear receptor, in astrocytes and microglia (Saijo et al., 2009). This complex is recruited to repress expression of inflammatory mediators in these cells and prevent neurodegeneration. In a recent study, the transition between multipolar and bipolar stages of newborn cortical pyramidal neurons is markedly delayed by knockdown of Rcor1, which profoundly affects the onset of their radial migration. This function of Rcor1 appears to be independent of REST but requires the histone demethylase Kdm1A (Fuentes et al., 2012).

Outside of the nervous system, the Rcor1complex has been shown to associate with repressors that are important to hematopoiesis, cancer progression and invasion and viral infection. Given the diverse number of functions, which have been proposed for Rcor1 through its interaction to different transcription factors, I decided to directly study Rcor1 function *in vivo*, by creating the first Rcor1 genetic knockouts. Specifically, the exon 4 of Rcor1 gene was floxed out and consequentially created a premature stop codon. Using these mice I specifically wanted to ask, what are the biological processes which depend

on the expression of Rcor1? In Chapter 2 I describe the preliminary studies of the Rcor1 function in the nervous system. To our surprise, I did not observe major defects due to loss of Rcor1 in this system despite the normally high levels of Rcor1, likely due to redundancy with other Rcor family members. In Chapters 3 and 4, I summarize the functions of Rcor1 in embryonic hematopoiesis and adult hematopoiesis. My studies demonstrated that Rcor1 is critical to hematopoetic lineage formation. Because so much is known about hematopoietic lineage differentiation and transcriptional regulation, I first summarize what we know about this system.

1.2 Lineage differentiation in hematopoietic system

The hematopoietic system is arguably the best studied system of stem cell differentiation and lineage determination (Orkin and Zon, 2008a, b). The hematopoiesis happens earliest in the yolk sac, where the hemangioblast generates endothelial cells (ECs) and primitive red blood cells (RBCs), characterized by large cell size and expression of embryonic hemoglobins (Lux et al., 2008; Sankaran et al., 2010). This early hematopoiesis is called primitive hematopoiesis since it generates primitive erythrocytes. Later, hematopoiesis moves to the AGM region (Aorta, Gonad, Mesonephros region) and the placenta, where hemogenic endothelial cells are capable of generating both hematopoietic stem cells (HSCs) and endothelial cells. The third hematopoietic tissue during development is the fetal liver. After birth, hematopoiesis moves to bone marrow and remains there for the entire lifetime. Since the hematopoiesis that occurs in the fetal liver and bone marrow generates smaller erythrocytes that only express adult hemoglobins, it is called definitive hematopoiesis. Within the definitive hematopoietic system, HSCs in fetal liver and bone

marrow have different properties. For example, HSCs in the fetal liver constantly undergo both self-renewal and differentiation; however, in the adult bone marrow, HSCs are normally quiescent and only divide when there is need for regeneration. In addition, HSCs in the fetal liver mainly generate RBCs, with less than 5% cells in other lineages, while HSCs in bone marrow generate all the blood lineages, including both the myeloid lineages and lymphoid lineages (Figure 1.2).

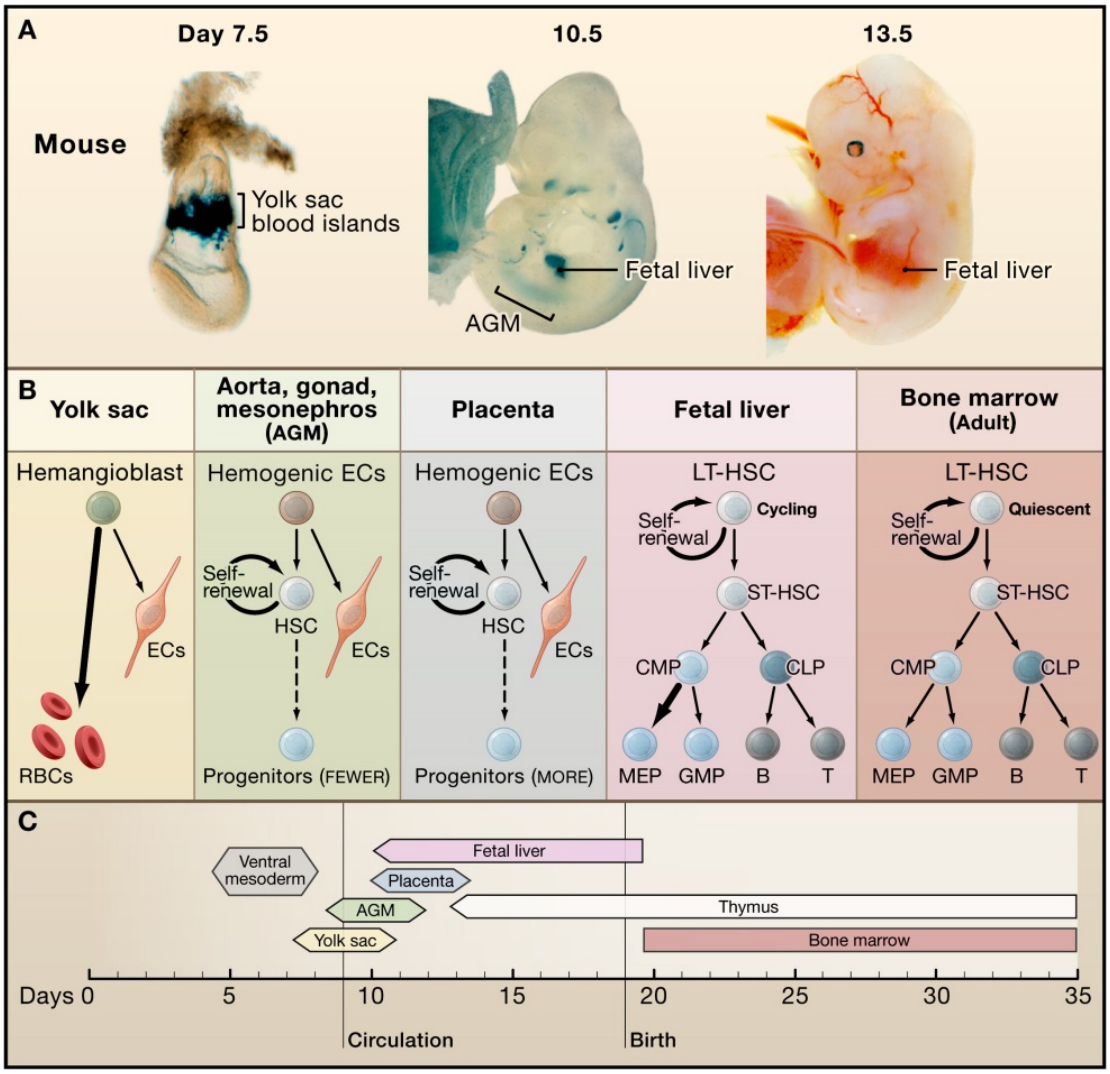

Figure 1.2. Developmental regulation of hematopoiesis in the mouse. (A) Hematopoiesis occurs first in the yolk sac blood islands and later at the aorta-gonad mesonephros (AGM) region, placenta, and fetal liver. Yolk sac blood islands (left), AGM and fetal liver (middle) are visualized by LacZ staining of transgenic embryo expression *GATA-1- LacZ* and *Runx1-LacZ* knockin mice, respectively. (Photos courtesy of Y. Fujiwara and T. North.) (B) Hematopoiesis in each location favors the production of specific blood lineages. Abbreviations: ECs, endothelial cells; RBCs, red blood cells;

LT-HSC, long-term hematopoietic stem cell; ST-HSC, short-term hematopoietic stem cell; CMP, common myeloid progenitor; CLP, common lymphoid progenitor; MEP, megakaryocyte/erythroid progenitor; GMP, granulocyte/macrophage progenitor. (C) Developmental time windows for shifting sites of hematopoiesis. Adopted from (Orkin and Zon, 2008a).

Stem cells and progenitors in the hematopoietic system have a number of properties that make them a relatively easy system to study. First, they are easily accessible: mature blood cells are free moving cells in circulation and the bone marrow is loose connective tissue that can be easily disrupted to isolate cells. Because of their ease of isolation, cell surface proteins are largely preserved, serving as markers to separate cells into different groups. Second, stem cells and progenitor cells can be transplanted: Simply taking them out of their niches and injecting them into the blood stream of a recipient, they survive, find their way back to their normal niches and retain their differentiation potential (Schroeder, 2010). Third, mature cells and some precursors in different lineages have distinct morphological characteristics, allowing them to be distinguished from one another. Studies using monoclonal antibodies and flow cytometry, together with *in vivo* transplants and *in vitro* culture, have established strong correlations between cell surface markers and differentiation potential.

The identification of the HSCs and many intermediate progenitors shaped the view of hematopoiesis into a hierarchical tree, starting first with the multipotent HSC, which can generate any cell in the hematopoietic system (Figure 1.3). The long-term HSCs first divide and generate short-term HSCs and multipotent progenitor cells (MPPs). MPPs then divide, differentiate and give rise to either the common myeloid progenitors (CMPs) or the common lymphoid progenitors (CLPs). The CLP further divides and differentiates leading to the formation of committed progenitors that give rise to all of the cells of the lymphoid lineage: T, B, natural killer (NK), and a subset of dendritic cells. The CMP is able to differentiate into two potentially isolatable progenitor populations, which include

the megakaryocyte-erythroid progenitor (MEP) and the granulocyte-monocyte progenitor (GMP). The MEP gives rise to lineage-committed progenitors that can undergo further differentiation to megakaryocytes and erythroid cells, whereas the GMP will generate precursors for mast cells, eosinophils, basophils, neutrophils, monocytes, macrophages and a subset of dendritic cells. (Dzierzak and Philipsen, 2013; Orkin and Zon, 2008a).

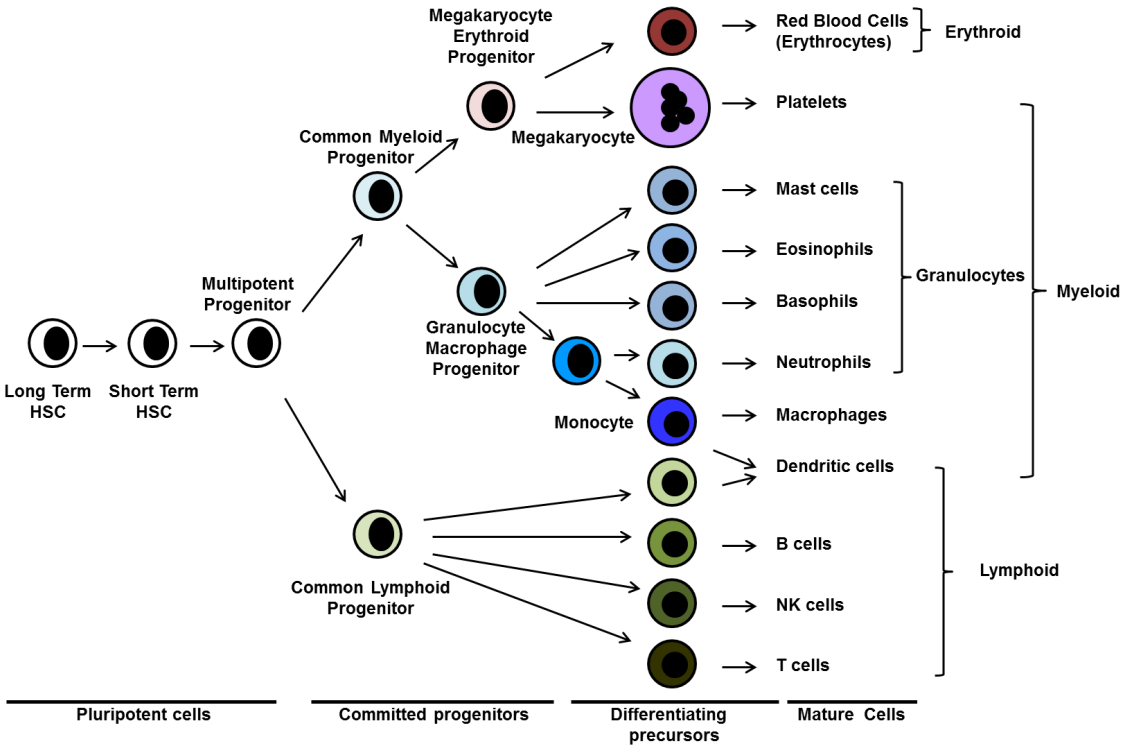

Figure 1.3. Hematopoiesis is a hierarchical differentiation process that leads to the formation of cells in all the blood lineages. Hematopoietic stem cells (HSC) can undergo self-renewing divisions. They can also divide and differentiate, leading to the formation of the common lymphoid progenitor (CLP) and the common myeloid progenitor (CMP). The CLP further differentiates and generates lymphocytes, whereas the CMP differentiates and forms the myeloid cells, including monocytes, granulocytes, megakaryocytes, and erythrocytes. Modified from (Dzierzak and Philipsen, 2013).

Markers of hematopoietic progenitors have been characterized and summarized in table 1. Mature cells in each lineage have their own markers. All the early progenitors do not express the lineage markers but are positive for the progenitor marker c-Kit, a tyrosine kinase receptor of Mast/stem cell growth factor. While HSC and MPP are enriched in the Sca1 positive population, CMP, GMP and MEP are Sca1 negative. The further distinctions of LT-HSC, ST-HSC and MPP are based on CD150 and CD48 and CD34. The further distinctions of CMP, GMP and MEP are based on CD34 and CD16/32.

Table 1.1: Surface markers for mature lineage cells and hematopoietic progenitors

Cell type	Lineage markers	Ckit	Sca1	CD48	CD150	CD34	CD16/32
LT-HSC	-	+	+	-	+	-	
ST-HSC	-	+	+	-	+	+	
MPP	-	+	+	+	+/-		
CMP	-	+	-			+	hi
GMP	-	+	-			+	low
MEP	-	+	-			-	-
RBCs	Ter119	-	-	-	-	-	-
Monocyte	Mac1+, Gr1-	-	-	-	-	-	-
Granulocyte	Mac1+, Gr1+	-	-	-	-	-	-
B cells	B220	-	-	-	-	-	-
T cells	CD3+	-	-	-	-	-	-
Megakaryocytes	CD41+	-	-	-	-	-	-

Because my research is mainly focused on the erythrocyte, myeloid, and megakaryocyte lineages, I will discuss their differentiation in more detail in the following three sections.

1.2.1 Erythropoiesis

Erythropoiesis is the process of generating erythrocytes or RBCs. RBCs are responsible for carrying oxygen from the lungs to other tissues in the body and for transporting carbon dioxide from the tissue to the lungs. There are two waves of erythropoiesis. The

first wave is known as primitive erythropoiesis, which transiently takes place in the yolk sac blood island during embryonic day E7.5-E11 in the mouse. It is characterized by the production of erythrocytes with unextruded nuclei and expression of embryonic globin genes. The second wave, or definitive erythropoiesis, in mouse occurs in the fetal liver during embryonic day E12 to birth, and then shifts to the bone marrow, where it sustains blood formation throughout the life of the individual. The product of definitive erythropoiesis is enucleated RBCs (Lodish et al., 2010).

Erythropoietic differentiation is a multiple step process (Figure 1.4). MEPs, upon the stimulation of growth factors, differentiate into erythropoietin – responsive erythroid burst forming unit-erythroid (BFU-E) and colony forming unit-erythroid (CFU-E). CFU-Es undergo three to five divisions, giving rise to several morphologically defined maturing erythroblasts, including proerythroblast (ProE), basophilic erythroblast (BasoE), polychromatophilic erythroblast (PolyE), and orthochromatic erythroblast (OrthoE). OrthoEs become hemoglobinized and extrude their nuclei to form reticulocytes, which then develop into mature, functional RBCs (Tsiftsoglou et al., 2009).

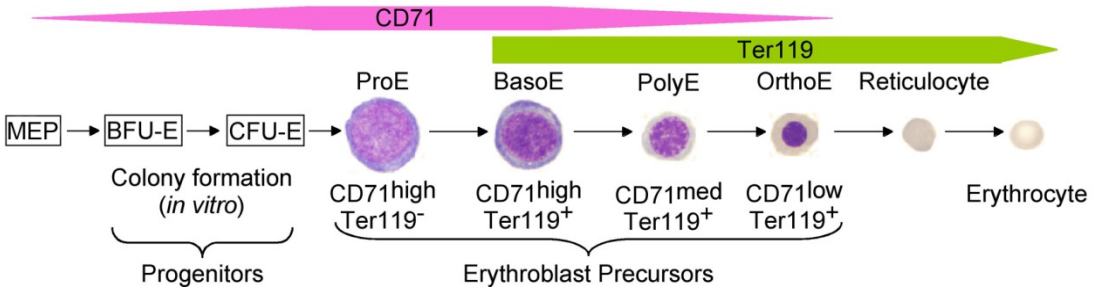

Figure 1.4. Schematic diagram of erythropoietic differentiation in the mouse. The early common progenitors for erythrocytes and megakaryocytes (MEP) divide and differentiate to the formation of the early erythroid progenitor (BFU-E), which further divides and differentiates and generates late erythroid progenitor (CFU-Es). Each CFU-E undergoes 3-5 cell divisions, differentiation, chromatin condensation, and enucleation, ultimately leading to the formation of the erythrocyte. Abbreviation: ProE, proerythroblast; BasoE, basophilic erythroblast; PolyE, polychromatophilic erythroblast; OrthoE, orthochromatic erythroblast.

The existence of all the different progenitor types can be determined by different experimental methods. MEPs have been identified by a series of surface markers (Table 1.1). There is no specific surface marker for BFU-Es or CFU-Es; however, their existence can be detected by *in vitro* colony-forming cell assays in methylcellulose medium. The erythroid colonies generated by BFU-E can be detected after 7-14 of culture as a large cluster of cells, and the colonies formed by CFU-Es can be detected after two days of culture as a small cluster of 8-32 cells. The later stage erythroblasts, from ProE to OrthoE, have limited ability to proliferate; therefore they do not generate any colonies in colony-forming cell assays. Instead, they exhibit differential expression of Ter119 and CD71, the combination of which is used to distinguish specific erythroblast stages by flow cytometric analysis (Zhang et al., 2003). Specifically, both CD71 and Ter119 are low in the early progenitors. As progenitors differentiate, the expression level of CD71 increases first and then the expression level of Ter119 increases. At the final stages of differentiation, the expression level of CD71 goes down but Ter119 stays high. This expression pattern is also faithfully reproduced during erythroid differentiation in *in vitro* culture of both fetal liver (Zhang et al., 2003) and adult erythroid progenitors (Shuga et al., 2007). These two cell surface markers therefore provide us a reliable method to trace the differentiation process of erythropoiesis.

1.2.2 Myelopoiesis

Granulocytes, monocytes, and their committed progenitors are collectively called myeloid cells. They are key mediators of innate immunity and inflammatory responses (Rosmarin et al., 2005).

Monocyte differentiation

Monocytes develop in the bone marrow from dividing CMPs followed by GMPs. Further differentiation of GMPs create monocyte/macrophage and dendritic cell progenitors (MDPs), which have lost the ability to generate granulocytes but provide the basis for monocytic lineage development, including monoblasts, promonocytes, and monocytes (Auffray et al., 2009) (Figure 1.5). Monocytes are subsequently released to the peripheral circulation as nondividing cells. The half-life of a circulating monocyte has been estimated to be around three days in humans and one day in mice. Monocytes can enter organs and tissues to differentiate into resident macrophages and dendritic cells, contributing to tissue hemostasis, such as clearance of senescent cells, tissue remodeling, repair, as well as the genesis and resolution of the inflammatory response (Figure 1.5) (Huber et al., 2014).

The markers for CMP and GMP have been described previously (Table 1.1). A clonogenic bone marrow MDP progenitor has been isolated with the surface marker of CX3CR1+, C-kit+, CD34+, CD16/32+ , and Lin-. These surface markers signify that MDPs are derived from GMPs, as they share all the markers of GMPs and also have an increase in CX3CR1expression. This progenitor can differentiate into macrophage (CD11b+, CD11c-) and dendritic cells (CD11blow CD11c+) both *in vivo* and *in vitro* (Fogg et al., 2006). Mouse bone marrow-resident and circulating blood monocytes are defined primarily by their expression of CD115 (the receptor for Monocyte-Colony Stimulating factor), F4/80 (a 125 KD transmembrane protein), CD11b (integrin beta2), and CX3CR1(a chemokine receptor) (Yona and Jung, 2010).

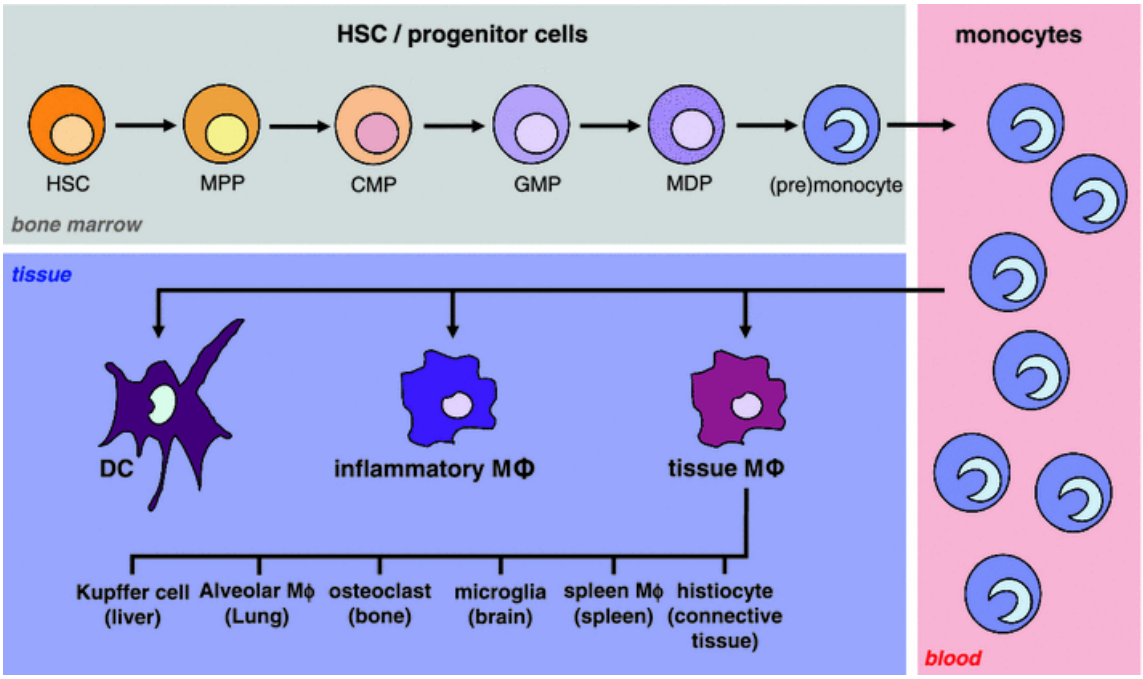

Figure 1.5. The differentiation of monocytic cells. The scheme shows monocytic maturation, beginning with self-renewing HSCs and involving several myeloid progenitors resulting ultimately in the mature blood monocytes. Further differentiaton steps yield the generation of macrophages and dendritic cells (DC) in different tissues. Further details are described in the text. (HSC hematopoietic stem cell, MPP multipotent progenitor, CMP common myeloid progenitor, GMP granulocyte/monocyte progenitor, MDP monocyte/macrophage and dendritic cell progenitor, MΦ, macrophage) Adopted from (Huber et al., 2014).

Granulocyte differentiation

Granulocytes actually include several different cell types: neutrophils, eosinophils, basophils, and mast cells. However, neutrophils are the most abundant within the granulocytic compartment and therefore have gathered the most attention. Except for the differentiation of neutrophils, the lineage commitment pathways and mechanisms are largely unsolved issues in hematology. In this thesis without specification, I use granulocytes to indicate neutrophils, as distinct from monocytes. Granulocytes and monocytes share the common progenitor GMP. After passing through the GMP stage, cells in granulocytic lineages gradually acquire specific features. The classification of progenitors of neurophils is mainly based on the characteristic nuclear shape and content of granules (McGarry et al., 2010). The maturation process therefore can be separated into a series of morphologically distinct stages, including myeloblasts, promyelocytes, myelocyte, metamyelocytes, and band cells /segmented granulocytes (Figure 1.6). At the myeloblast/promyelocyte (MB/PM) stages the cells still proliferate and generate primary granules with their constituting proteins. At the myelocyte/metamyelocyte (MC/MM) stages, cell proliferation and expression of primary granule proteins stop concomitantly with the successive generation of secondary and tertiary granules and their constituting granule proteins. Finally, the synthesis of granule proteins ceases, and the cells acquire their full antimicrobial potential when maturation proceeds toward the stages of neutrophils with band shaped (BCs) and segmented polymorphic nuclei (PMNs). The granulocytic progenitors described above can be roughly separated based on their characteristic forward-scattered light (FSC), side-scattered light (SSC), and surface

markers (Satake et al., 2012). Specifically, as progenitors mature, they decrease in the progenitor maker c-Kit expression and increase in the lineage specific maker, Lymphocyte Ag6 complex, locus G (Ly6G; a member of the Ly-6 family of GPI-anchored proteins).

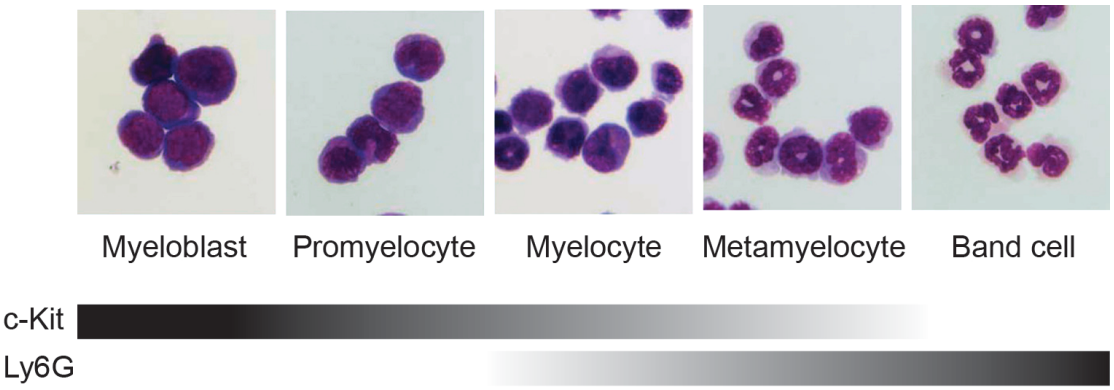

Figure 1.6. The differentiation of granulocytes. The maturation process of granulocytic progenitors can be separated into a series of morphologically distinct stages, including myeloblasts, promyelocytes, myelocyte, metamyelocytes, and band cells, revealed by wright–Giemsa staining. As progenitors mature, they decrease in the progenitor maker c-Kit expression and increase in the lineage specific maker, Lyphocyte antigen 6 complex, locus G (Ly6G). Modified from (Satake et al., 2012).

1.2.3 Megakaryoctye differentiation

A third cell type that I have focused on is megakaryocytes. They are very rare and only account for ~0.01% of nucleated bone marrow cells (Nakeff and Maat, 1974). The best defined progenitors that can give rise to megakaryocytes are the MEPs and committed clonogenic megakaryocyte progenitors (MkPs) that have the surface markers of $CD41^{+,}$ $CD9^{+}$, $Ckit^{+}$, $Scal^{+}$, $Fc\gamma R^{lo}$, IL-$7R\alpha^{-}$, Lin^{-} (Nakorn et al., 2003; Pronk et al., 2007). Mature or maturing megakaryocytes are the most easily distinguished cells in the bone marrow because they are several times larger than the surrounding cells. They also have a very large nucleus owing to repeated endonuclear duplication and bulky excessive cytoplasm. Megakaryocytes can be quantified by flow cytometry based on expression of CD41 and polyploidy. It is believed that all these unique maturation behaviors serve to the ultimate function of megakaryocytes, which is to produce platelets. Platelets are small, anucleate cell fragments in the blood that help to form blood clot (Machlus and Italiano, 2013).

1.3 Transcriptional regulation in hematopoiesis

Over the past couple of decades, efforts have been made to understand the molecular mechanisms that determine these cell fate decisions. As intrinsic determinants of cellular phenotype, transcription factors are known to govern the hematopoietic lineage determination. Although the list is still growing and new functions of known transcription factors are emerging, an overview of transcriptional regulation of different lineages is provided in Figure 1.7.

It is important to note that both transcriptional activation and repression are required for specific lineage formation. While transcription factors and their co-activators promote lineage specific gene expression, transcription repressors and co-repressors suppress alternative lineage gene expression, serving as an additional molecular mechanism to reinforce lineage commitment. It is common to see cross antagonism between transcription factors for different lineages. The importance of the antagonism is demonstrated at multiple stages from early progenitors to late precursors. A few transcription factors that have been shown to recruit Rcor1/Kdm1A complex are marked with red color (Figure 1.7).

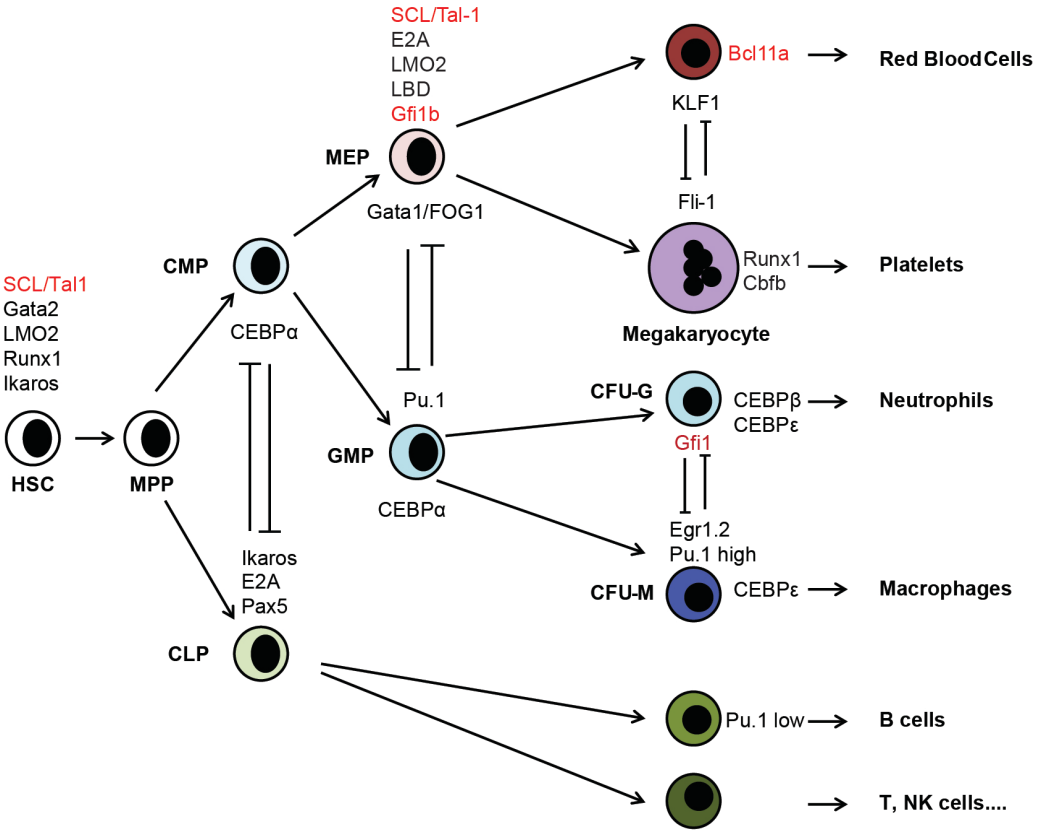

Figure 1.7. Key transcription factors that are involved in determining hematopoietic lineages. Transcription factors that are important for each lineage are labeled besides icons representing each cell type. A few pairs of transcription factors cross antagonize each other to influence lineage determination. Rcor1 interacting transcription factors are colored in red. Modified from (Friedman, 2007).

1.3.1 Transcriptional regulation of early hematopoietic development

Since purifying and biochemically studying very rare HSC populations is very difficult, the role of specific transcription factors in HSC fate decision was first derived largely from genetic strategies, primarily gene-targeting and retroviral infection/overexpression experiments (Zhu and Emerson, 2002). When tested in chimeric mice, ES cells that lack SCL/Tal (Robertson et al., 2000), Gata2 (Tsai et al., 1994), or Lmo2 (Yamada et al., 1998) cannot contribute to any primitive and definitive hematopoietic compartments, while ES cells lacking Runx1 failed to generate definitive hematopoietic tissues (Okuda et al., 1996), suggesting these factors are important for HSC specification. Other transcription factors are more important for HSC function. For example, Homobox genes (Sauvageau et al., 1995) and IKaros (Nichogiannopoulou et al., 1999) are important for HSC self-renewal, as deletion of them impair long term repopulation ability of HSCs. While Gfi1 is required for restricting stem cell proliferation and preserving HSC quiescence (Hock et al., 2004), Gfi1b retains dormant HSCs in the endosteal niche to keep its quiescence (Khandanpour et al., 2010).

1.3.2 Transcriptional regulation of erythropoiesis and megakaryocyte differentiation

The best studied transcription factor in erythropoiesis and megakaryocyte differentiation is the zinc finger transcription factor Gata1. It is perhaps also the best-studied hematopoietic transcription factor. Gata1 activates a large number of genes that promote erythropoiesis and megakaryocyte generation together with an activation complex

including SCL, E2A, LMO2 and LDB1. On the other hand, it interacts with FOG-1/NuRD repression complex to repress genes and maintain lineage fidelity (Dore and Crispino, 2011; Perry and Soreq, 2002).

Another important transcription factor common to these two lineages is Gfi1b (Foudi et al., 2014; Saleque et al., 2002), which has been show to function as a transcription repressor through interaction with Rcor1/Kdm1A/HDCA complex (Saleque et al., 2007). Depletion of Gfi1b or Kdm1A resulted in block of differentiation in erythroid and megakaryocyte lineages (Foudi et al., 2014; Kerenyi et al., 2013; Saleque et al., 2002). However, the molecular mechanism mediated through Gfi1b and how it cooperated with Gata1factor in these two lineages differentiation is not very clear.

Although many transcription factors are required for both erythroid and megakaryocyte differentiation, others are lineage specific. The best example is the mutual antagonism between KLF1 and FLI1 (Starck et al., 2003). KLF1 is critical for activation of β-globin transcription. Mice lacking KLF1 die in utero due to severe anemia demonstrating the requirement of KLF1 for proper RBC production (Nuez et al., 1995; Perkins et al., 1995). KLF1 also represses megakaryocyte differentiation through interaction with the megakaryocytic ETS factor Fli-1, which is important for megakaryocyte differention. Homozygous loss of Fli1 in mice results in embryonic lethal and severe dysmegakaryopoiesis (Hart et al., 2000; Spyropoulos et al., 2000). Conversely, FLI-1 is capable of repressing KLF1 target genes. Several *in vivo* and *in vitro* studies support a model that in a bipotential erythro-megakaryocytic progenitor cell type, a marginal and

probably stochastic increase in KLF1 or FLI-1 levels may drive cell fate decision toward either erythroid or megakaryocyte lineage (Dore and Crispino, 2011).

In addition to the Fli1, GATA-2 overexpression in a multipotent human leukemia cell line (K562) also drives megakaryocytic differentiation at the expense of erythroid differentiation (Ikonomi et al., 2000).Other transcription factors, such as RUNX1 and CBFβ, are important for megakaryopoiesis (Elagib et al., 2003), but not essential for erythropoiesis (Wen et al., 2011).

1.3.3 Transcriptional regulation of myelopoiesis

There is no single, master regulator of transcription in myeloid cells, as seen with MyoD in muscle cells (Tapscott, 2005) and Pax5 in B lymphocytes (Medvedovic et al., 2011). Rather, transcriptional regulation in myeloid cells is the result of the combinatory effect of a few key transcription factors (Rosmarin et al., 2005). Among them, Pu.1 and CEBPα are important for making the early myeloid decision, whereas Pu.1, Egr1/2 and Gfi1 are important for later stage decision-making within the myeloid lineages (Friedman, 2007).

PU.1 is expressed in many different myeloid cell types but not in the erythroid lineage, mature granulocytes or T cells. Consistent with the idea that Pu.1 promotes myeloid differentiation, its expression increases during differentiation of granulocytic and monocytic precursors (Cheng et al., 1996b). Binding sites for Pu.1 are found on almost all myeloid specific promoters, such as CD11b and CD18, and the receptors for the cytokines, M-CSF, GM-CSF, and G-CSF. In addition, Pu.1 binds and regulates its own promoter (Rosmarin et al., 2005). Another mechanism for Pu.1 to promote myeloid

differentiation is the mutual antagonism between Pu.1 and Gata1. Overexpression of Pu.1 in erythroid lineage cells blocks erythroid differentiation and lead to erythroleukemia in mice (Paul et al., 1991). Conversely, ectopic expression of Gata1 in myelo-monocytic cells transforms them into erythroid, megakaryocytic and esoinophilic cells (Kulessa et al., 1995; Visvader et al., 1992). This occurs through the direct interaction and cross-antagonism between Pu.1 and Gata1.

While Pu.1 promotes myeloid differentiation, within myeloid lineages Pu.1 expression level influences the fate choice between granulocytes and monocytes lineages. Sustained, high-level expression of PU.1 fosters macrophage development and blocks granulocytic differentiation (McIvor et al., 2003), consistent with the fact that Pu.1 is not expressed in mature granulocytes.

Interestingly, not only the presence or absence of Pu.1 influences lineage choices, but the amount of PU.1 also seems to determine lineage choices. Singh's group made the important observation that high levels of PU.1 induce commitment to the myeloid lineage, while lower levels drive B lymphoid development (DeKoter and Singh, 2000).

Another important transcription factor is the CEBP family protein C/EBPα, which is expressed in myeloid progenitors and increases during early differentiation towards the GMP (Cheng et al., 1996b). It contributes to myeloid lineage commitment in early development stages. Similar to PU.1, CEBPα suppresses erythroid lineage formation but promotes the differentiation of the myeloid lineage (Suh et al., 2006). In addition, CEBPα inhibits the lymphoid lineage in CLP and B cells by antagonizing Pax5 (Hsu et al., 2006)

and Notch signaling. Transduction of lymphoid cells like CLP, B cells, and T cells with C/EBPa induces macrophage but not neutrophil development (Fukuchi et al., 2006; Heavey et al., 2003; Laiosa et al., 2006; Xie et al., 2004), suggesting CEBPα also promotes monocyte differentiation. However, it is dispensable for terminal monocyte maturation, since deletion of CEBPα in GMP did not alter the distribution of mature macrophages or granulocytes (Zhang et al., 2004).

Within the regulatory network that determines lineage fate decision between granulocyte and Monocyte/macrophage, the counter action between repressors Gfi1 and Pu.1-Egr1/2 is the best studied mechanism. As mentioned previously, high level of Pu.1 promotes monocytic differentiation. This is partly due to induction of Egr-1/2 expression by high level of Pu.1. While Pu.1 can activate both granulocyte and monocyte specific genes, Egr-1/2 specifically inhibits granulocytic genes to achieve the monocyte cell fate. In contrast, Gfi1 enhances granulocytic differentiation. In *Gfi1*$^{-/-}$ mice, neutrophil development is impaired and the mutant granulocytic cells mis-express macrophage genes (Hock et al., 2003). Mechanistically, both Egr1/2 and Gfi1 are repressors that can bind to each other's promoter to directly repress each other's expression level. In addition, Gfi1 also inhibits Pu.1 by direct repression of the Pu.1 gene. Gfi1 and Pu.1 can also inhibit each other's function by competing for DNA binding in promoters of target genes or through protein–protein interaction (Laslo et al., 2006; Spooner et al., 2009). This is another great example of the importance of repressors in lineage determination.

1.3.4 Principles in transcriptional regulation of hematopoiesis

Through the extensive studies of the key transcription regulators, such as those have been mentioned above, several principles and concepts have emerged in terms of how transcription factors control lineage differentiation (Orkin and Zon, 2008a).

1. All of the HSC transcription factors (such as SCL/Tal-1, Gata2, Runx1) also serve roles later within differentiation of individual blood lineages, and conversely, factors that appear to have more lineage-restricted roles (such as Pu.1, Gfi-1, CEBPα) act within HSCs. The redeployment of transcription factors at different stages of blood cell development complicates analysis of *in vivo* requirements. Both temporal and lineage-restricted conditional inactivation is often needed to reveal a meaningful phenotype.

2. Lineage determination requires both promoting target lineage differentiation while simultaneously acting against factors favoring other choices. Therefore, both transcription activators and repressors are required to provide an efficient means for resolving and reinforcing lineage choices. This can also be achieved by combining the positive and antagonistic roles of the major regulators. In both cases, understanding the interaction between transcription factors and different cofactor complexes is very important.

3. Cellular differentiation is not fixed or unidirectional. Although the traditional hierarchical model of hematopoiesis provides us an important reference for hematopoiesis, progenitors display plasticity. Cells of one lineage can be converted to another through the forced expression of chosen transcription factors or loss of them.

Knowledge of the functions of transcriptional regulation provides a strong foundation for cellular reprogramming.

4. Hematopoietic cell fate is intertwined with the origins of leukemias. Of the more than two-dozen regulators designated ‘‘hematopoietic transcription factors,’’ nearly all are intimately associated with hematopoietic malignancy. Indeed, the majority of genes encoding these factors were discovered either through analysis of chromosomal translocations found in human leukemias or study of cooperating leukemia genes during insertional mutagenesis in the mouse. Disturbance of the homeostatic balance of the critical transcriptional regulators is a defining feature of leukemias.

1.4 Significance of studying Rcor1 function in hematopoiesis

Rcor1 has been suggested to play important roles in hematopoiesis through its interaction with a few key transcription factors important for different lineages. For example, it can be recruited by growth factor-independent-1 transcription factor, Gfi1 and Gfi1b (Saleque et al., 2007). While Gif1 is required to maintain hematopoietic stem cells and generate neutrophils and lymphocytes, Gif1b is necessary for both erythropoiesis and megakaryopoiesis (van der Meer et al., 2010). In addition, the Rcor1/Kdm1A complex interacts with BCL11A (Xu et al., 2013) and SCL/Tal1 (Hu et al., 2009). BCL11a is important for the development of lymphocytes (Liu et al., 2003) and serves as a fetal globin switch during erythropoiesis (Sankaran et al., 2008). SCL/Tal1 has a broad spectrum of activity in hematopoiesis. It is required for the development of all hematopoietic lineages (Porcher et al., 1996; Sanchez et al., 2001) and can function as

both activator and repressor depending on different associated cofactors (Huang and Brandt, 2000; Huang et al., 2000; Huang et al., 1999). In addition, a mouse model specifically knocking out Kdm1a in the hematopoietic system has recently been generated. Kdm1a depletion causes a strong HSC defect and block of erythropoiesis and myelopoiesis(Kerenyi et al., 2013). However, since transcription factors can recruit multiple cofactors and Kdm1a can also associate with other cofactor complexes, the transcription network is still not clear without knowing the function of the transcription co-factors. Therefore, it is important to tease out Rcor1 dependent functions in hematopoiesis, which is the main goal of my thesis work.

KDM1a overexpression has been shown in a few cancer types, and several publications have shown that KDM1A inhibitors can induce apoptosis and differentiation of a few tested types of acute myeloid leukemia (AML) cells *in vivo* and *in vitro* (Fiskus et al., 2014; Harris et al., 2012; Schenk et al., 2012). These findings point to KDM1A as one of the most promising epigenetic targets in drug discovery design. However, current KDM1A inhibitors do show some toxicity to the cells when used at the effective concentration. The efficacy of these drugs is significant although they do not substantially increase survival times. In addition, it is interesting to note that in each case, KDM1A only affects a subset of genes and increases H3K4 dimethylation marks in specific promoters. These changed genes and promoters were different among individual studies. These results led to an interesting hypothesis that maybe inhibiting KDM1A function by disrupting a specific complex will reduce cell toxicity and therefore allow for the usage of higher concentration of inhibitors to achieve a better treatment. In addition,

if the transcription network is clarified in the normal condition, different complex-specific inhibitors can be used to achieve targeted induction of tumor suppresser genes or differentiation pathways in different patient cases. Studying the function of the Rcor1 complex and its targets will provide knowledge to achieve that goal.

Although diseases caused by Rcor1 mutation have not been reported, our work and others in knocking out or knocking down KDM1A clearly indicate that normal cell differentiation cannot be maintained without a sustained level of Rcor1 or KDM1A. The disease phenotypes showed in our Rcor1 knockout mice will help to identify new mutations and understand pathogenesis of certain blood diseases.

CHAPTER 2: Preliminary studies of Rcor1 function in nervous system

Introduction

As mentioned above, Rcor1 was identified in my mentor's laboratory as a corepressor of REST (Andres et al., 1999), which is a master repressor that regulates thousands of neuronal genes (Otto et al., 2007; Schoenherr et al., 1996). In the mice genome, there are three Rcor1-like genes: Rcor1 on chromosome 12, Rcor2 on chromosome 19, and Rcor3 on Chromosome 1. The roles of RCOR2 and RCOR3 are unknown.

Rcor1 is expressed in both non-neuronal cells and neurons (Grimes et al., 2000). The REST-Rcor1complex has been shown to play an important role in regulating neuronal gene expression and neuronal stem cell fate (Ballas et al., 2005). However, in mature neurons, the function of Rcor1 may not be dependent on REST, because REST is largely depleted in mature neurons, although recent studies in my mentor's and other laboratories indicate that REST is expressed in some subpopulations of adult neurons (Calderone et al., 2003; Gao et al., 2011; Lu et al., 2014). Rcor1 also interacts with other transcription factors, such as Nurr1 (Saijo et al., 2009), NAC1 (Korutla et al., 2007), and Znf217 (Cowger et al., 2007). The biological function of Rcor1 in the nervous system is not clear; however, there is evidence that Rcor1 may be involved in the regulation of learning and memory. The first evidence came from nervous system HDAC2 knockout mice, which have enhanced learning and memory. HDAC2 is found primarily in three distinct multi-protein corepressor complexes: Sin3a, NuRD, and Rcor1 (Cunliffe, 2008). In a wildtype brain, HDAC2 and HDAC1 showed equal ability to bind the Sin3a, NuRD complex, but only HDAC2 showed binding ability to the Rcor1 complex. In HDAC2 knockout mice, HDAC1 showed increased binding to Sin3a and NuRD, but not Rcor1

(Guan et al., 2009). Therefore, knocking out of HDAC2 seems affect the function of Rcor1 complex more severely than other two cofactor complexes. It is possible that HDAC2 knockout may lead to derepression of Rcor1 targets but not to Sin3a and NuRD targets. This suggests that Rcor1 targets in the brain may be important for memory formation. In addition, in neurons Rcor1 can bind to neuronal plasticity genes, such as BDNF and Calbindin through interaction with the methyl CpG binding protein MeCP2, where it has been linked to activity-dependent regulation of gene expression during memory consolidation (Chen et al., 2003; Schoch and Abel, 2014). To study the biological function of Rcor1 in the brain, we first had Ozgene generate a mouse line that has the Exon 4 of Rcor1 flanked by LoxP sites.

Materials and methods

Mice

Floxed Rcor1 mice were generated by Ozgene, Inc. The targeting vector was constructed by inserting three fragments: a 5.6 kb 5' homology arm, a 0.8kb LoxP arm and a 4.7kb 3' homology arm into the Ozgene plasmid FLSniper. Between the LoxP arm and 3' homology arm, there is a PGK-Neo-pA-SD selection cassette for clonal selection. This cassette was flanked by flippase recognition target (FRT) sites. The targeting vector was electroporated into w9.5 embryonic stem cells. Following homologous recombination and selection with neomycin, the clonal ES cells containing $Rcor1^{flox\_neo/+}$ allele were injected into blastocysts to generate chimeric mice. These mice were crossed with C57BL/6J mice for germline transmission. The PGK-Neo cassette was deleted by

crossing *Rcor1*$^{flox\_neo/+}$ mice to the FLPe deleter strain in which FLPe was driven by the human ACTB promoter (The Jackson Laboratory, stock # 003800). Nervous system knockout of Rcor1 were generated by crossing *Rcor1*$^{flox/flox}$ mice to *Nestin-Cre* transgenic mice (The Jackson Laboratory, stock # 003771). *Rcor1*$^{+/-}$ mice were obtained by crossing *Rcor1*$^{flox/+}$ mice to *Meox2-Cre* transgenic mice (The Jackson Laboratory, stock # 003755) to recombine LoxP sites and remove exon 4 sequences in germ cells. *Rcor1*$^{+/-}$ mice were outcrossed from *Meox-Cre* transgene and backcrossed into C57BL/6J. The primers A3: 5'-atttgtgtcatgtgtcatgta-3' and B2: 5'- gggaagctcatctataggcaa-3' were used to distinguish Rcor1+ (1.1 kb) and Rcor1- alleles (350 bp). The primers A2: 5'-gtagttgtcttcagacactcc-3' and B2 were used to distinguish Rcor1flox (550 bp) and Rcor1+ alleles (400bp).

Constructs

The coding DNA sequence (CDS) of human Rcor1 has been clonied into pFL-Big vector with N-terminal flag tag previously in my mentor's laborotory.

Constructs pOBT-hRcor2 and pCMV-SPORT6-hRcor3 were purchased from Openbiosystem, and contain human Rcor2 and human Rcor3 complementary DNA (cDNA) sequences respectively. For the pCGN- hemagglutinin tag(HA)-hRcor2 construct, hRcor2 cDNA was PCR amplified from pOBT-hRcor2, digested with XbaI and Kpn1, and ligated to pCGN-HA vector (Mandel construct 510) pre-cut with XbaI and Kpn1.

For pCGN-HA-hRCor3, the N-terminus of human Rcor3 cDNA sequence was PCR amplified from pCMV-SPORT6-hRcor3, digested with XbaI and BspE1, and then ligated

to Mandel construct 510 (pCGN-HA-1434, missing N-terminal of hRcor3) pre-digested with XbaI and BspE1.

Cell culture

Human Embryonic Kidney 293T cells were maintained in Dulbecco's Modified Eagle Medium (DMEM) with 10% 10% fetal calf serum (FCS), 1% penicillinstreptomycin (Pen/Strep), and 1% L-glutamine and split every three days to keep the cell density under 90% confluence.

Rcor1-3 Antibodies

The rabbit polyclonal N-Rcor1 antibody was generated against the human Rcor1 N-terminal sequence "MVEKGPEVSGKRRGRN". The rabbit polyclonal P-71 antibody (in house (Ballas et al., 2005) and Millipore 07-455) and the mouse monoclonal antibody (NeuroMab, clone K72/8) both were generated against protein amino acids 109-293 of the human Rcor1 sequence. The rabbit polyclonal antibody against Rcor3 was generated in house with peptide: "KSTDEEEEAQTPQAPRTL".

The rabbit polyclonal antibody against Rcor2 was generated in Dr. Michael Rosenfeld's Laborotory at UCSD against protein sequence: "SAGSGILSRSRAKTVPNGGQPHSEDDSSEEEHSHDSMIRVGTNYQAVIPECKPES PARYSNKELKGMLVWSPNHCVSDAKLDKYIAMAKEKHGYNIEQALGMLLWHK HDVEKSLADLANFTPFPDEWTVED".

Western blot analysis

Cell or tissue samples were lysed in cold RIPA buffer (50 mM Tris•HCl pH 7.6, 150 mM NaCl, 1mM EDTA,1% NP-40, 1% sodium deoxycholate, 0.1% SDS) containing proteinase inhibitors (Roche) and 2mM NaVO3 and 10mM NaF. Samples were sonicated briefly to shear DNA. Protein concentration was measured with a BCA Protein Assay kit (Thermo Scientifc, Pierce). Blotting with primary antibodies was carried out at 4°C overnight followed by incubation with the appropriate infrared IRDye-labeled secondary antibodies for one hour. Membrane were scanned with Odyssey infrared imaging system (LI-COR). Kdm1A antibody (ab17721) and GAPDH antibody (ab9484) was from Abcam.

Frozen tissue sections

Mice were anaesthetized with an intraperitoneal injection of 0.5 ml 2% Avertin. They were transcadially perfused with PBS for 10 minutes, followed by PBS-buffered 4% paraformaldehyde for 15 minutes. Brains were further fixed in 4% paraformaldehyde overnight, cut into big pieces and cryopretected by immersion in 30% sucrose for one or two days. To freeze brain blocks, brains were first equilibrated in 1:1 of 30% sucrose and tissue freezing medium (TFM, Cat# TFM-5, TBS) for 30mins-1hr, then put into plastic molds and covered with TFM. The models were transferred onto dry ice sheet and pressed for a few minutes. When the whole block was frozen, tissue blocks were stored in -80°C or cut into 14μm- 20μm sections with cryostate at -22°C.

Immnuostaining

Brain sections were dried on a slide warmer (Thermo Fisher Scientific) at 65°C for two hours, then fixed in 3.7% formaldehyde for eight minutes. Antigen retrieval in antigen-

unmasking solutions (Vector laboratories, H-3300) was performed following the manufacturer's instructions. Cells were permeabilized in PBS-buffered 0.3% triton for 1-2 hrs, and then blocked for 1-2hrs with 0.3% triton containing 10% normal donkey serum (NDS) and 2.5% BSA. Sections were incubated in primary antibody diluted in 10% NDS/ 0.1% triton at 4°C overnight, followed by three 10 minutes-long wash with 0.1% Tween-20. Secondary antibody were diluted in 10% NDS/0.1% triton and applied to sections for 1 hour at room temperature, also followed by three 10 minutes-long wash with 0.1%Tween-20. To label neurons, slides were incubated with NeuroTrace® 530/615 red fluorescent Nissl stain (Life Biotechnologies) at RT for 30 minutes, which were diluted 200 times in 10% DNS. Slides were mounted with ProLong® Gold Antifade Reagent (with or without DAPI) (Life Biotechnologies). Primary antibody: mouse anti-Rcor1 monoclonal antibody (K72/8, NeuroMab, 1:500 dilution); Rabbit anti- Glial Fibrillary Acidic Protein (GFAP) antibody (Dako Cytomation, 1:500 dilution). Secondary antibody: Alex Flour® 594 donkey anti mouse IgG; Alex Flour® 488 donkey anti mouse IgG (Invitrogen); Alex Flour® 488 donkey anti Rabbit IgG (Invitrogen). Images were acquired at room temperature using Ziess Axiovert S-100 (Carl Zeiss) and AxioCam HRc camera, and processed with AxioVision Rel 4.8 (Carl Zeiss) and Photoshop (Adobe).

Hematoxylin and Eosin Staining of frozen sections

Frozen sections were placed in 95% ethanol for 5 minutes and rinsed with water. They were stained in Hematoxylin for 45s, then acid alcohol for one dips, ammonia water for 20 dips and 80% ethanol for 15 dips. Slides were rinsed with running tap H2O in between these steps. Slides were then stained in Eosin for 12 dips, followed by dehydration in

95% ethanol, 100% ethanol and finally Xylene. Slides were mounted with Permount toluene solution (Fisher Scientific).

Subjects

All mice used for behavior test were bred into the C57BL/6J background for two generations. Mice ranging in age from three to six month old were used in the experiments. Animals were allowed free access to laboratory chow and water during all experiments. Subjects were maintained on a 12-h light/dark cycle (lights on at 0600 h). All experiments were performed during the animal's light cycle, started at 12:00 pm ± 1 hour.

Mouse general activity test

All animals used in the experiment were handled for 1-2 minutes and brought in the experimental procedure room for 1 hour every day for 3 days before experiments. Locomotor activity was recorded for 30 min with a pinhole camera (Polaris USA Video, Inc. product EM100/E-3; Norcross, GA) mounted in the ceiling of a chamber (21.5×21.5×23cm). Velocity and distance travelled was analyzed using the EthoVision XT video tracking system (Noldus, Wageningen, Netherlands) (Stafford et al., 2012).

Contextual and cued fear conditioning

The contextual fear conditioning test apparatus were Plexiglas chambers (21.5×21.5×23cm) placed on a grid floor. Scrambled shock was delivered through the floor by a shock generator (Coulbourn Instruments product H24□61). An infrared activity monitor was fixed to the top of each chamber to record freezing. The whole

apparatus was placed inside a sound attenuating chamber, but the chamber was illuminated throughout the experimental session with a light. All animals used in the experiment were handled for 1-2 minutes and brought in the experimental procedure room for 1 hour every day for 3 days before the first contextual exposure. On the day of conditioning, mice were placed into the conditioning apparatus for 3 minutes in total. From 2 minutes to 2.5 minutes, a noise was provided and at 2 minutes 28s, a 2s 0.35mA scrambled foot shock was given. The test for the memory of context was performed 24h later by re-exposing the mice for 6 minutes to the conditioning context without noise or shock. The test for the memory of cued condition was performed by placing the mice in a new context for 6 minutes and with a noise at 2-5 minutes. Freezing behavior was defined as the absence of detected movement for at least 3 seconds and analyzed with colbourn fear conditioning v1.0. (Stafford and Lattal, 2009).

Statistical analysis

Statistical comparisons between two samples were made using student t- tests. Multiple-group comparisons were analyzed by a one-way ANOVA with Newman-Keuls post-hoc test in Prism 6 (GraphPad Software).

Results

Characterization of antibodies for Rcor1, 2, 3

Because there are three Rcor family proteins in both human and mouse, it is important to have tools to distinguish them. In our laborotory, one antibody against Rcor3 and three antibodies against Rcor1 have been generated: N-Rcor1, p71 antibody, and a mouse

monoclonal antibody. An antibody against Rcor2 has been generated in Dr. Michael Rosenfeld's Laborotory at UCSD. We expect these antibodies to detect both human and mouse proteins, because the peptides used to generate antibodies were about highly identical between the two species.

To test the specificities of these antibodies, I first transfected HEK 293T cells with full length human Rcor1, Rcor2 or Rcor3 constructs. The hRcor1 construct has an N-terminal Flag tag, whereas the hRcor2 and hRcor3 constructs have single N-terminal HA tags. Two days after transfection, whole cell lysate was prepared and western blot analysis was performed with different Rcor and epitope antibodies. As shown in Figure 2.1, Rcor1 monoclonal antibody and N-Rcor1 antibody detected Flag-hRcor1 and endogenous Rcor1 in the 293T lysates. P71 supernatant detected both Rcor1 and Rcor3. Anti-Rcor2 and Rcor3 antibodies were specific to their targets. These results ensured that I had the right antibodies to monitor the Rcor1, 2 and 3 expression levels.

Generation of *Rcor1* knockout mice

To study Rcor1 function *in vivo*, we decided to use the Cre-Lox system to knock out Rcor1 in the mouse. This system is useful because depending on which Cre recombinase-expression mice line I use, Rcor1 can be knocked out in different tissues or at different time points. Ozgene Inc helped us to generate a $Rcor1^{flox/flox}$ mouse line, in which exon 4 of *Rcor1* gene is flanked by loxP sites (Figure 2.2). Removal of exon 4 by Cre recombinase will result in a premature stop codon and consequently a 52 amino acid long peptide, which is not known to have any particular function.

To study Rcor1function in the nervous system, Tamilla Nechiporuk, a postdoctoral fellow in the lab, initiated generation of both a global knockout (also called germ line knockout) line and a nervous system specific knockout line. By comparing the phenotypes of these two knockouts to control mice, I should reveal clear roles of Rcor1 in the nervous system and outside the nervous system. Germ line knockout of Rcor1 was generated with a *Meox2-Cre* line, in which expression of Cre recombinase is observed in epiblast-derived tissues as early as embryonic day 5, including the primordial germ cells. Subsequently, she bred the Meox2-Cre away from the recombined Rcor1allele ($Rcor1^{-}$) and intercrossed $Rcor1^{+/-}$ mice to generate global knockouts. To obtain nervous system Rcor1 knockouts, she crossed the $Rcor1^{flox/flox}$ mice with a *Nestin-Cre* line, where the Cre recombinase is expressed in Nestin expressing neural progenitor cells by embryonic Day 11 (Zimmerman et al., 1994). While Cre recombinase activity is very strong in the nervous system, it is already known that Nestin promoter can also express in other tissues postnatally, such as kidney and lung (The Jackson Laboratory).

Depletion of Rcor1 in the brain does not affect brain development

Given previously proposed functions for Rcor1 in neuron differentiation, I expected to see developmental defects in the nervous system in *Nestin-Cre,* $Rcor^{fl/fl}$ mice compared to controls. However, neither knockouts showed consistent developmental defects in the brain. The global Rcor1 knockouts were embryonic lethal around embryonic day 16.5 due to anemia (further described in Chapter 3). However, their heads and brain appeared normal at E13.5. A very small number of E13.5 global Rcor1 knockout embryos had deformed heads or were missing one eye, but the frequency was so extremely low that I

did not pursue that phenotype. *Nestin-Cre*, *Rcor1*$^{flox/flox}$ mice were born in Mendelian Ratio, and by eyes could not be distinguished from their litter mates. I observed no obvious change in brain anatomy (Figure 2.3) or in body weight (Figure 2.4).

I attribute the lack of distinguishable phenotypes to one of three possibilities: 1) Rcor1 does not play a role in neural development; 2) knockout of Rcor1 is incomplete 3) other Rcor family proteins compensated for Rcor1 function. To investigate the second possibility, I used Western blot analysis to detect the expression levels of Rcor1, 2 and 3 in both of these Rcor1 knockouts. As shown in Figure 2.5, Rcor1 and Rcor2, but not Rcor3, were expressed in the control E13.5 brain. In *Rcor1*$^{-/-}$ mice, I observed a total loss of Rcor1 but no change of Rcor1 expression level. This observation was consistent with the third possibility that Rcor2 may be able to compensate Rcor1 function in the developing brain. To test that hypothesis, I started to generate Rcor1 and Rcor2 double knockout. Because both germ line Rcor1 and Rco2 knockouts were embryonic lethal, I used *Nestin-Cre* line to knockout Rcor1 and Rcor2 in the nervous system. *Nestin-Cre, Rcor2*$^{flox/flox}$ mice were provided by Dr. Michael Rosenfeld's Laborotory at UCSD. *Nestin-Cre, Rcor2*$^{flox/flox}$ mice were smaller than their little mates. Interestingly, *Nestin-Cre*, *Rcor1*$^{flox/flox}$, *Rcor2*$^{flox/flox}$ mice die around birth with a smaller brain. These observations suggested that Rcor2 do compensate Rcor1 function during embryonic brain development. Another graduate student in our laborotory is currently further characterizing the double knockout mouse phenotype because I chose to focus on the strong hematopoietic phenotype in the global knock out mouse (Chapter 3).

To examine Rcor1, 2 and 3 expression levels in the adult brain, Western blots were performed on extracts from several brain regions from three-month old adult mice. As shown in the Figure 2.6, when equal amounts of total protein were loaded per lane, I observed ubiquitous expression of Rcor1 throughout the control adult brain., However Rcor1 is mostly absent from the *Nestin-Cre*, *Rcor1*$^{flox/flox}$ brain, with a low level of Rcor1 detected in olfactory bulb. In other brain regions, such as the cortex and hippocampus, Rcor1 levels were barely detectable. This low level of residual Rcor1 expression could be explained by incomplete deletion of Rcor1. However, Rcor1 will still be expressed in non-neural-progenitor-derived cells in the brain, such as endothelia cells and microglial cells, which are more likely to be the sources of residual Rcor1. This could be tested by immunostaining with markers specific for the different non-neuronal cell types. Interestingly, no Rcor2 and Rcor3 proteins can be detected in the adult brain, indicating they are not required for adult brain function.

In conjunction with Western blotting, immnuostaining was used to exam the expression pattern of Rcor1 and to confirm the depletion of Rcor1 from neurons in the *Nestin-Cre*, *Rcor1*$^{flox/flox}$ brain. I observed clear expression of Rcor1 in neurons in control brains, which were counter labeled with NeuroTrace. While only staining in cortex and hippocampus are shown (Figure 2.7), Rcor1 is expressed throughout the entire brain, consistent with our western blotting results. Importantly, although Rcor1was readily detected in control mice, it was absent from the *Nestin-Cre*, *Rcor1*$^{flox/flox}$ brain. I also noticed that Rcor1 expression in glial cells seemed to be much lower than in neurons, with staining signals that were only slightly detectable above background (Data not

shown). In contrast, Rcor1 protein was detected in cultured wild type astrocytes from P0 brain (Figure 2.8), however, more analysis need to be done *in vivo*.

Previously, Rcor1 knock down by shRNA was shown to affect Kdm1a stability (Shi et al., 2005). To test if it is true in the Rcor1 knockout mouse brain, I performed western blot analysis and found that depletion of Rcor1did not affect the expression of Kdm1a in the brain (Figure 2.9). However, in the liver and spleen Lsd1 level slightly decreased, indicating different regulatory mechanisms in different tissues.

Because Rcor1 appears to be the only Rcor protein expressed in the adult mouse brain, I decided to investigate its functions there. However, as shown by Western blot and immunostaining analysis, Rcor1 expression is ubiquitous throughout the brain, which makes it hard to predict its function based on expression pattern. We therefore did a few basic analyses based on previously published functions of Kdm1a or HDAC1/2, two key components of the Rcor1 complex. At that time, one interesting hypothesis was that loss of Rcor1 complex activity in HDAC2 knockout mice was responsible for observed improvement in learning and memory. If this was correct, the *Nestin-Cre*, *Rcor1*$^{flox/flox}$ mice should show improved memory assessed by fear conditioning test. Because general activity levels can obscure fear conditioning test results, I first determined the general activity level of Rcor1 knockout mice. As shown in Figure 2.10, no obvious differences in moving distance, moving duration, or velocity were observed between *Nestin-Cre*, *Rcor1*$^{flox/flox}$ mice and control groups. Since general activity level appeared unchanged, I could now safely perform the fear conditoning test.

The fear conditioning test consisted of several steps. On the first day of conditioning, mice were placed into the conditioning apparatus for a total of 3 minutes. From 2 minutes to 2.5 minutes, a noise was provided and at 2 minutes 28s, a 2s 0.35mA scrambled foot shock was given. To test for memory of the conditioning context, mice were placed into the same apparatus 24h later for 6 minutes without noise or shock. To test for the memory of cued condition (the noise), mice was placed in a novel context for 6 minutes and subjected to a noise from minutes 2-5. Freezing behavior was defined as the absence of detected movement for at least 3 seconds (Stafford et al. 2009). The test showed that all the experimental mice remembered the shock when they were put into the same context that they received the shock. They also remembered the noise that was associated with the shock. However, there was no difference between control, heterzygous and homozygous mutant (Figure2.11), indicating that Rcor1 knockout had no effect on the learning and memory as assayed by this fear conditioning test.

Discussion

In this chapter, I studied Rcor1 function during nervous system development using both a global and conditional knock out of Rcor1. To my surprise, no obvious defect was observed. Consistent with these results, when Rcor1 was knocked down by in utero electroporation in the embryo brains, migration of cortical neurons was only temporarily blocked and no major differences can be observed three days after knockdown of Rcor1 (Fuentes et al., 2012). The results taken together with my results indicate that other mechanisms can compensate decrease of Rcor1. Therefore, I surmise that the Rcor proteins do play an important role in brain development; however, Rcor2 compensates

Rcor1's function in this process. Interestingly, Rcor2 single knockout mice are smaller than their control littermates, suggesting Rcor2 has its own unique function. Further characterization of Nestin-Cre, Rcor1 single knockout, Rcor2 single knockout and Rcor1/Rcor2 double knockout should be able to tease out the unique roles of Rcor2 vs common role for Rcor1 and 2. These studies are being carried out by another graduate student in the lab, Caitlin Monaghan.

In contrast to embryonic brain, western blot analysis from whole cell lysate showed that Rcor1 was the only Rcor protein expressed in the adult brain. Neither Rcor2 nor Rcor3 overexpression was observed in the Rcor1 knockout brains, therefore, it is unlikely that they can compensate the Rcor1's function. Because the adult brain is primarily populated with post-mitotic, terminal differentiated neurons and glial cells, which constantly integrate and response to internal and external stimuli, transcriptional regulation with epigenetic modification in the adult brain is more likely to be activity dependent. Activity dependent gene regulation in neurons is the best understood in the context of regulation of HATs and HDACs (Peixoto and Abel, 2013). Because histone deacetylation is a key negative regulator of hippocampal gene expression during memory consolidation, I tested whether mice depleted with Rcor1 are responsible for the improved learning and memory observed in the HDAC2 knockout mice (Guan et al., 2009). I chose the fear conditioning test because it has been used to demonstrate that HDAC2 knockout mice have better learning and memory than control mice. However, I didn't observe any difference between control and knockout mice. Even though we observed no change, I cannot completely rule out the potential role of Rcor1 in regulating learning and memory. First,

mice background has been shown to affect behavior test results (Bailey et al., 2006). The mice that I used for behavior tests had mixed background of C57BL/6J and 129; therefore it is possible that variation caused by mixed background masks the effect caused by knocking out of Rcor1. Future tests with C57BL/6J background mice should resolve this issue. Second, different behavioral paradigms require the functions of different brain regions. The fear conditioning test is usually used to test the hippocampus and amygdala dependent learning and memory (Maren, 2001). The fact that there is no change in this test does not rule out the possibility that Rcor1 is required for other types of learning and memory.

Because our central hypothesis is that Rcor1 plays a role in activity dependent transcription regulation in adult brain, it may affect other types of behavior, not just learning and memory. For example, drug habituation is another form of adaptive behavior that requires activity dependent gene regulation. Rcor1 may be involved in this process through interaction with NAC1, which was initially isolated from the nucleus accumbens of the rat a structure in the mammalian forebrain that influences the response to addictive drugs (Korutla et al., 2007). However, NAC1 is widely expressed in both neuronal and non-neuronal tissues. Therefore, without test, it is hard to know whether Rcor1 truly has a function in drug addiction.

Overall, much literature on Rcor1 focuses on identifying catalytic and transcription factor binding partners, however the impact of these interactions on biological processes is frequently not clear. The Rcor1 knockout mice model is a great tool to study the *in vivo* function of Rcor1 complex.

Acknowledgements

I thank Jennifer Miller, Travis Polston and Andrea Ansari for mouse genotyping and animal care; Tamilla Nechiporuk for initially generating Rcor1 global knockout mice and *Nestin-Cre* conditional knockout mice model.

Figures and legends

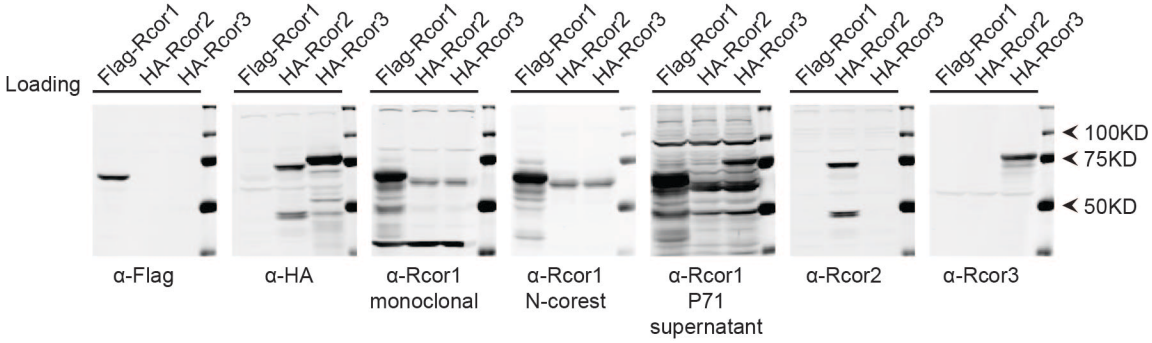

Figure 2.1 Characterization of the the Rcor antibodies. HEK293 cells were transfected with constructs containing Flag-hRCor1, HA-hRcor2 or HA-hRcor3. Two days after transfection, cells were harvested for Western Blot analysis. Antibodies used for each blot are labelled at the bottom, whereas sample names are indicated at the top of each lane. Anti (α)-Rcor1 monoclonal antibody and N-Rcor1 antibody detected both Flag tagged hRcor1 (lane1) and endogenous hRcor1 (lane2 and lane3) in 293T cells. p71 antibody supernatant detected both Rcor1 and Rcor3 protein. Anti-Rcor2 and Rcor3 antibodies had high specificity.

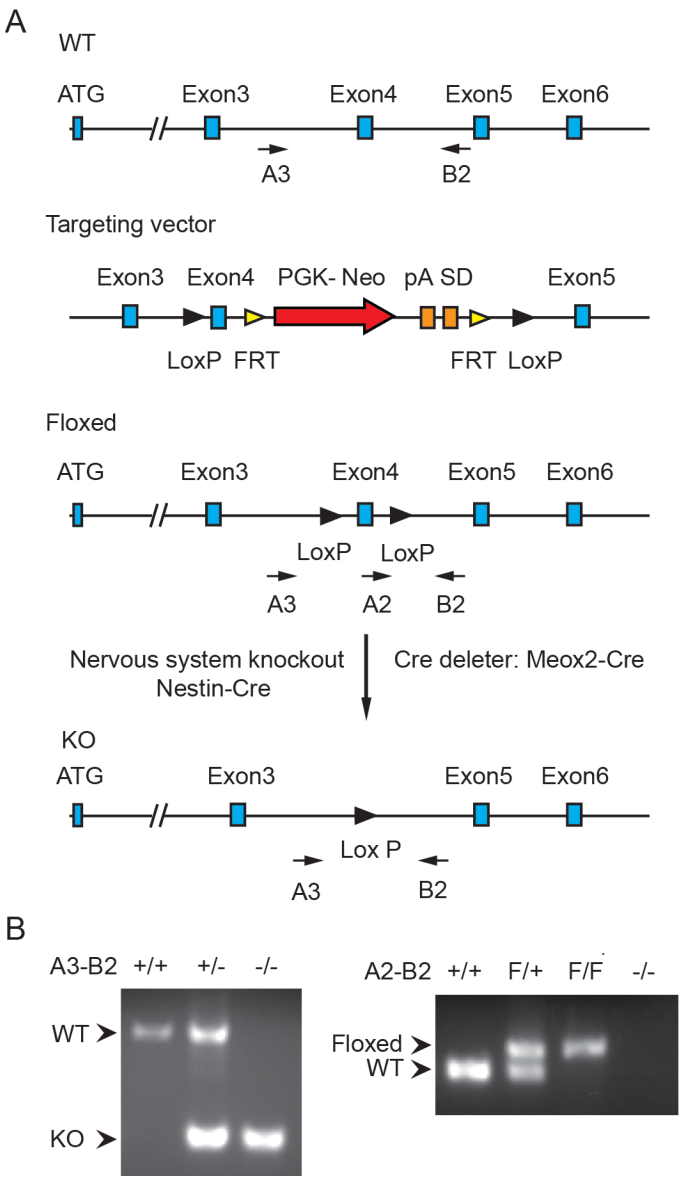

Figure 2.2 Generation of Rcor1 knockout mice. (A) Gene targeting strategy for the *Rcor1* locus: Illustration of the wild type (WT) $Rcor1^{+}$ allele, targeting vector, $Rcor1^{flox}$ allele (Floxed) and mutant $Rcor1^{-}$ allele (KO). $Rcor1^{flox/+}$ mice were crossed with *Meox2-Cre* and subsequently outcrossed to obtain $Rcor1^{+/-}$ mice. Nervous system knockout was generated by crossing $Rcor1^{flox/flox}$ mice with a *Nestin-Cre* mice line. FRT, flippase recognition target sites; PGK-Neo, neomycin resisance cassette; pA, polyadenylation site;

SD, splice donor. Arrows indicate positions of the A3, A2 and B2 genotyping primers. (B) Left panel: PCR analysis with primers A3 and B2 to resolve wild type and mutant Rcor1 alleles (KO) in E13.5 embryos. Right panel: PCR analysis with primers A2 and B2 to resolve wild type and floxed (F) Rcor1 allele in E13.5 embryos.

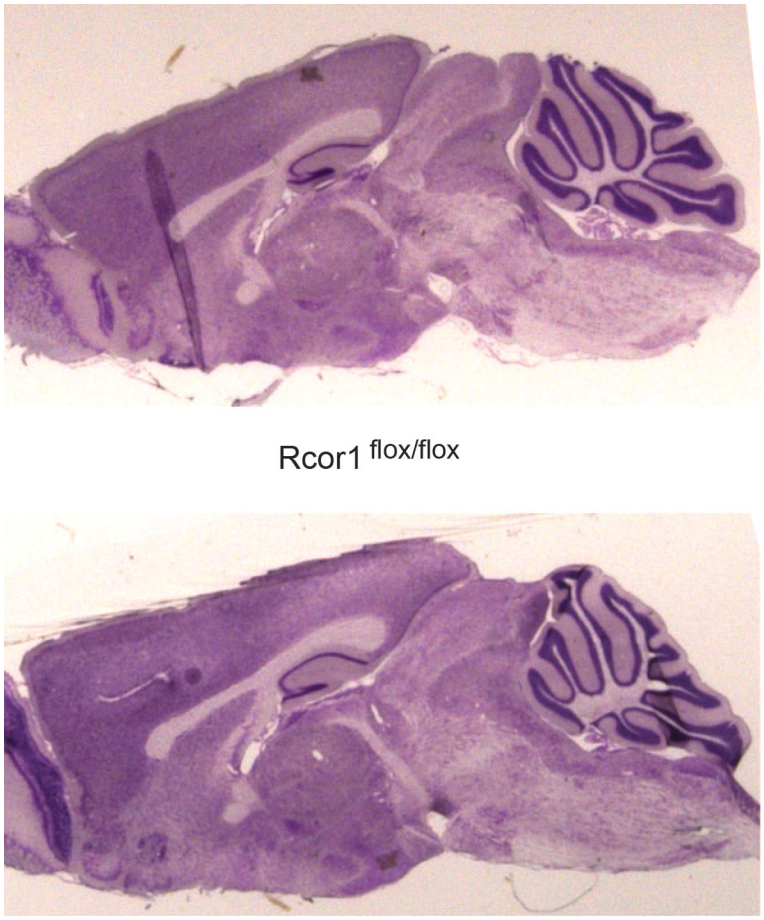

Figure 2.3 Morphological comparisons between *Nestin-Cre, Rcor1*$^{flox/flox}$ brain and control *Rcor1*$^{flox/flox}$ brain. Sagittal sections are shown here with rostral end on the left and caudal end on the right. No obvious change was observed.

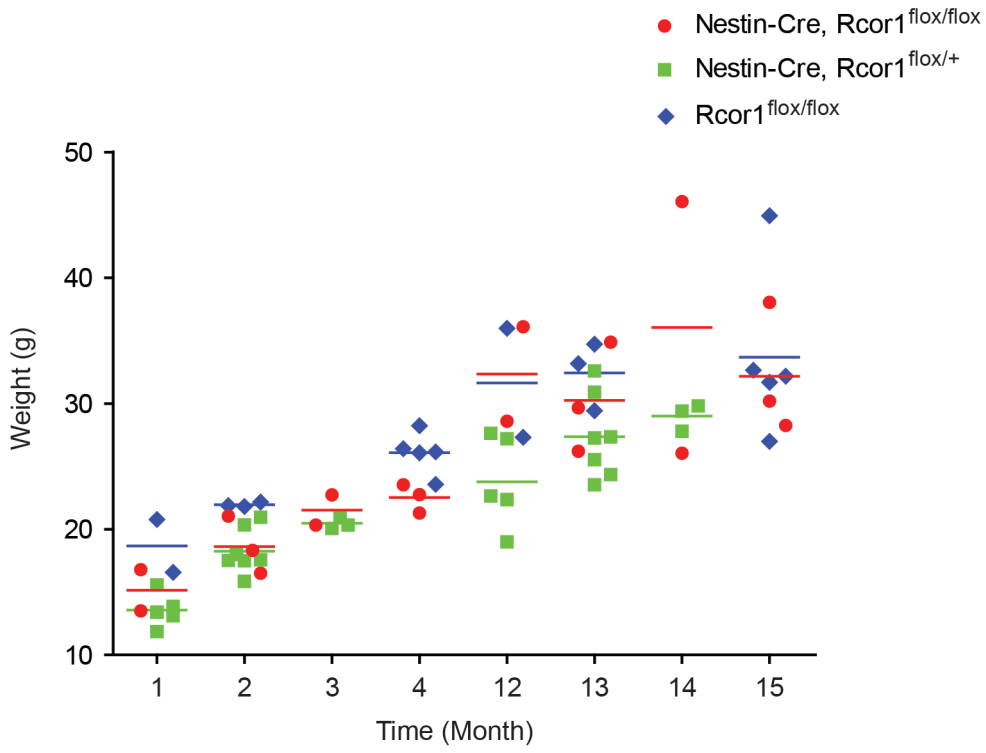

Figure 2.4 Body weight comparisons between *Nestin-Cre, Rcor1*$^{flox/flox}$ mice and litter mate controls. No significant changes in body weight were observed.

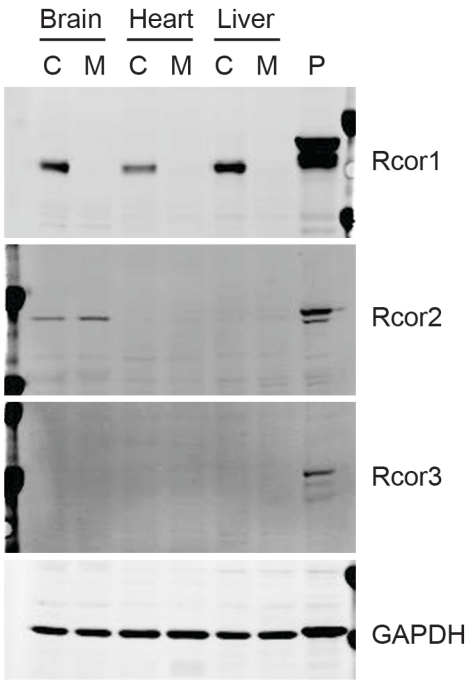

Figure 2.5 Expression levels of Rcor1, 2 and 3 in embryonic tissues. Tissue lysate was prepared from E13.5 embryos. C, control, *Rcor1*$^{+/+}$ embryo; M, mutant, *Rcor1*$^{-/-}$embryo. P, positive control, 293T cell lysate transfected with Flag-hRcor1, HA-hRcor2 and HA-hRcor3 constructs, respectively. GAPDH was used as loading control.

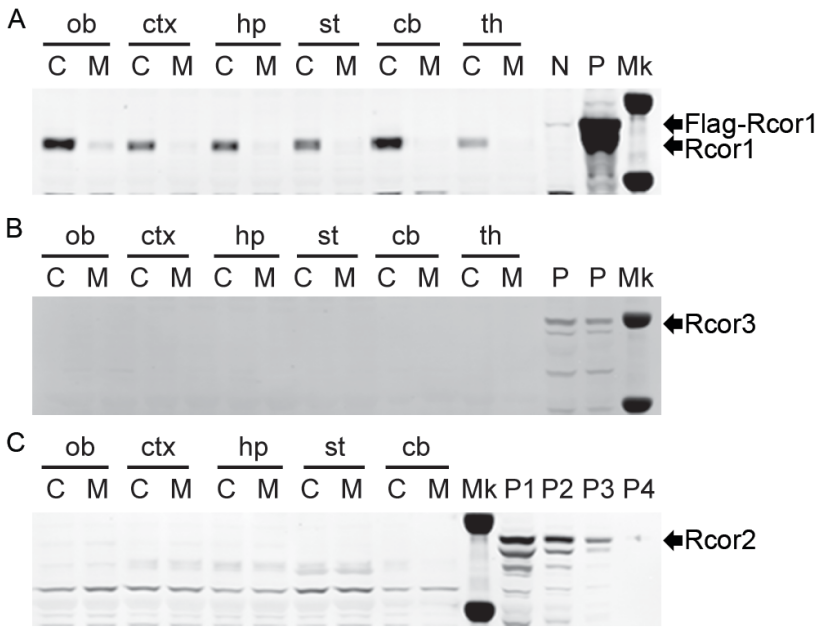

Figure 2.6 Rcor1-3 expression levels in adult brain. Cell lysate prepared from three-month old brain. M, mutant, *Nestin-Cre, Rcor1*$^{flox/flox}$ mouse; C, control, *Rcor1*$^{flox/flox}$ mouse; ob, olfactory bulb; ctx, cortex; hp, hippocampus; st, striatum; cb, cerebellum; th, thalamus. (A) Western blot analysis with Rcor1 antibody. N (negative control), *Rcor1*$^{-/-}$ tissue lysate; P (positive control), 293T cells transfected with Flag-Rcor1 construct. (B) Western blot analysis with anti-Rcor3 antibody. P (positive control), 293T cells transfected with HA-Rcor3 construct. (C) Western blot analysis with anti-Rcor2 antibody. P1-4 (positive control), 293T cells transfected with HA-Rcor2 construct. The total protein loaded for P1-4 is 30, 10ug, 3ug, 0.3ug, respectively. Mk, protein marker. Upper band, 75KD; Lower band, 50KD.

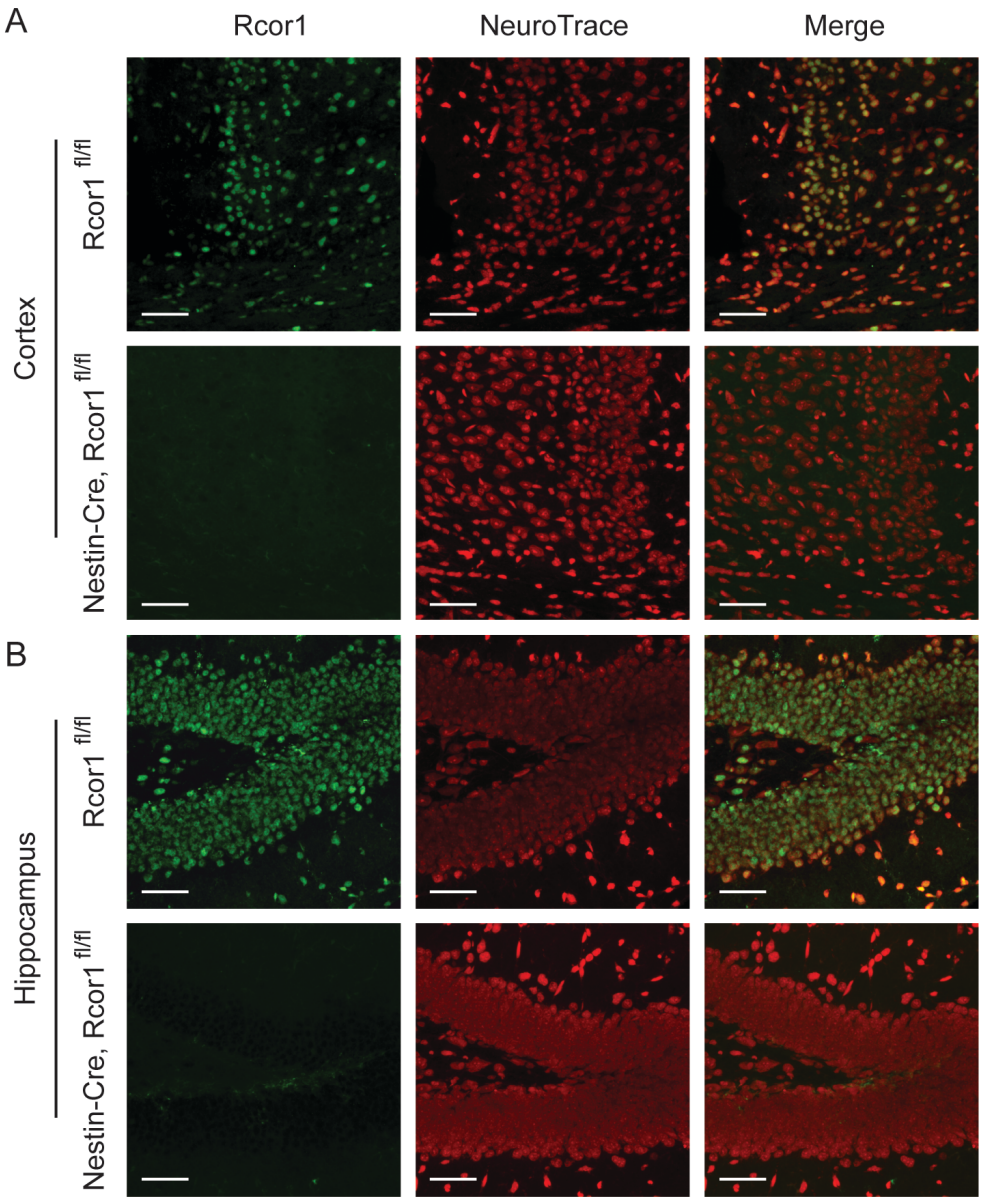

Figure 2.7 Immunostaining of Rcor1 in the adult mice brain. Rcor1 can be detected in *Rcor1*$^{flox/flox}$ mouse brain but not in *Nestin-Cre, Rcor1*$^{flox/flox}$ mouse brain. Staining in (A) Cortex and (B) Hippocampus are shown. Scale bar, 50μm.

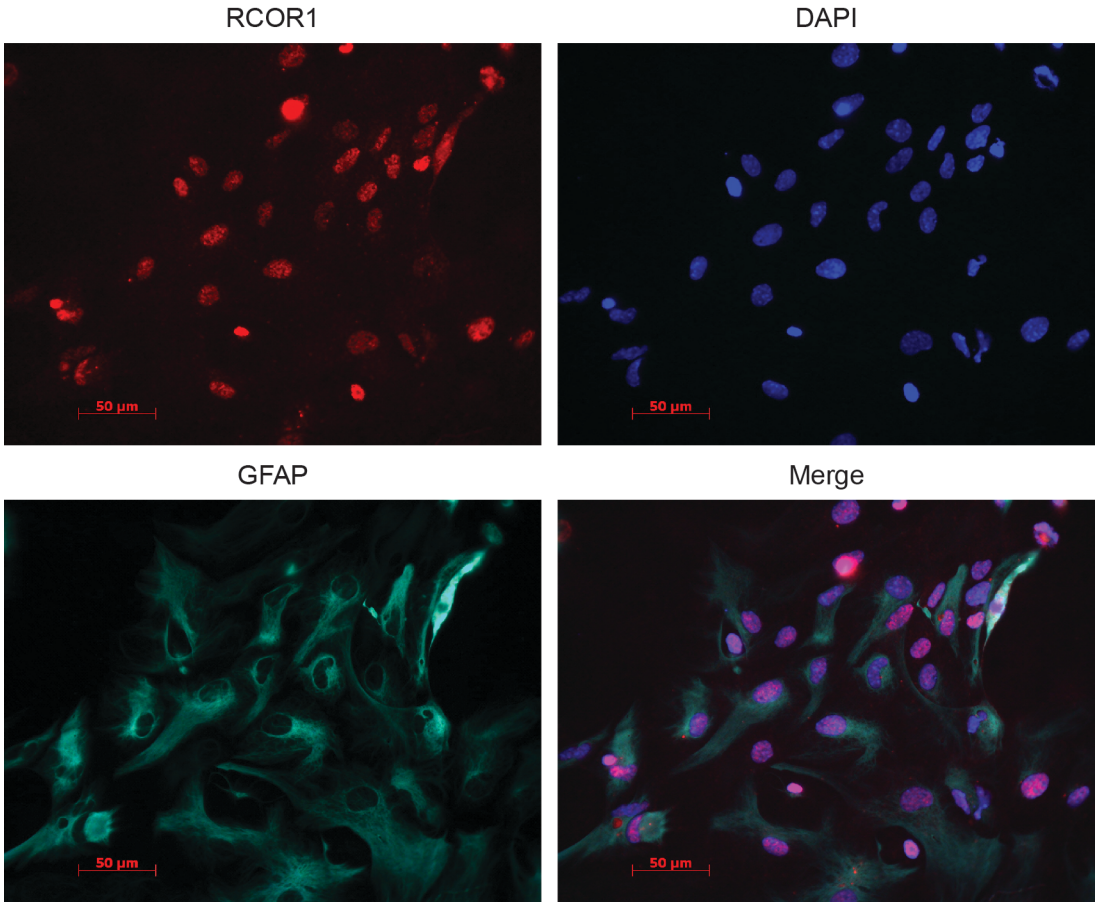

Figure 2.8 Immunostaining of Rcor1 in cultured wild type astrocytes. DAPI was used to label nuclei. GFAP is astrocyte marker.

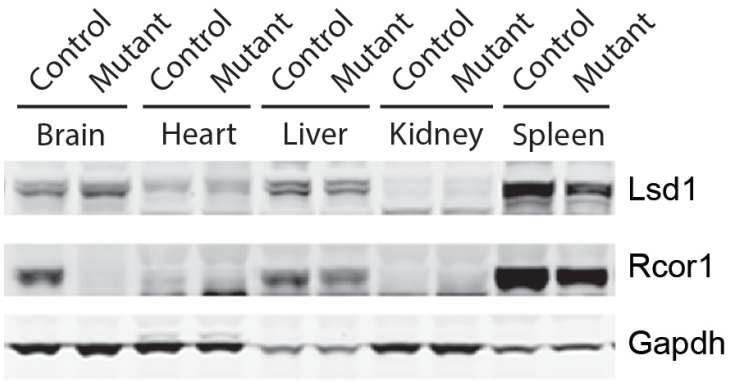

Figure 2.9 Rcor1 and Kdm1a protein levels in adult tissues. Tissues lysate from three-month old mice was used. Gapdh was used as a loading control. Control, *Rcor1*$^{flox/flox}$ mouse; Mutant, Nestin-Cre, *Rcor1*$^{flox/flox}$ mouse.

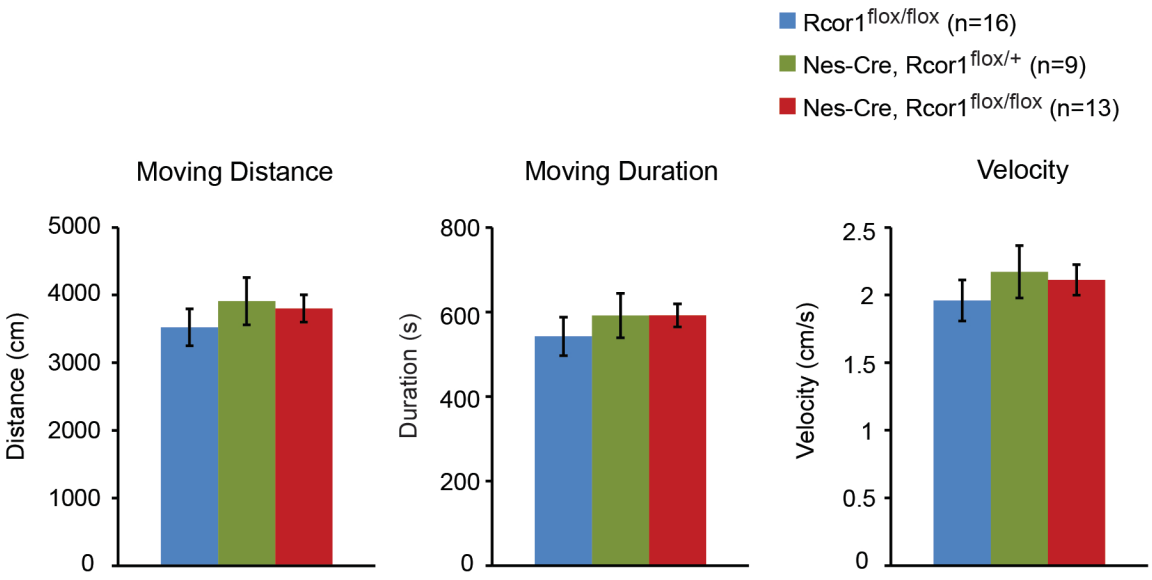

Figure 2.10 Comparison of the general activity levels between *Nestin-Cre, Rcor1$^{flox/flox}$* mice and their littermate controls. Mean and the standard error of the mean (SEM) are shown here. There was no significant change between different groups.

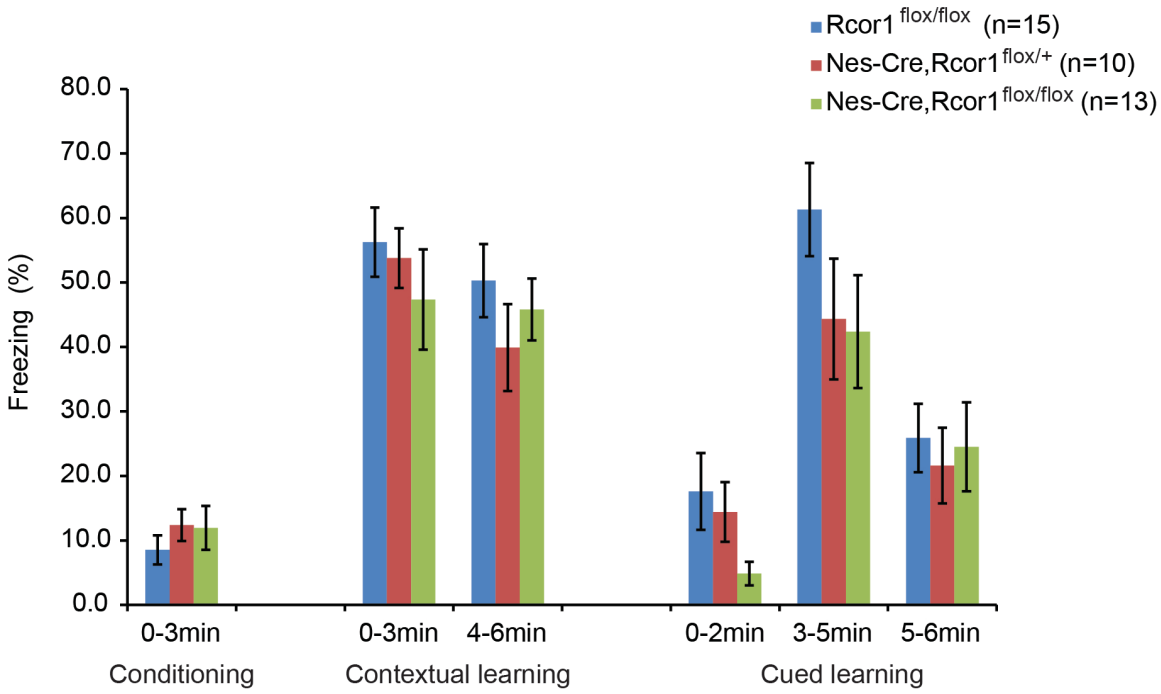

Figure 2.11 Test of learning and memory by contextual and cued fear conditioning tests. No significant difference was observed between Nestin-Cre, *Rcor1*$^{flox/flox}$ mice and their littermate controls.

CHAPTER 3: The co-repressor Rcor1 is essential for murine erythropoiesis

(Reprinted from Yao et al., *Blood*. 2014; 123(20):3175-84.)

Introduction

Histone modifications, and their deregulation, have been implicated in many hematological disorders, including severe anemia, myelodysplastic disorders and leukemias.(Kelly et al., 2010; Kiefer et al., 2008) Furthermore, inhibitors of the enzymes that catalyze histone modifications, histone deacetylases (HDACs) and demethylases, have been used in the clinic.(Kelly et al., 2010). For this reason, considerable effort has been invested in determining the roles of chromatin modifiers throughout hematopoiesis. The specificity of these modifiers, however, is conferred by transcription factors and their co-factors.

A predominant co-factor in cells is Rcor1 (also called CoREST). Rcor1 is present in complexes containing several chromatin modifiers associated with transcriptional repression, including the histone3 lysine4 demethylase, Kdm1a, which binds to Rcor1 directly,(Yang et al., 2006) and HDACs.(Humphrey et al., 2001; Lee et al., 2005) Proteins with chromatin binding properties, such as the High Mobility Group protein 20b (Hmg20b), are also present.(Hakimi et al., 2002) A potential role for Rcor1 in red blood cell (RBC) development has been suggested by the interaction of Rcor1 and Kdm1a with Gfi1b,(Saleque et al., 2007) a member of the Gfi zinc-finger transcriptional repressors, which is essential for erythropoiesis.(Saleque et al., 2002) However, in Kdm1a knockout mice, erythropoiesis is impaired(Kerenyi et al., 2013) while knock down of another Rcor1 cofactor, Hmg20b, promotes terminal differentiation of both a mouse fetal liver cell line (I/11) and primary fetal liver proerythroblasts.(Esteghamat et al., 2011) Similarly, HDACs both inhibit the growth of early erythroid precursors and promote erythropoietin-

mediated differentiation and survival of erythroid precursors.(Yamamura et al., 2006) These seemingly contradictory results likely reflect recruitment of the histone modifying enzymes through different co-repressors. To begin to dissect this complexity, we have determined the role of Rcor1 function *in vivo*.

Materials and methods

Mice

Rcor1$^{flox/+}$ mice were generated by Ozgene, Inc (details in materials and methods, Chapter 2). and crossed to *Meox2-Cre* transgenic mice (The Jackson Laboratory, stock# 003755) to create *Rcor1*$^{+/-}$ mice. *Rcor1*$^{flox/+}$ and *Rcor1*$^{+/-}$ mice were backcrossed with C57BL/6J for at least ten generations. *Mx1-Cre* mice (The Jackson Laboratory, stock# 003556) were used to generate *Mx1-Cre; Rcor1*$^{flox/-}$ embryos. The primers A3: 5'-atttgtgtcatgtgtcatgta-3' and B2: 5'- gggaagctcatctataggcaa-3' were used to distinguish *Rcor1*$^{+}$ (1.1 kb) and *Rcor1*$^{-}$ alleles (350 bp). The primers A2: 5'-gtagttgtcttcagacactcc-3' and B2 were used to distinguish *Rcor1*^{flox} (550 bp) and *Rcor1*$^{+}$ alleles (400bp).

Flow cytometry analysis and cell sorting

Cells from mechanically dissociated E13.5-E15.5 fetal livers were pre-incubated with mouse Fc block, stained with CD71-FITC, TER119-PE and propidium iodide (PI) and either analyzed with a LSRII (BD biosciences), or sorted with an Influx cell sorter (BD biosciences) for making RNA-seq libraries. To isolate R1 (Lineage^{-}, CD71^{low}) and R2 (Lineage^{-}, CD71^{hi}) cells for colony forming assays, cells were stained with CD71-FITC, a lineage cocktail (TER119, Gr1, Mac1, B220, CD3, CD4 and CD8)-PE and PI and sorted

with an Influx cell sorter. To analyze CMP, GMP and MEP, single cell suspensions were stained on ice for 1hr with IL-7Rα-PE, Lineage panel (B220, CD3, CD4, CD8, Gr1, Ter119, CD19, IgM) -PE, Sca1-PE, C-kit-APC, CD34-FITC, CD16/32-PE/Cy7. To detect Csf2rb expression on Pre-CFU, CFU-E and Pro Ery, single cell suspensions were stained in Brilliant Stain Buffer (BD Horizon™) on ice for 30mins with a lineage cocktail (CD4, CD5, CD8, B220, Gr1, Mac1, Sca-1, CD16/32, CD41)-FITC, CD131-PE, CD71-PECY7, CD105-APC, Ckit-APC-H7, CD150-BV421, TER119-BV650. Cells were analyzed with a BD Fortessa cell analyzer. Pre-CFU, CFU-E and ProEry cells were identified as previously described. Data were analyzed using FlowJo (Tree Star, Inc)..

Flow cytomertry antibody clones

CD71 (R17217), Mac1 (M1/70), Gr1 (RB6-8C5), CD3 (145-2C11), B220 (RA3-6B2), C-kit-APC (2B8), CD16/32 (93), IgM (eB121-15F9) all eBioscience; CD4 (H29.19), CD8 (53.6.7), CD16/32 (2.4G2), CD131 (JORO50), CD34 (RAM34), CD19 (1D3), CD5 (53-7.3), Ckit-APC-H7 (2B8,) TER119-BV650 all BD Pharmingen; TER119-PE, IL-7Rα (A7R34), Sca1 (D7), CD41 (MWReg30), CD105 (MJ7/18), CD150-BV421 (TC15-12F12.2) all Biolegend.

***In vitro* colony forming assay**

FACS-sorted R1 (Lineage-, CD71low) and R2 (Lineage-, CD71hi) fetal liver cells were plated in triplicate in mouse methylcellulose complete medium (R&D systems, HSC007) according to the manufacturer's protocol. 500 R1 cells or 5000 R2 cells were plated for each sample. CFU-E colonies were counted at Day3. BFU-E, CFU-G, CFU-M and CFU-

GM were counted at D7, CFU-GEMM were counted at D12. To confirm CFU-GEMM identity, benzidine (Sigma) staining solution was added in each plate and stained for 5 minutes before counting. Mouse interferon alpha (R&D Systems,) and JAK2 inhibitor TG101384 (Selleckchem) were used at 1000U/ml and 500nM, respectively.

Cytospin preparations

10,000-50,000 fetal liver cells or individual colonies were cytospun onto slides for 5 minutes at 500rpm using a Cytospin3 (Thermo Shandon) and air-dried.

Fetal liver transplantation and engraftment analysis

To evaluate engraftment of the red cell compartment, donor CD45.2 Hbbs cells were transplanted into double congenic CD45.1 Hbbd recipients maintained in an SPF facility at OHSU. Recipients were irradiated with 500cGy using an RS2000 Xray irradiator (Rad Source). Immediately following irradiation, each mouse was infused intravenously with 2x106 fetal liver cells. After four and 12 weeks, peripheral blood leukocytes were obtained after erythrocyte depletion by sedimentation in 3% dextran (Amersham Pharmacia) and hypotonic lysis. Multi-lineage hematopoietic engraftment was analyzed with antibodies to CD45.1 (A20, eBioscience) conjugated to PE or PE-Cy7 and CD45.2 (104,eBioscience) conjugated to FITC, and the lineage markers Mac1-PE, Gr-PE, B220-PE and CD3-PE, as previously described.2

Hemoglobin electrophoresis

Hemoglobin electrophoresis was performed as described.3 Briefly, peripheral blood was lysed, the hemoglobin in lysate was separated on a cellulose acetate plate (Helena Laboratories, Beaumont, TX) and stained with Ponceau S.

Fetal liver erythroid progenitor cell separation

Erythroid progenitors were enriched from mouse E13.5 or E14.5 fetal liver by depleting mature erythrocytes and differentiated nonerythroid cells, according to a protocol kindly provided by the Lodish laboratory (Boston) and described in (Zhang et al. 2003). Briefly, single cell fetal liver suspension was incubated with chromPure Rat IgG (Jackson ImmunoResearch), Ms Lineage Panel (Fisher Scientific) containing biotin conjugated TER119, Mac1, Gr1, CD3 and B220. After washing, the biotin -labeled cells were depleted with Streptavidin Particles Plus - DM and cell separation magnet (BD Biosciences) according to the manufacturer's protocol.

To further enrich the R2 population, TER119- cells were incubated with FITC-conjugated CD71 antibody followd by anti-FTIC Microbeads (MACS Miltenyi Biotec). CD71+ cells were isolated by passage over a MACS MS column according to the manufacturer's protocol.CSF2 stimulation

Approximately one million purified control and mutant cells were incubated in basal medium (IMDM, 10% FBS, 100U/ml penicillin/streptomycin and 2mML-glutamine) at 37°C for one hour. To stimulate the cells, recombinant murine CSF2 (50ng/ml PeproTech) or DMSO was added and the cells incubated at 37°C for 15 mins. The cells

were collected by centrifugation and then resuspended in SDS-PAGE buffer immediately to lyse the cells.

Western blot analysis

To detect protein expression, tissues were lysed in cold RIPA buffer containing proteinase inhibitors (Roche). To detect phosphorylation of proteins, cells were lysed in SDS-PAGE buffer (62.5mM Tris ph 6.8, 10% Glycerol, 2% SDS) containing proteinase inhibitors (Roche) and 2mM NaVO3 and 10mM NaF. Antibodies to Jak2 (#3230), Stat5 (#9363), phospho-Stat5(#9351) were from Cell Signaling. Actin antibody (JLA20) was from DSHB. GAPDH antibody (ab9484) was from Abcam.

Immunostaining

FACS-sorted cells were fixed with 4% formaldehyde for 10 minutes, spun onto slides and dried overnight. Cells were then fixed in 4% formaldehyde for eight minutes. Antigen retrieval in antigen-unmasking (Vector laboratories, H-3300) was performed following the manufacturer's instructions. Cells were permeabilized in 0.3% triton, and then blocked with 10% normal donkey serum and 2.5% BSA. Mouse anti-CoREST1 monoclonal antibody (K72/8, NeuroMab, 1:500 dilution) and Alexa-594-conjugated donkey anti mouse IgG (Invitrogen) were used as primary and secondary antibodies. Images were acquired at room temperature using Ziess Axiovert S-100 (Carl Zeiss) and AxioCam HRc camera, and processed with AxioVision Rel 4.8 (Carl Zeiss) and Photoshop (Adobe).

RNA-seq and computational analysis

R2 cells from E13.5 fetal livers were sorted directly into TRIzol LS (Invitrogen). 2μg total RNA from pooled samples was used to make one Illumina-compatible indexed library using the Illumina mRNA-Seq Sample Preparation Kit. Four libraries (two biological replicates each for control and mutant) were mixed at equal concentration and sequenced by an Illumina HiSeq 2000 using version 3 sequencing reagents at Genomics core facility (University of Oregon). An in-house, open-source pipeline for RNA-Seq was used that is compliant with the Standards, Guidelines and Best Practices for RNA-Seq proposed by the ENCODE consortium (V1.0 June 2011). This included "quality assessment / quality control" of the FASTQ file generated by the sequencer using an automated script that generates a detailed report for each sample, based around the FastQC utility. These metrics include per base sequence quality, per sequence GC Content, detection of over-represented kmers and sequences etc. In addition to FastQC's flags of "Pass", "Warn" and "Fail", we have developed additional flags to guide processing of the reads, if needed, prior to alignment. Every report was manually reviewed to ensure no anomalies occured. Examination of read quality via FastQC led us to trim the read length to 30bp for each library. The "read processing" component of the workflow included mapping of the reads and local alignment via the Bowtie aligner (allowing 2 mismatches). Only the uniquely mapping reads were utilized for the primary analysis. The multi-mapping reads, which could represent putative repetitive transcripts, are excluded from the primary analysis but retained for future follow-up. For "Normalization and Differential Transcript Modeling" a linear model was fit to the unit of analysis (in this case, gene level utilizing Ensembl gene annotation) via the EdgeR framework. All p-values were then False Discovery Rate adjusted.

Accession numbers

The GEO accession number for all unpublished gene expression data is GSE50708.

Gene set enrichment analysis

Genes used for gene set enrichment analysis (GSEA) were selected based on fold change and tag counts. Genes with (mutant/control) > |2| and an FDR adjusted p-value <0.05 were further evaluated for tag counts. For tag count evaluation, the total reads from each library were adjusted to that of the library with the smallest total number of reads. To minimize the influence of genes with extremely low expression levels, only genes with a difference of >50 adjusted reads between genotypes were used for GSEA.

Genes differentially expressed between control and mutant cells were further analyzed by gene set enrichment analysis (GSEA). GSEA is a computational method that determines whether a previously defined set of genes shows statistically significant, concordant differences between different phenotypes or biological states.4 Briefly, the 760 up-regulated genes and 87 down-regulated genes were defined as Rcor1 up-regulated gene set and Rcor1 down-regulated gene set, respectively. Two microarray data sets published previously were used to generate phenotypic classifications: 1) GSE65065 which includes gene expression data from different cell lineages: long term hematopoietic stem cell (LT-HSC), NK cell, monocyte, granulocyte, erythrocyte, naive CD4 cell, naive CD8 cell, active CD4 cell, active CD8 cell, B cell; 2) GSE37256 which has gene expression data for HSC, CMP, GMP and MEP. After up-loading the input files, the dataset was collapsed to gene symbols, and 1000 permutations were run.

RNA extraction and real time PCR (qPCR)

RNA was extracted using TRIzol (Invitorgen) and treated with DNAse (Ambion). Reverse transcription reactions were performed using Superscript III (Invitorgen). qPCR was performed in an Applied Biosystems PRISM 7900HT Fast Real Time PCR system with SYBR green PCR master mix (Applied Biosystems) using the same cycling conditions. Relative abundance of each cDNA was determined according to the standard curve and normalized to 18S RNA level. Primer sequences are shown in Table 3.1.

Chromatin immunoprecipitation analysis

MEL-745A cl. DS19 cells were provided by Stuart Orkin and maintained in DMEM with 10% FCS, 1% Pen/Strep and 1% L-Glutamine.

ChIP analyses were carried out as described (Ballas et al. 2001). Briefly, chromatin from ten million MEL cells, 5x106 control R2 (CD71+, TER119-) fetal liver cells or 5x106 mutant fetal liver cells were immunoprecipitated overnight at 4°C using 5ul Rcor1 antibody (Andres et al. 1999) or Gfi1b antibody (D-19, from Santa Cruz Biotech). After reversal of cross-links, DNA and 10% input samples were purified using Qiagen columns. For qPCR analyses, primers are shown in supplementary Table 3.2. ChIP DNA amounts were determined from standard curve and normalized to the input DNA.

Statistical analysis

Statistical comparisons between two samples were made using student t- tests. Multiple-group comparisons were analyzed by a one-way ANOVA with Newman-Keuls post-hoc

test in Prism 6 (GraphPad Software). Two- way ANOVA was used for matched CFU analyses within genotypes treated with and without TG101348.

Table 3.1 Real-time primers for gene expression analysis.

Name	Forward primer	Reverse primer
Csf2rb	ATAGTCCTCATCCTGGTCTTTCTCA	CTTCCACTTCCTGTACGTCCTGTAT
Csf2rb2	AGGATGGAGGTAAAGGTCTCTGG	CGTTGTTGTCTTCCAAATGTTCATA
Tec	TATGAGGTGATGCTGAGATGCTG	ATTTCTTCCTCTTGCCTTGGAAACT
1700025G04 Rik	ATGTGTTTGGCGATGAGTATAGGAT	TTTCTTGGTTTCTGGCTGCTATTT
Fli	AAAGTTCACTGCTGGCCTATAACAC	TATTATTGTTCCATGCTCCTCTCCT
Hbb-Y	AACTTCAAACTCTTGGGTAATGTGC	TAGAGAGAGGGCTCAGTGGTACTTG
Sfpi1	ATTCAGAGCTATACCAACGTCCAAT	GTGTGCGGAGAAATCCCAGTAGT
Bh1	TGGACAACCTCAAGGAGACC	ACCTCTGGGGTGAATTCCTT
Gata2	CGCCTGTGGCCTCTACTACAA	TTTCTTGCTCTTCTTGGATTTGCT
Id2	TGAGCTTATGTCGAATGATAGCAAA	CTGGTGAAATGGCTGATAACAAA
Id1	ACGTCCTGCTCTACGACATGAAC	AGGATCTCCACCTTGCTCACTTT
Runx1	GATCCATCACCTCTTCCTCTGTC	CGGAGCCGTTGAGAGTCG
Lmo4	GGTTTCACTACATCAATGGCAGTTT	TTACTCTGACCTCTCAGCAGACCTT
CEBPa	GGACCATTAGCCTTGTGTGTACTG	AGCTTGTCATAACTCCAGTCCCTCT
Ckit	GGTCAAAGGAAATGCACGAC	CCATAGGACCAGACATCACTTTCA
Gata1	TGTATCACAAGATGAATGGTCAGAA	GAGTGTTGTAGTGGTCGTTTGACAG
Fog1	CCCAAGTCCACCCAGAGAAG	GGCCTCATCTCCAACTCCTG
Sox6	AGGAGATGCGACAGTTCTTCACT	AATAGCACCAGGATACACAACACCT
18S	CTCAACACGGGAAACCTCAC	CGCTCCACCAACTAAGAACG

Table 3.2 Real-time primers for ChIP analysis.

Name	Forward primer	Reverse primer
β-actin	TAACAATGGCTCGTGTGACAA	AAGTTCAGTGTGCTGGGAGTCT
Meis1	CACTGGCTGGTTGGAGACTT	CCCAGACCTCCATCTCTCAA
Meis1 (NC)	TTCTCTATCATCTATCACCAAATCG	AATGTCGTTTATGCTCTCCTGATTA
Runx1	ACTGCTGAGATTTCTACCTGTGGTT	AGTGGCTTAGTGGTCTAGGCAAAG
Runx1(NC)	TATAATTTCTTTCACCTTCAGAGCA	GAGTACCAGAAGTGTTAGGGTTGG
Cbfb	GAGGAAGGAGCAGGGTTTCAC	CTCTAGCAAACAAGACGCACCAT
Cbfb(NC)	TATGTAATGTCCTGCTTCTGATCCT	GGAGAGACAGATTGGTTCCTGTAG
Csf2rb	TGGCAGAACTAAATGTCGTGAGTAT	AACAGAGAGCAGATTGAGGAAGTTG
Csf2rb(NC)	TGGAACCTAATGTCTGTACTGGAAC	ACAAGTGGCTTACTATGATTTCTGG

NC: negative control

Results

Disruption of the *Rcor1* gene causes embryonic lethality.

As mentioned previously (Chapter 2, Figure 2.2), we used the *Meox2-Cre* deleter strain(Tallquist and Soriano, 2000) to generate mice carrying germline $Rcor1^{-}$ allele. The resulting $Rcor1^{+/-}$ mice, after genetic removal of the Cre transgene, appeared normal and fertile. Intercrosses of $Rcor1^{+/-}$ mice showed that $Rcor1^{-/-}$ embryos were present at the expected Mendelian ratios at E13.5, but no viable $Rcor1^{-/-}$ offspring survived to P7 (Table 3.3). By E15.5, almost all mutant embryos were severely edematous, and by E16.5, ~75% of mutant embryos were dead. Importantly, no Rcor1 protein was detected in the $Rcor1^{-/-}$ embryos (Figure 2.5), suggesting that the loss of *Rcor1* resulted in embryonic lethality.

$Rcor1^{-/-}$ embryos die due to a defect in definitive erythropoiesis.

Phenotypic analysis revealed that starting from E13.5, the mutant embryos exhibited pale livers (Figure3.1A, B). Although embryo size was not significantly different among genotypes, the mutant fetal livers were much smaller (Figure3.1 B), with 72% fewer cells than control littermates ($Rcor1^{+/+}$: 9.9±0.74x10^6 cells/liver; $Rcor1^{+/-}$: 9.14±2.89X10^6 cells/liver; $Rcor1^{-/-}$: 2.77±0.71x10^6 cells/liver). Because no significant differences between $Rcor1^{+/+}$ embryos and $Rcor1^{+/-}$ embryos were measured in any experiments, we refer to them collectively as control.

Between E13.5 and E16.5, the fetal liver is the major site of definitive erythropoiesis (Wong et al., 2011), and most of the liver is comprised of nucleated erythropoietic precursors distinguished on the basis of size, nuclear morphology and Giemsa staining.

Cytospin preparations showed that mutant fetal liver were primarily early erythroblasts, while control fetal livers contained cells in all the different stages of erythropoiesis (Figure3.1 C). Consistent with the absence of later stage erythroid precursors in the mutant fetal liver, E15.5 mutant peripheral blood lacked mature, enucleated red blood cells (Figure 3.1 D). By contrast, peripheral blood from E15.5 control embryos contained more than 90% enucleated red cells (Figure3.1 E). No other overt morphological changes were observed in the mutant embryos. Based on these findings, I attributed the lethality in *Rcor1* $^{-/-}$ embryos to defects in erythropoiesis.

Rcor1 is required for the proerythroblast to basophilic erythroblast transition.

To identify which stage of erythropoiesis was affected in the *Rcor1* $^{-/-}$ mice, I performed flow cytometry analysis of CD71 and TER119(Zhang et al., 2003) markers on fetal liver cells (Figure 3.2 A). By E14.5, most control cells progressed through the proerythroblast stage (R2) to the basophilic, chromatophilic, and orthochromatophilic erythroblast stages (R3 and R4). In contrast, most mutant liver cells were arrested at the proerythroblast stage (R2 to R3).

To determine whether the accumulation of R2 and R3 cells in the mutants reflected a differentiation arrest, rather than aberrant marker expression, I examined the morphology of the FACS-sorted cells. Mutant R2 and R3 cells were identical to their control counterparts at these stages (Figure 3.2 B). Thus, the altered expression pattern of TER119 and CD71 in the mutants represented a differentiation arrest. Immunostaining of sorted control fetal liver cells showed that Rcor1 protein is present in all of the cells

from R0 to R3 (Figure 3.2 C), supporting our results that the disruption of the Rcor1 complex plays an important role at these differentiation stages.

To determine whether mutant erythroid progenitors would eventually form mature red blood cells over time, I performed a transplant experiment wherein fetal liver cells from control and mutant CD45.2 embryos with the beta hemoglobin haplotype Hbbs were transplanted into sub-lethally irradiated C57BL/6 mice congenic for both CD45.1 and the beta hemoglobin haplotype Hbbd (Figure 3.3 A). Host blood was analyzed for donor hemoglobin contribution at four weeks (data not shown) and 12 weeks after transplantation. Mutant fetal liver cells generated leukocytes with a frequency similar to control cells (Figure 3.3 B); however, no mutant peripheral RBCs were detected (Figure 3.3 C), indicating that mutant erythroid progenitor differentiation was blocked rather than temporarily arrested.

Rcor1 null erythroid progenitors have a cell autonomous defect and potential for myeloid differentiation.

To determine whether the developmental arrest of *Rcor1*$^{-/-}$ erythroid cells is a cell intrinsic defect, I performed *in vitro* colony forming assays using lineage-depleted E13.5 fetal liver cells. Equal numbers of R2 cells (Figure 3.4 A) were cultured in methylcellulose medium containing recombinant erythropoietin, stem cell factor, IL-3 and IL-6, which support the growth of erythroid and myeloid progenitors. As expected, control R2 cells generated almost exclusively Colony Forming Units -Erythroid (CFU-E). By contrast, very few, if any, CFU-E were detected in *Rcor1*$^{-/-}$ R2 cells (Figure3.4 A),

consistent with the erythroid defect observed *in vivo*. Instead, large numbers of heterogeneous myeloid colonies were detected (Figure3.4 A, C). Immature granulocytes, mast cells and macrophages were present in individual cytospun colonies stained with May-Grunwald Giemsa reagent (Figure3.4 D).

I also cultured R1 cells (Figure3.4 B) from control and mutant fetal livers. Control R1 cells contain mostly less mature erythroid progenitors (BFU-E) and few primitive erythroid progenitors (CFU-Granulocyte, Erythroid, Monocyte, Megakaryocyte; GEMM). Similar to mutant R2 cells, mutant R1 cells produced few, if any, erythroid colonies and generated large numbers of myeloid colonies that were not qualitatively different than the myeloid colonies in mutant R2 cultures (Figure3.4 B). Mutant R1 cells formed more CFU-GEMMs than control; however, they were pale, consistent with defective erythroid differentiation. Together with the lack of differentiated mutant erythroid cells in wild type hosts after transplantation (Figure3.3 C), these findings suggest that a cell intrinsic defect causes the arrest in erythropoiesis in Rcor1 mutants.

The dramatic increase in myeloid colony frequency in mutant cell cultures suggested either that mutant erythroid progenitors have the potential to become myeloid cells, or that an atypical myeloid progenitor accumulates in the *Rcor1* constitutive knockout fetal liver. I reasoned that inducing Rcor1 deletion following the isolation of normal progenitors would allow us to distinguish these two possibilities. *Rcor1*$^{flox/flox}$ mice were mated with *Mx1-Cre* mice, to generate embryos in which the expression of Cre recombinase is inducible by interferon α (IFNα; Figure3.5 A).(Kuhn et al., 1995) Sorted R1 cells from E13.5 *Mx1-Cre; Rcor1*$^{flox/-}$ fetal livers were plated into methylcellulose

culture medium with or without IFNα.(Kerenyi et al., 2013) Interestingly, I observed a decrease of BFU-E, and a concomitant, proportional increase of myeloid colonies in the IFNα treated cells (Figure3.5 B). Complete recombination of the floxed allele was confirmed in 22/23 myeloid colonies by PCR analysis (Figure2.2 B and data not shown). By contrast, the floxed *Rcor1* allele was detectable in fully hemoglobinized CFU-GEMM. Cre-deficient *Rcor1*$^{flox/-}$ R1 cells cultured with or without IFNα had indistinguishable CFU activity, indicating that IFNα itself does not influence myeloid cell production (Figure3.5 C). Thus, the increase in myeloid colonies is associated specifically with depletion of Rcor1 in progenitors that make BFU-Es.

In parallel experiments using R2 cells from *Mx1-Cre; Rcor1*$^{flox/-}$ fetal livers, no difference in CFU-E and myeloid colony output was observed following IFNα treatment (Data not shown). I suspect that turnover of Rcor1 was not fast enough to direct the lineage switch in CFU-E progenitors.

To test for aberrant white blood cell potential in Rcor1 mutant mice *in vivo*, I measured myeloid and lymphoid cells by flow cytometry. Although Mac1/Gr1^{+} myeloid cells in the mutant fetal livers increased five-fold in frequency (Figure3.6 A), their absolute number per liver was not different from controls. B cell (B220^{+}) and T cell (CD3^{+}) numbers were both decreased in the mutant fetal livers (Figure3.6 B). Evaluation of common myeloid progenitors (CMP), granulocyte-monocyte progenitors (GMP), or megakaryocyte-erythroid progenitors (MEP)(Traver et al., 2001) in the mutant fetal liver revealed a 1.8-fold decrease, 2.8-fold decrease and a very modest 13% increase in their frequency, respectively (Figure 3.7). Thus, in the Rcor1 mutants, there is not a propensity to

inappropriately expand the myeloid lineage. Presumably, the myeloid lineage-supporting cytokines present in the culture medium are absent or inactive in the fetal liver.

Rcor1 represses myeloid lineage and hematopoietic stem cell/ progenitor genes in erythroid progenitors.

I performed mRNA profiling to investigate the underlying molecular mechanisms for both the block of erythropoiesis and increased myeloid potential in Rcor1-deficient R2 cells. Our bioinformatic analysis identified genes in the mutant cells that were either up- (n=760) or down- (n=87) regulated by two-fold relative to the controls (Figure3.8A and Appendix 1). A good correlation (R^2= 0.9816) between RNA-Seq and qPCR was observed for the 18 genes assayed (Figure3.8 B, C).

To gain insight into the differentiation programs regulated by Rcor1, I employed Gene Set Enrichment Analysis (GSEA)(Subramanian et al., 2005) to compare the up-regulated and down-regulated gene sets from *Rcor1*$^{-/-}$ R2 cells with that of reference gene expression profiles. I exploited published microarray data sets for long term (LT)-HSCs, monocytes, granulocytes, naive and active T cells, B cells, Natural Killer cells (NK cells), and nucleated (immature) erythrocytes.(Chambers et al., 2007) Genes enriched in monocytes (Figure3.9A) and granulocytes (Figure3.9 B) were highly enriched in the *Rcor1*$^{-/-}$ up-regulated genes. These results suggested that myeloid genes were expressed ectopically and inappropriately in the *Rcor1*$^{-/-}$ cells, consistent with their myeloid differentiation potential in the colony forming assays.

Interestingly, transcripts associated with LT-HSCs were enriched in both the up- and down-regulated genes in the Rcor1 mutants, with a much higher enrichment score for the up-regulated gene set (Table3.4). Because multipotent progenitors were not included in the HSC/differentiated cell comparison,(Chambers et al., 2007) this HSC signature may not truly represent HSCs. I therefore performed GSEA analysis using published expression profiles for HSC, CMP, GMP and MEP cells.(Krivtsov et al., 2006) This analysis revealed an enrichment of HSC (Figure3.9 C) and CMP (Figure3.9 D) transcripts in the up-regulated genes in mutant R2 cells (Table3.5), further suggesting that both HSC and early progenitor genes are de-repressed in *Rcor1*$^{-/-}$ cells.

Interestingly, no major changes in the expression levels were detected in a subset of factors critical for erythropoiesis,(Tsiftsoglou et al., 2009) including Gata1, Zfpm1/Fog1, Scl /Tal1, Klf1/Eklf, Lmo2, Tcf3/E2A, and erythropoietin receptor (EpoR; Figure3.10 A). Thus, it is unlikely that the differentiation block in the Rcor1 mutant is due to a lack of positively acting regulators for erythropoiesis. Instead, our data suggest that Rcor1 promotes erythroid differentiation by repressing myeloid genes and HSC/progenitor genes (Figure3.10 B). Examples of myeloid genes include transcription factors, such as RARα,(Friedman, 2007) PU.1(Rekhtman et al., 1999) and Id1,(Leeanansaksiri et al., 2005) which promote myelopoiesis, as well as the cytokine CSF2/IL3/IL5 receptor beta common chain (Csf2rb and Csf2rb2) and macrophage colony-stimulating factor receptor (Csf1r). Similarly, genes encoding factors that are important in maintaining HSCs and early progenitors, including Gata2,(Tsai et al., 1994) Meis1,(Azcoitia et al., 2005) Pbx1(Ficara et al., 2008) and CD34,(Cheng et al., 1996a) were de-repressed. Notably,

overexpression of PU.1,(Rekhtman et al., 1999) Id1,(Lister et al., 1995) Meis1,(Cai et al., 2012) Gata2,(Briegel et al., 1993; Persons et al., 1999) Fli1(Athanasiou et al., 2000) and the Runx1/Cbfb complex(Cammenga et al., 2007; Kundu and Liu, 2003; Lorsbach et al., 2004) can interfere with normal erythropoiesis.

Increased CSF2 signaling in Rcor1 mutant erythroid cells contributes to their myeloid potential.

To identify which genes were direct Rcor1 targets, we performed Chromatin Immunoprecipitation analysis followed by qPCR. Gfi1b binding was also assessed given the previously demonstrated interaction between Gfi1b and Rcor1 and their shared binding at many hematopoietic genes.(Saleque et al., 2007) I focused on *Runx1* and *Cbfb* as their overexpression is detrimental to erythroid development.(Cammenga et al., 2007; Kundu and Liu, 2003; Lorsbach et al., 2004) *Csfr2b* was also assayed because of its robust induction in *Rcor1*$^{-/-}$ cells (300-fold; Figure3.10 B). *Meis1*, a known target of Gfi1b and Rcor1,(Chowdhury et al., 2013) was included as a positive control. To guide our design of ChIP primers, I used published Kdm1a ChIP-seq sites that were close to Transcriptional Start Sites.(Kerenyi et al., 2013) Primer sites located more than two kilobases away from Kdm1a or Gfi1b binding sites, as well as the expressed β-actin gene, served as negative controls. In our initial screen of the mouse erythroleukemia (MEL) cell line, binding of both Rcor1 and Gfi1b was detected at the promoter regions of *Meis1*, *Runx1* and *Csf2rb* (Figure3.11 A-B). Similar binding patterns of Rcor1 and Gfi1b at these targets were confirmed in control R2 cells prepared from fetal livers (Figure3.11 C-D); however, in R2 cells, Gfi1b binding was also detected at the *Cbfb* promoter. As expected,

in mutant fetal liver cells, Rcor1 was depleted from these promoters (Figure3.11 C). These data indicate that Rcor1 directly regulates these genes in fetal liver cells *in vivo*, likely together with Gfi1b.

The Csf2rb gene encodes the receptor beta subunit shared by the cytokines CSF2, IL3, and IL5, which stimulate proliferation, differentiation, survival, and functional activation of myeloid cells.[39] I therefore hypothesized that over-expression of Csf2rb in *Rcor1*$^{-/-}$ erythroid precursors might influence their response to cytokines and contribute to the inappropriate generation of myeloid colonies (Figure3.4-3.5). A four-fold increase in anti-Csf2rb staining on the mutant fetal liver cells was detected using flow cytometry (Figure3.12 A, median fluorescence intensity of control: 166.4±24.2, n=10; median fluorescence intensity of mutant: 692±136.9, n=5; $p<0.0001$). Notably, cell surface expression of Csf2rb was also detected in immunophenotpyically defined erythroid progenitor populations(Pronk et al., 2007) in *Rcor1* mutants but not controls (Figure3.12 B-C).

The aberrant increase of Csf2rb led us to interrogate whether I could detect changes in Csf2rb signaling pathways in *Rcor1*$^{-/-}$ cells. Because Jak-Stat pathway is one of predominant pathways downstream of cytokine treatment (Figure3.13 A), I determined weather this pathway was changed when treated with cytokines. The alpha subunits that associate with Csf2rb determine the cellular cytokine response, and I noted that the alpha subunit of the CSF2 receptor is expressed at a higher level than the alpha subunits of IL-3 and IL-5 receptors in our mutant RNA-seq data sets. Upon stimulation of R2 cells with CSF2, levels of phospho-Stat5, an important downstream mediator of CSF2 signaling,

were increased five-fold in mutant cells (Figure3.13 B), whereas total Jak2 and Stat5 protein levels were the same in control and mutant cells. To test whether this altered signaling pathway in *Rcor1*$^{-/-}$ erythroid cells contributed to their generation of myeloid colonies, the Jak/Stat pathway was blocked with a specific Jak2 inhibitor, TG101348.(Wernig et al., 2008) This inhibitor reduced the number of myeloid colonies formed by mutant cells by 40% (Figure3.13 C). Taken together, these results suggest that hyper-activation of the Csf2rb signaling pathway contributes to the generation of myeloid cells by mutant erythroid progenitors.

Discussion

This study provides the first *in vivo* evidence that Rcor1 is an essential co-repressor in erythropoiesis. Rcor1 is present in protein complexes with Kdm1a and HDACs in different cell types, and Rcor1 can bind Kdm1a directly.(Yang et al., 2006) Nonetheless, the germline knock outs of Kdm1a and HDAC mice exhibit a more severe phenotype than the Rcor1 knockouts, dying by E7.5 (Wang et al., 2007) and E10.5 (Lagger et al., 2002) respectively, compared to ~E16.5 for Rcor1 mutants. However, elimination of Kdm1a or Rcor1 in the RBC lineage blocks erythropoiesis at the transition of proerythroblast to basophilic erythroblast.(Kerenyi et al., 2013) Thus, the transcription factors that recruit Rcor1 are predicted to be only a subset of the factors that recruit Kdm1a.

In cells with erythroid potential, Rcor1 has been shown to physically interact with Gfi1b,(Saleque et al., 2007) SCL/Tal (Hu et al., 2009) and Bcl11a(Xu et al., 2013).

Rcor1 and Gfi1 bind to 720 common targets in MEL cells (25.8 % of total Rcor1 targets(Saleque et al., 2007)), and numerous erythroid maturation defects are shared by *Rcor1*$^{-/-}$ and *Gfi1b*$^{-/-}$ mice. Both knockout mice die at ~E15.5-E16.5 because of arrested definitive erythropoiesis. Furthermore, *Gfi1b*$^{-/-}$ cells (Saleque et al., 2002) and *Rcor1*$^{-/-}$ cells cannot form typical BFU-E and CFU-E, and instead exhibit the potential to form mast cell colonies in cytokine-supplemented cultures (Figure 4). Collectively, these data suggest that Gfi1b and Rcor1 work together to regulate early steps in definitive erythropoiesis *in vivo*. Given that functional erythropoiesis is preserved in BCL11A – deficient erythroid cells and their major phenotype at the transcriptional level is failure to repress embryonic β-like and α-like globin gene expression (Xu et al., 2011), BCL11A is not a likely candidate for mediating early definitive erythroid cell maturation together with Rcor1. SCL is important but not essential for the generation of mature RBCs (Hall et al., 2005) , and SCL and Rcor1 share a number of gene targets (Kassouf et al., 2010; Saleque et al., 2007) however, the functional interactions between SCL and Rcor1 in early erythroid cell differentiation remain to be explored.

One of the more striking findings of our studies is that Rcor1-deficient cells enriched for erythroid precursors have vastly increased myeloid potential *in vitro*. Our use of a conditional Rcor1 knockout model to delete Rcor1 from phenotypically normal R1 cells revealed a decrease in BFU-E accompanied by a proportionate increase in myeloid colony formation. These data suggest that BFU-E or earlier stage progenitors can transition to a myeloid phenotype after deletion of Rcor1. This could also account for the higher frequency of CFU-GEMM, colonies comprised of both erythroid and myeloid

cells, observed in the induced mutant R1 cultures. Our transcriptome analysis of *Rcor1*$^{-/-}$ proerythroblasts suggests that pro-erythroid gene expression is not affected by loss of Rcor1, and the de-repression of genes associated with hematopoietic stem cell/ progenitor cell function and myeloid differentiation likely drive this myeloid lineage switch. An alternative explanation for the observed increase in myeloid colonies in the R1 culture may be that loss of Rcor1 can increase proliferation of a pre-existing myeloid progenitor pool. Given the lower frequency of phenotypic GMP and CMP observed in the mutants (supplemental Figure 3), these primitive myeloid progenitors are unlikely candidates.

The most robustly up-regulated transcript in *Rcor1*$^{-/-}$ proerythroblasts was *Csf2rb* and Csf2rb was readily detectable on mutant erythroid cells. Our ChIP results indicated that both Gfi1b and Rcor1 occupy the *Csf2rb* promoter *in vivo*, suggesting that this complex directly represses *Csf2rb* expression in wild type erythroid cells. Interestingly, a recent study also shows Kdm1a at this site.(Kerenyi et al., 2013) Moreover, the myeloid transcription factors PU.1 and C/EBP(van Dijk et al., 1998; van Dijk et al., 1999) both overexpressed in the mutant erythroid cells, can directly activate the Csf2rb gene. Several studies showed that increasing the activity of Csf2rb is sufficient to induce myeloid colony formation from both fetal liver cells and bone marrow. (D'Andrea et al., 1998; Hisakawa et al., 2001) Similarly, overexpression of an activated form of the human Csf2rb in fetal liver cells induces growth factor-independent proliferation and differentiation of mast cell and neutrophils.(McCormack and Gonda, 1997) I demonstrated that Csf2rb overexpression in the mutant erythroid cells makes them hypersensitive to CSF2 stimulation. Moreover, inhibition of Jak2, a major effector of

Csf2r signaling, significantly reduced the myeloid colony forming capacity of Rcor1-deficient cells (Figure 6G). Thus, overexpression of Csf2rb in Rcor1 mutant erythroid cells likely contributes to the adoption of a myeloid cell fate in colony forming assays.

Previously, Gfi1b was shown to directly repress the TGFb receptor gene, Tgfbr3, and thereby modifies TGF-beta signaling to facilitate the differentiation of immature progenitors (MEP) toward the erythroid lineage.(Randrianarison-Huetz et al., 2010) Our transcriptome analysis of Rcor1-deficient committed erythroid precursors did not reveal a large increase in TGFb receptor expression relative to control cells. Specifically, Tgfbr3 was down-regulated (Mut/control=0.779 fold), whereas Tgfbr1 (Mut/control=1.64 fold) and Tgfb2 (Mut/control=1.94 fold) were modestly up-regulated. Thus, the Gfi1b/Rcor1 complex likely has different targets at specific stages of erythropoiesis.

In summary, our work revealed an essential role for Rcor1 in promoting erythroid progenitor maturation and restricting their differentiation towards alternative myeloid lineages.

Acknowledgements

I thank Jennifer Miller, Travis Polston and Andrea Ansari for mouse genotyping and animal care, Devorah Goldman, Hyunjung Lee and Kimberly Hamlin for the blood analysis. The work was supported by NIH grants to GM (NS22518), to SK and SKM (5UL1RR024140) (5P30CA069533) and to WHF (HL069133). HY was supported by an American Heart Association predoctoral fellowship. SHO and GM are Investigators of the Howard Hughes Medical Institute.

Figures and legends

Age	Genotype (number/percentage)			Total
	+/+	+/-	-/-	
E13.5	88(24.4%)	188(52%)	85(23.6%)	361
P7	88(35.7%)	158(64.3%)	0	246

Table 3.3 Targeted disruption of murine *Rcor1* results in embryonic lethality.

Genotypes resulting from *Rcor1* heterozygote matings.

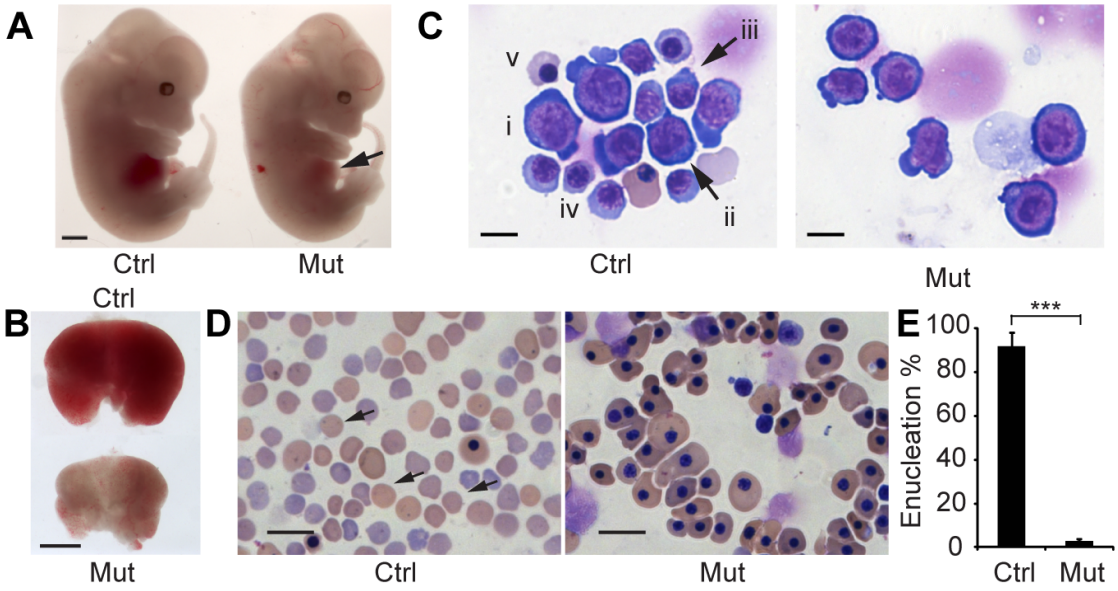

Figure 3.1 Rcor1 null embryos exhibit defective embryonic erythropoiesis.

(A) E13.5 control and mutant littermates. Note pale liver in mutant (arrow). Scale bar: 1mm. (B) Comparison of E13.5 control and mutant fetal livers. The mutant fetal liver is smaller and paler than the control fetal liver. Scale bar: 1mm. (C) May-Grunwald Giemsa staining of E13.5 fetal liver cytospin preparations. The control liver contains early erythroid progenitors (i, BFU-E or CFU-E like cells; ii, proerythroblast) and late erythroid precursors (iii, early basophilic erythroblast; iv, late basophilic erythroblast; v, orthochromatophilic erythroblast). The mutant fetal liver contains primarily early stage erythroid progenitors. Scale bar: 10μm. (D) May-Grunwald Giemsa staining of E15.5 peripheral blood smears showing enucleated definitive erythrocytes (arrow) in the control that are lacking in the mutant. In the mutant, nearly all the circulating blood cells are primitive wave erythroid cells of normal appearance. Scale bar: 20μm. (E) Mean of enucleated RBC frequency in control (n=5) and mutant (n=3) E15.5 peripheral blood.

Error bars show standard deviation (SD). *** indicates that P<0.001. Images for A-B were taken with a Zeiss SteREO Lumar.V12 microscope, a Neo-Lumar S 0.8x FWD 80mm objective and an AxioCam HRc camera. Images for C-D were acquired with a Zeiss Axiovert S-100 (Carl Zeiss), an AxioCam HRc camera and either a Zeiss plan-neofluar 100X/1.30 oil lens (C) or a Zeiss plan-neofluar 40x/1.30 oil lens (D).

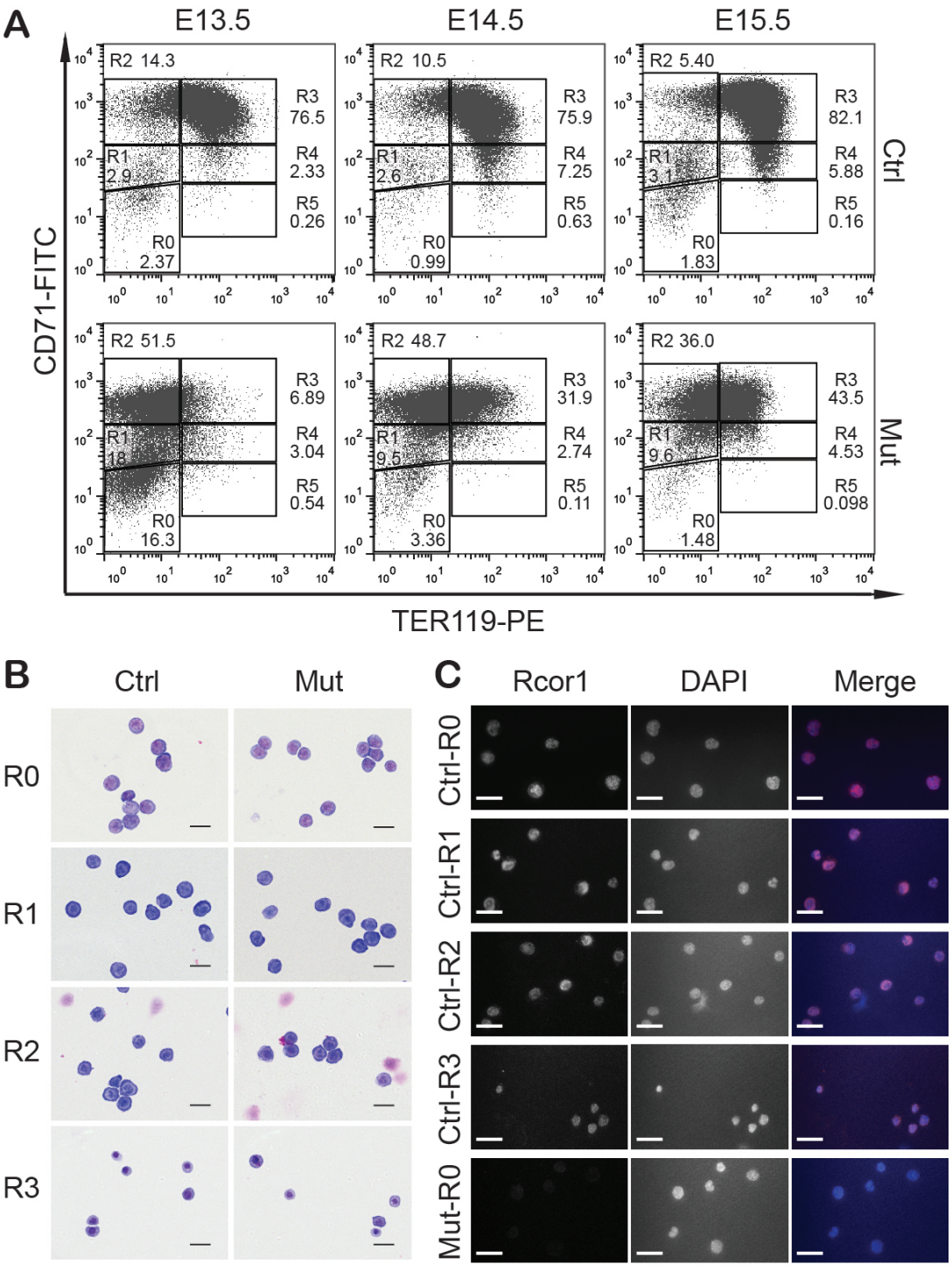

Figure 3.2 Erythropoietic differentiation in Rcor1 knockout mice is blocked at the proerythroblast to basophilic erythroblast transition.

(A) Flow cytometry profiles of fetal liver cells stained with CD71 and TER119. R0-R5: Gates of different erythroblast populations according to their expression levels of CD71 and TER119. R0 contains mixed populations of HSC and early progenitors, such as CMP, GMP and MEP; R1 consists of mostly immature RBC progenitors, including BFU-E and CFU-E; R2 is comprised mainly of proerythroblasts and early basophilic erythroblasts; R3 contains early and late basophilic erythroblasts; R4 is composed of chromatophilic and orthochromatophilic erythroblasts; R5 contains late orthochromatophilic erythroblasts and reticulocytes. Note that the transition from R2 to R3 is arrested in the mutant fetal liver. (B) May-Grunwald Giemsa staining showing similar morphology of FACS-sorted mutant and control E14.5 fetal liver cells. Scale bar: 20μm. (C) Immunostaining for Rcor1 protein in FACS-sorted E14.5 fetal liver cells. Mutant R0 cells serve as a negative control. DAPI labeled nuclei. Scale bar: 20μm. Images in this figure were acquired with a Zeiss Axiovert S-100, a Zeiss plan-neofluar 63X/1.25 oil lens and an AxioCam HRc camera.

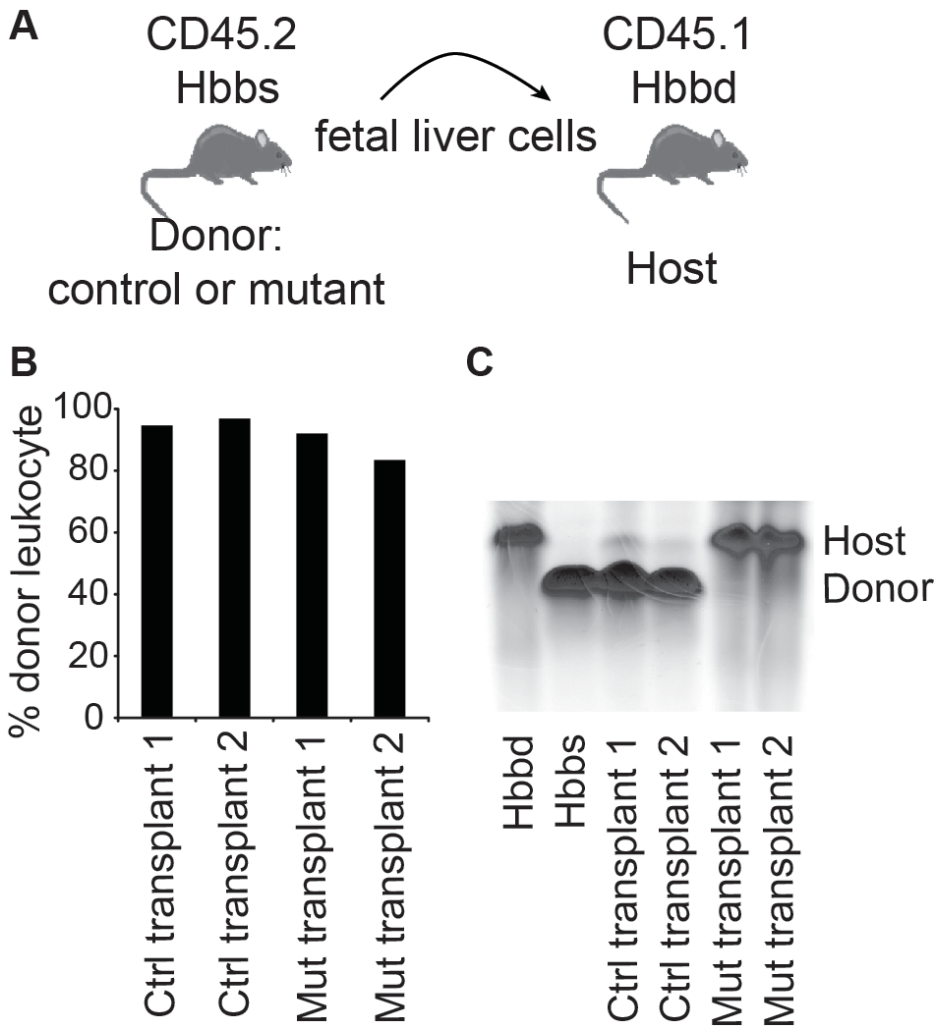

Figure 3.3 Rcor1 knockout feta liver cells do not generate erythrocytes in wild type host.

(A) Schematic diagram showing transplant of fetal liver cells that express CD45.2 and beta-globin haplotype Hbbs (donor) into irradiated mice double congenic for CD45.1 and beta-globin haplotype Hbbd (host). (B) Donor cell contribution to circulating leukocytes of adult WT mice transplanted with 2 million E13.5 mutant or control fetal liver cells. (C) Hemoglobin electrophoresis analysis indicates that mutant fetal liver cells cannot generate RBCs after transplantation into wild type adult mice.

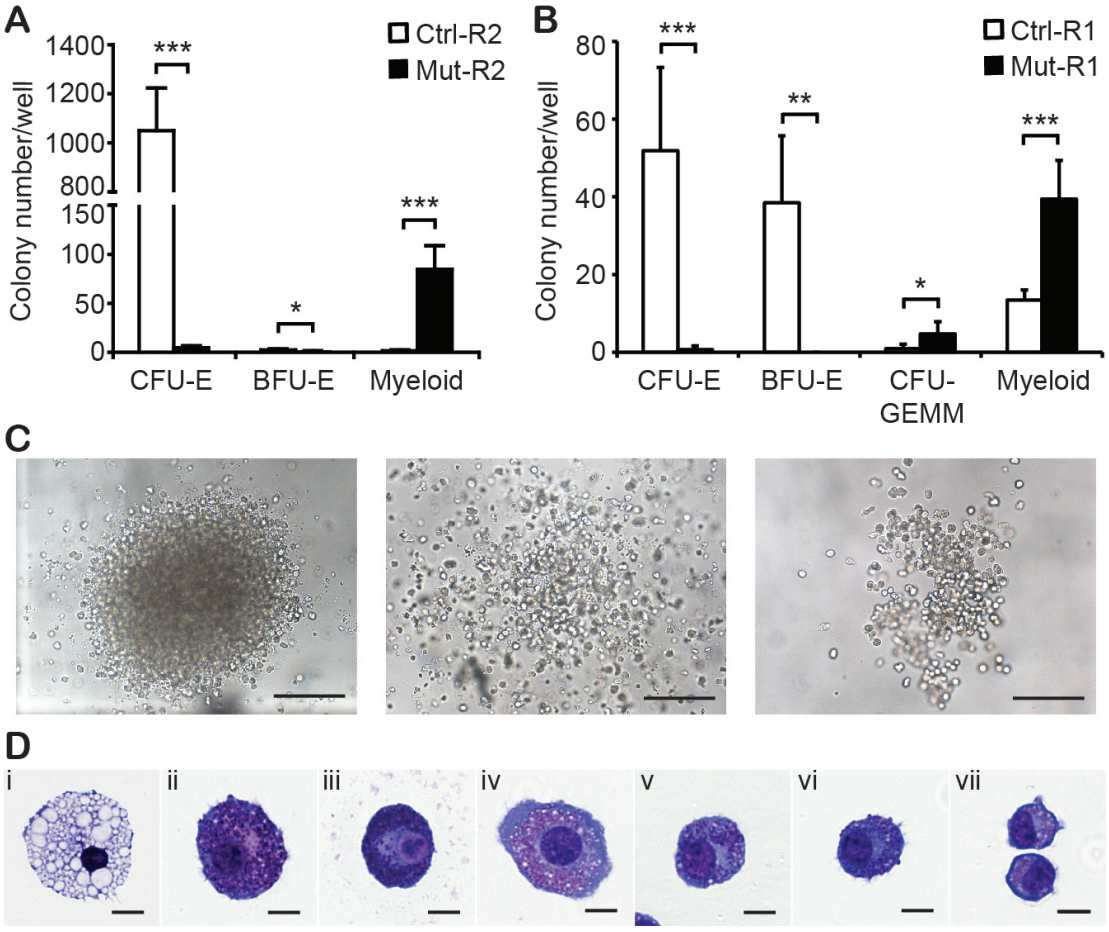

Figure 3.4 *In vitro* colony forming assays reveal a cell autonomous defect in erythropoiesis and enhanced myeloid potential in Rcor1 deficient erythropoietic progenitors.

(A, B) Numbers of colonies generated from FACS sorted R2 fetal liver cells (A) or R1 fetal liver cells (B) in methylcellulose culture. CFU-E: colony forming units- erythrocyte; BFU-E: burst forming units-erythrocyte; CFU-GEMM: colony forming units-granulocyte, erythrocyte, macrophage and megakaryocyte; Myeloid colonies: colonies containing mast cells, granulocytes and/or macrophages. Results from 4 experiments for R2 and 5 experiments for R1 are shown (mean±SD). Equal numbers of control and mutant cells

were plated in each experiment. * $P<0.05$, **$P<0.01$,***$P<0.001$. (C) Representative myeloid colonies generated from methylcellulose cultures of mutant R2 cells. Scale bar: 200μm. (D) Representative cells from cytospin preparations of mutant myeloid colonies stained with May-Grunwald Giemsa. (i) Macrophage; (ii-iii) Mast cells; (iv-vii) granulocytes. Scale bar: 10μm. All images were acquired using a Zeiss Axiovert S-100 and AxioCam HRc camera. A Zeiss Fluar 10X/0.5 objective was used for the images in panel C and a Zeiss plan-neofluar 100X/1.30 oil objective was used for the images in panel D.

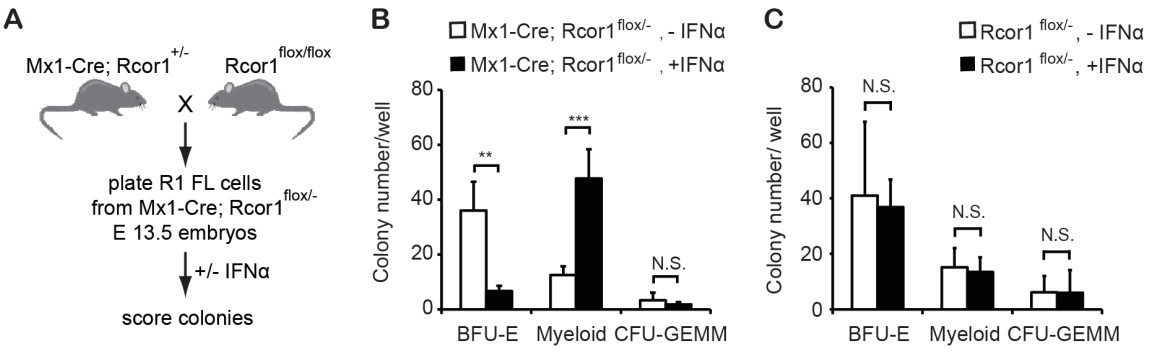

Figure 3.5 Induction of Rcor1 recombination *in vitro* with IFNα increases myeloid colonies and decreases erythroid colonies.

(A) Schematic diagram for generating inducible *Rcor1* deletions in R1 fetal liver (FL) cells. (B) Numbers of colonies generated from FACS sorted R1 *Mx1-Cre; Rcor1$^{flox/-}$* fetal liver cells cultured in methylcellulose with or without IFNα. (C) Treatment of R1 *Rcor1$^{flox/-}$* cells with IFNα does not influence colony outcomes. Results from 6 experiments are shown (mean±SD). * P<0.05, **P<0.01,***P<0.001, N.S., non-significant. BFU-E, burst forming units-erythrocyte; CFU-GEMM, colony forming units-granulocyte, erythrocyte, macrophage and megakaryocyte; Myeloid colonies, colonies containing mast cells, granulocytes and macrophages.

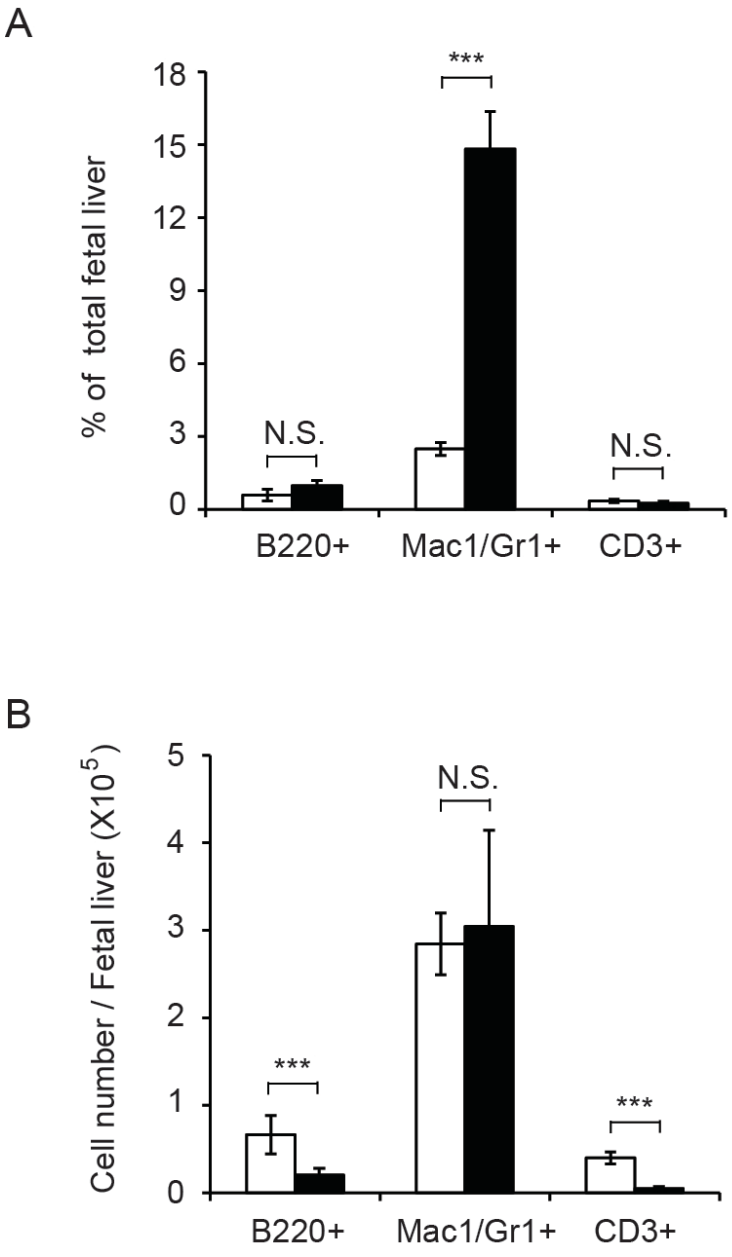

Figure 3.6 Increase in the percentage but not absolute cell number of myeloid cells in *Rcor1*$^{-/-}$ fetal livers

(A) Percentage of lineage positive cells in E13.5 fetal livers. (B) Absolute number of lineage positive cells in individual E13.5 fetal liver. Graphs show mean±SD. $N_{control}=4$, $N_{mutant}=4$. ***, $P<0.001$, N.S., non-significant.

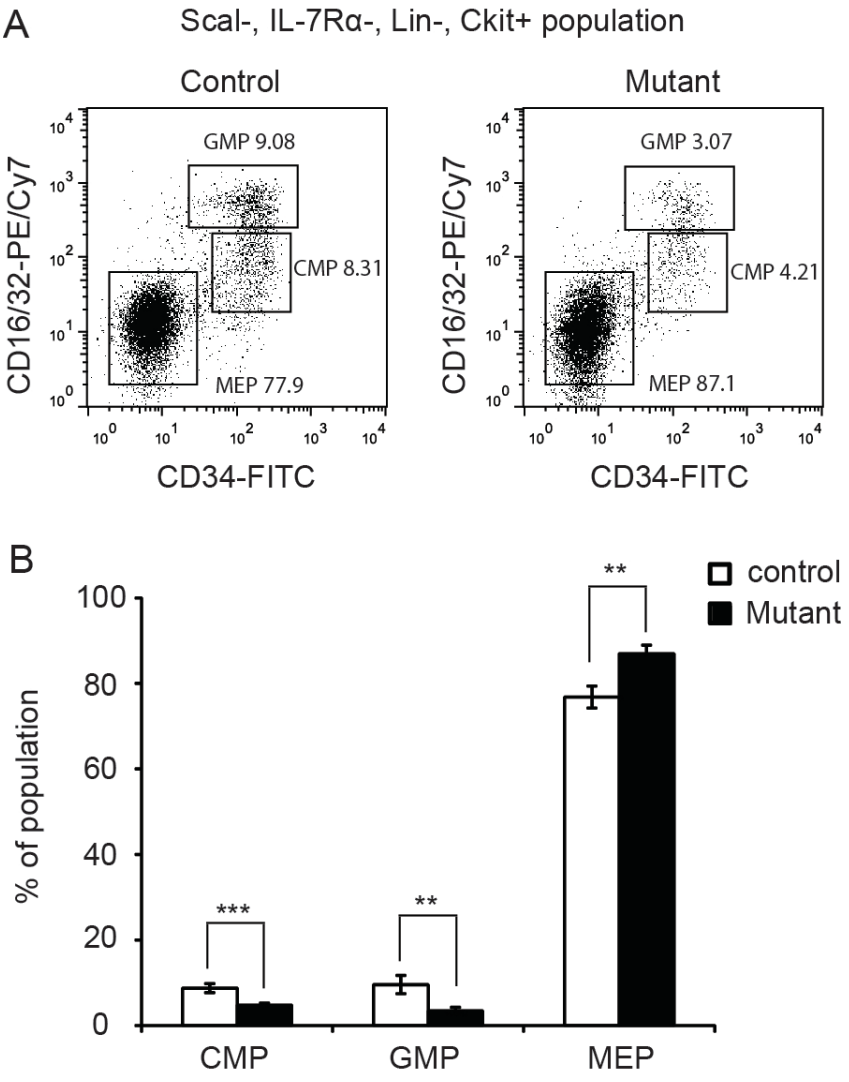

Figure 3.7 Modest changes in CMP, GMP and MEP frequency in *Rcor1*$^{-/-}$ fetal livers

(A) Representative flow cytometry profiles of E13.5 control and mutant fetal liver stained with markers for CMP, GMP and MEP. (B) Quantification and statistical analysis of CMP, GMP and MEP flow cytometric data (Mean±SD). $N_{control}=7$, $N_{mutant}=3$. **, $P<0.01$; ***, $P<0.001$

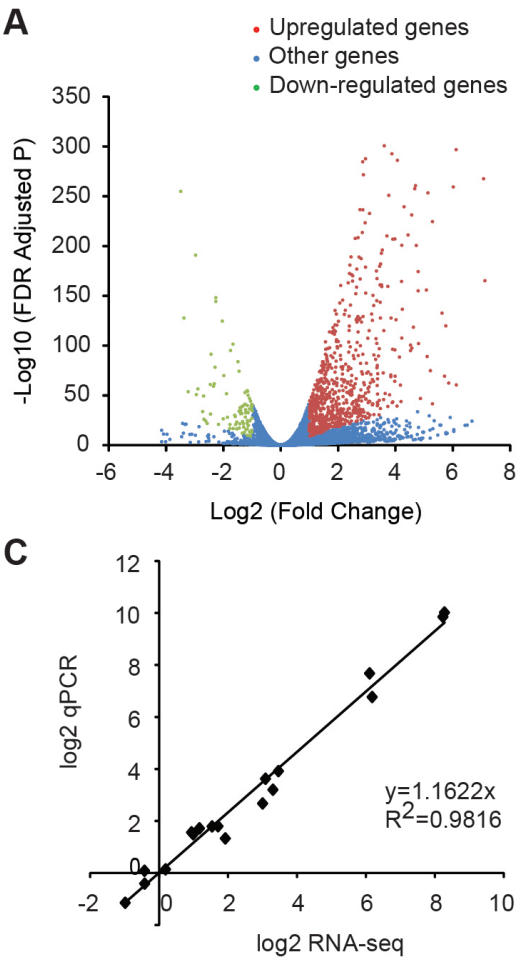

B

	Fold change (Mut/ WT)	
Gene name	log2 RNA-seq	log2 qPCR
Csf2rb	8.285	10.015
Csf2rb2	8.244	9.849
Tec	6.188	6.767
1700025G04Rik	6.116	7.673
Fli1	3.472	3.913
Hbb-Y	3.313	3.202
PU.1	3.096	3.621
Bh1	3.010	2.667
Gata2	1.929	1.322
Id2	1.715	1.793
Id1	1.544	1.787
Runx1	1.178	1.714
Lmo4	0.997	1.485
CEBPa	0.950	1.561
Ckit	0.194	0.138
Gata1	-0.413	-0.415
FOG1	-0.413	0.084
Sox6	-0.976	-1.152

Figure 3.8 Knockout of Rcor1 results in the up-regulation of myeloid genes.

(A) Volcano plot from RNA-seq showing all expressed genes. The Y-axis shows statistical significance. A false discovery rate (FDR) adjusted p-value of 0.05 is 1.3 on this scale. The X-axis shows the magnitude of change (Mutant/Control). Red dots, all up-regulated genes with fold change equal to or larger than 2, $p < 0.05$ and an adjusted tag number of >50 (average mutant reads minus average control reads, see materials and methods for details). Green dots, all down-regulated genes with fold change equal to or smaller than 2, $p < 0.05$, and an adjusted tag number of >50 (average control reads minus

average mutant reads). Blue dots, all other genes. (B) Confirmation of representative RNA-seq results by quantitative PCR. (C) Correlation between qPCR and RNA-seq data based on data points from (B).

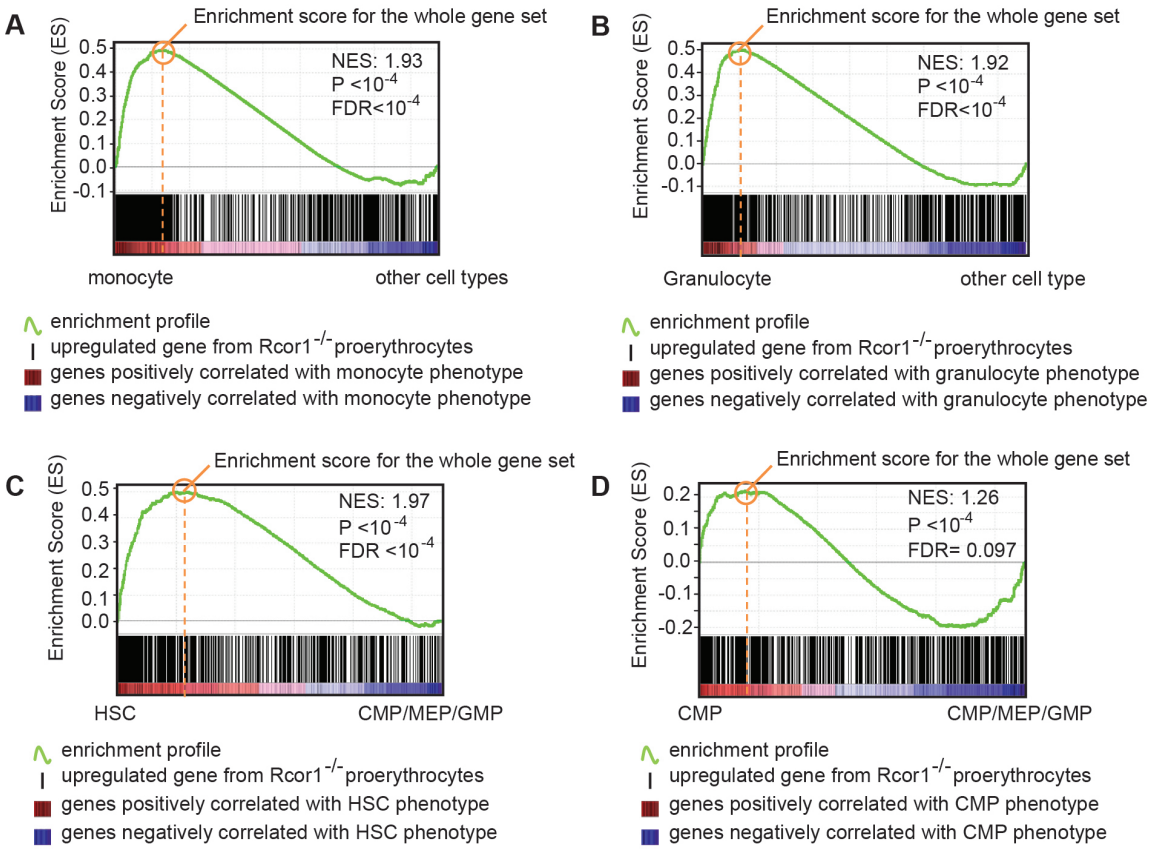

Figure 3.9 Knockout of Rcor1 results in the up-regulation of myeloid and HSC/progenitor genes.

(A-B) Gene Set Enrichment Analysis (GSEA) showing that genes that are up-regulated in mutant *Rcor1*$^{-/-}$ cells correlate positively with genes that are enriched in monocytes (A) and granulocytes (B). Heat map: genes are ranked according to their relative expression levels in monocytes to "other" hematopoietic cell types (LT-HSC, NK cells, monocytes, granulocytes, erythrocytes, naive CD4 cells, naive CD8 cells, active CD4 cells, active CD8 cells, B cells).[20] Red, highly enriched in monocytes. Black vertical lines represent single genes from the up-regulated *Rcor1*$^{-/-}$ gene set, which are positioned with respect to the ranked list of the reference cell type expression data set. The green line is the running

sum for calculating the enrichment score (ES). Positive and negative ES indicate enrichment at the top and bottom of the ranked reference list, respectively. ES is normalized (NES) based on differences in gene set size and correlations between gene sets, and is used to compare GSEA results across experiments. (C-D) Gene Set Enrichment Analysis showing that genes up-regulated in *Rcor1*$^{-/-}$ cells are correlated positively with genes that are highly expressed in HSC (C) and CMP (D). Heat map: genes are ranked according to their relative expression levels in HSC relative to CMP, GMP and MEP.[21] Colors and NES as described in D.

Table 3.4 The myeloid signature and the HSC signature are enriched in *Rcor1*$^{-/-}$ increased gene set.

GSEA comparison	Rcor1 null increased genes			Rcor1 null decreased genes		
to blood lineages	NES	p-value	FDR q-value	NES	p-value	FDR q-value
LT-HSC vs others	1.7675	$<10^{-4}$	$<10^{-4}$	1.07	0.325	0.263
NK cells vs others	1.3282	0.005	0.0357	N.S.	-	-
Monocyte vs others	1.9336	$<10^{-4}$	$<10^{-4}$	N.S.	-	-
Granulocyte vs others	1.9243	$<10^{-4}$	$<10^{-4}$	N.S.	-	-
Erythrocyte vs others	N.S.	-	-	2.437	$<10^{-4}$	$<10^{-4}$
CD4 naive vs others	N.S.	-	-	N.S.	-	-
CD8 naive vs others	N.S.	-	-	N.S.	-	-
CD4 active vs others	N.S.	-	-	N.S.	-	-
CD8 active vs others	N.S.	-	-	N.S.	-	-
B cells vs others	N.S.	-		N.S.	-	-

NES indicates normalized enrichment score; N.S. indicates not significant

Table 3.5 The HSC signature and the CMP signature are enriched in *Rcor1*$^{-/-}$ increased gene set when compared to early hematopoietic progenitors.

GSEA comparison to hematopoietic progenitors	Rcor1 null increased genes			Rcor1 null decreased genes		
	NES	p-value	FDR q-value	NES	p-value	FDR q-value
HSC vs others	1.968	$<10^{-4}$	$<10^{-4}$	0.966	0.5135	0.5775
CMP vs others	1.2637	$<10^{-4}$	0.0968	N.S.	-	-
GMP vs others	N.S.	-	-	N.S.	-	-
MEP vs others	N.S.	-	-	1.971	$<10^{-4}$	$<10^{-4}$

NES indicates normalized enrichment score; N.S. indicates not significant

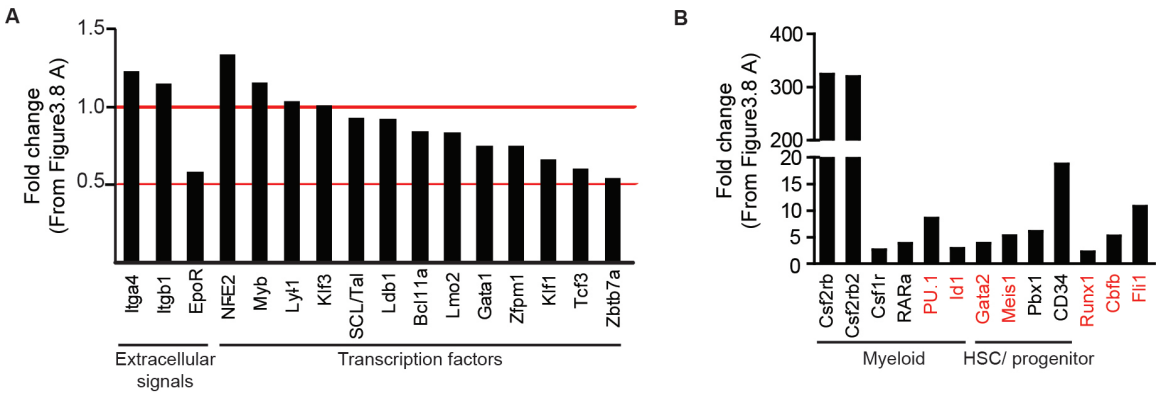

Figure 3.10 Knockout of Rcor1 results in the up-regulation of myeloid genes.

(A) Expression levels of positive regulators of erythropoiesis are not significantly altered in Rcor1 null proerythroblasts. (B) Examples of de-repressed genes from *Rcor1*$^{-/-}$ cells. Red colored genes have been reported to block erythropoiesis when de-repressed in RBC progenitors. Fold change, mutant/control.

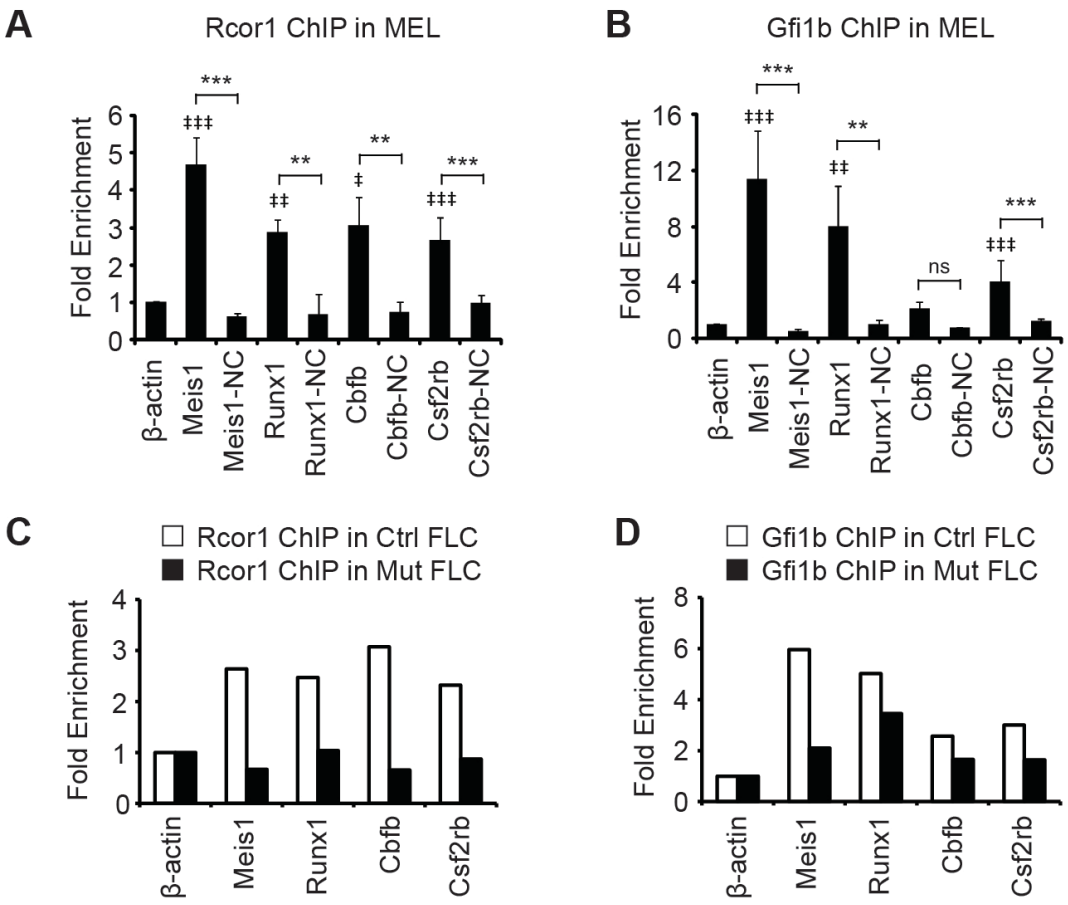

Figure 3.11 Identification of Rcor1 and Gfi1b targets by CHIP analyses.

(A-B) Rcor1 and Gfi1b occupy the promoters of indicated target genes measured by Rcor1 ChIP (A) and Gfi1b ChIP (B) analysis in the murine erythroleukemia (MEL) cell line. Binding is represented as fold enrichment relative to a negative region from the β-actin gene intron. For each gene, a site 2-8kb away from the positive binding site was used to serve as internal negative control (NC). Results from 3 experiments are shown (mean ± SD). ‡ indicates comparisons to β -actin: ‡ P< 0.05, ‡‡ P<0.01, ‡‡‡ P<0.001. * indicates comparison to internal negative control: * P<0.05, **P<0.01,***P<0.001. (C-D) Rcor1 ChIP (C) and Gfi1b ChIP (D) analysis in primary control R2 fetal liver cells

(FLC) and mutant total fetal liver cells. Binding is represented as fold enrichment relative to a negative region from the β-actin gene intron. The mean of two independent experiments is shown.

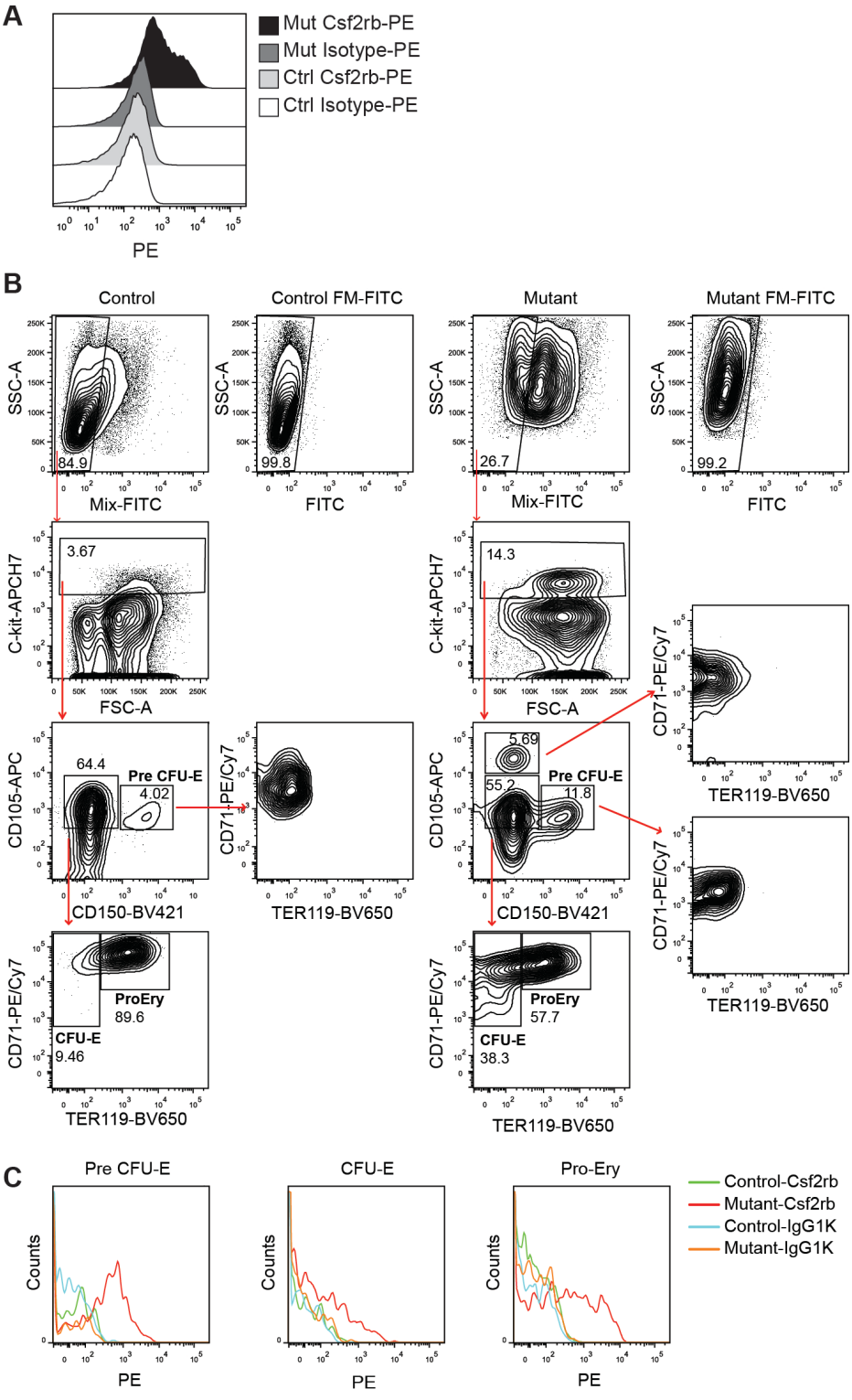

Figure 3.12 Aberrant increases of Csf2rb expression in *Rcor1*$^{-/-}$ fetal liver cells.

(A) Representative flow cytometry analysis of Csf2rb expression level in E13.5 control fetal liver (n=10) and mutant fetal liver (n=5). Phycoerythrin (PE) conjugated anti-Csf2rb or PE conjugated IgG1 (isotype control) were used. (B) Staining and gating strategies for analyzing Pre CFU-E, CFU-E and proerythroblasts (ProEry) from E13.5 control and mutant fetal liver. (B) Csf2rb expression level in gated Pre CFU-E, CFU-E and ProEry population from control and mutant fetal liver. Profiles are representative of 4 individually stained control or mutant fetal livers.

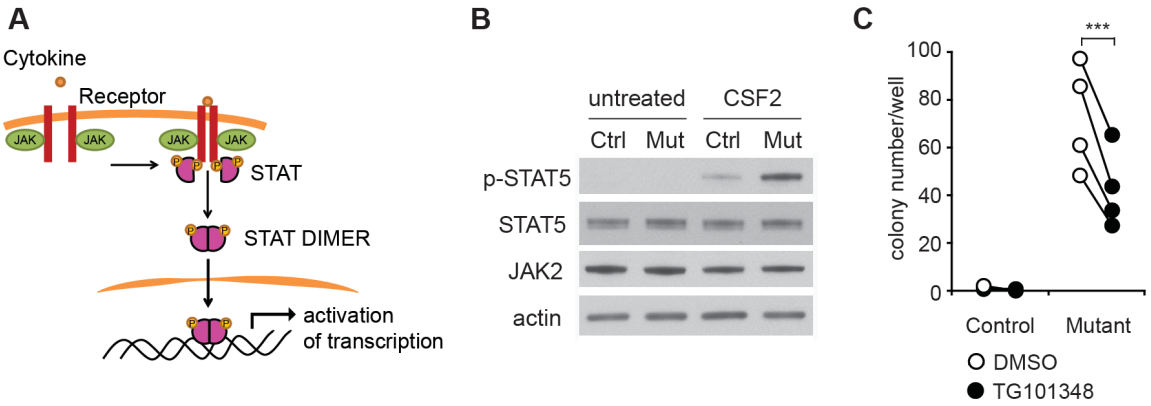

Figure 3.13 Rcor1 mutants exhibit a hypersensitive CSF2 signaling pathway.

(A) Illustration of JAK-STAT pathway which is downstream of cytokine treatment. (B) Western blot analysis showing that purified TER119- mutant cells have higher levels of p-Stat5, but similar levels of total Stat 5 and Jak2 protein, following treatment with CSF2. This experiment was repeated once more with the same result. (C) Colony forming assay results showing that the Jak2 inhibitor TG101348 reduces CFU-GM colonies generated from mutant fetal liver R2 cells. Results from 4 independent control or mutant fetal livers treated with TG101348 or DMSO are shown (mean ± SD). ***P<0.001.

CHAPTER 4: Rcor1 deficiency disrupts myeloerythroid lineage differentiation and causes severe myelodysplasia in mice

(In collaboration with Dr. Devorah Goldman, submitted for publication)

Introduction

Transcriptional co-repressors are critical components of gene expression regulatory machinery. Their primary function is to serve as a platform to couple a variety of different histone modification activities that regulate gene expression. Through diverse transcription factor and cofactor interactions, tightly regulated gene expression patterns can be achieved by a limited number of proteins. Among the best characterized transcription co-repressors is Rcor1 (CoREST)(Andres et al., 1999), a core component of a chromatin-modifying repressor complex that includes histone deacetylase 1/2 (HDAC1/2)(Humphrey et al., 2001; Lee et al., 2005) and the histone 3 lysine 4 (H3K4) demethylase, Kdm1a (also known as LSD1)(Yang et al., 2006). HDAC1/2 removes acetyl groups from histone tails whereas Kdm1a removes di-/tri-methylation marks from H3K4. Although much attention has been focused on understanding the biochemical functions of Rcor1, its functional role *in vivo* has only begun to be explored.

To begin to understand the biological function of Rcor1 *in vivo*, we recently generated *Rcor1* knockout mice (Yao et al., 2014). These null mutants had severe defects in fetal liver erythropoiesis, resulting in a profound anemia that caused lethality late in gestation. We demonstrated that Rcor1's major function in maturing proerythroblasts is to repress genes enriched in both hematopoietic stem/progenitor cells and the myeloid lineage, many of which are detrimental to erythropoiesis.

Numerous lines of evidence suggest that the repressor activities of Rcor1 are not restricted to the erythroid lineage. For example, knocking down Rcor1 expression in fetal

liver cells blocks *in vitro* differentiation of megakaryocytes (Saleque et al., 2007; Upadhyay et al., 2014). In addition, biochemical studies have identified several DNA binding transcription factors that physically interact with Rcor1/Kdm1a in different hematopoietic cell types. These transcription factors, including Gfi1 and Gfi1b (Saleque et al., 2007), have been shown to regulate key aspects of hematopoietic differentiation *in vivo*. For example, the zinc finger protein Gfi1 is critical for granulocyte differentiation (Hock et al., 2003; Karsunky et al., 2002) and also regulates the production of common lymphoid progenitors as well as B-cell and T-cell differentiation (van der Meer et al., 2010). The Gfi1 homolog, Gfi1b, is necessary for both erythroid and megakaryocytic differentiation (Foudi et al., 2014; Saleque et al., 2002). Although these interactions suggest potential roles for Rcor1 in myelomonocytic, lymphoid and megakaryocytic differentiation, it is not yet known which hematopoietic cell lineages are functionally dependent on Rcor1 activity.

To assess Rcor1 function throughout the hematopoietic system and to bypass the embryonic lethality in the whole-animal Rcor1 knockout model, we generated an *Mx1-Cre* driven (Kuhn et al., 1995) *Rcor1* knockout mouse and studied the effects of *Rcor1* ablation in adult hematopoiesis. The loss of Rcor1 in adult hematopoietic cells leads to a complex phenotype that includes a complete block in erythroid and neutrophil differentiation along with a sparing of the megakaryocyte lineage. These findings, along with a marked increase in abnormal monocytes, reveal that Rcor1 deficiency results in a severe myelodysplasia/myeloproliferative disorder.

Materials and methods

Mice

Generation of *Mx1-Cre; Rcor1*$^{flox/-}$ mice (B6.CD45.2) and genotyping was performed as previously described (Yao et al., 2014). To induce Rcor1 deletion (*Rcor1*$^{flox/-}$→*Rcor1*$^{-/-}$), 8-12 week old mice were injected every other day (3 injections total) with 250-350µl of double stranded polyinosinic:polycytidylic acid (poly(I:C); 0.5mg/ml, Amersham Biosciences). Age-matched *Mx1-Cre; Rcor1*$^{flox/+}$, *Rcor1*$^{flox/-}$ mice treated with poly(I:C) were used as controls. For transplantation studies, B6.CD45.1, B6.CD45.2/ B6 Thy1.2 CD45.1 hybrids or double congenic B6.CD45.1 Hbbd mice (8-12 weeks old) were used as primary recipients and maintained on acidified water for at least 1 week prior to irradiation with an RS2000 X-ray irradiator (Rad Source) or a Cs^{137} irradiator (J.L. Shepherd). 1-3x10^6 control or *Rcor1*$^{-/-}$ unfractionated bone marrow was transplanted into sublethally irradiated (500-700 Gy) recipient mice. Sorted Lin$^-$Sca1$^-$c-kit$^+$ (LSK) cells (1500-2500 cells) from untreated or poly(I:C) treated *Mx1-Cre; Rcor1*$^{flox/-}$ and control donors were co-transplanted with competitor bone marrow (1-2 x10^5 cells) from B6.CD45.1 or B6.CD45.1 EGFP$^+$ (TgN(act-EGFP)OsbY01) donors into lethally irradiated recipient mice (1000cGy). Transplant recipients were provided antibiotic-supplemented water for 1 month as previously described (Li et al., 2010). All animal procedures were performed in accordance with the Institutional Animal Use and Care Committee at Oregon Health & Science University.

Flow cytometry analysis and fluorescence activate cell sorting (FACS)

Single cell suspensions from bone marrow, spleen and red-cell depleted peripheral blood were prepared as previously described (Goldman et al., 2009). Immunophenotyping of myeloerythoid progenitors (Pronk et al., 2007) and CMP/GMP/MEP progenitors (Akashi et al., 2000) was carried out following published methods and analyzed on either an LSRII, Canto, FACS Calibur or Fortessa cytometer (BD). For apoptosis analysis, an Annexin-V Apoptosis Detection Kit I (BD Pharmingnen) was used together with 7-Aminoactinomycin D according to the manufacturer's instructions. Cell sorting was performed using a BD Influx or a BD Vantage sorter. Dead cells were excluded with propidium iodine and doublets were excluded using FSC-A, FSC-H and trigger pulse width parameters. Data were analyzed with FlowJo software (Tree Star, Inc).

Antibody used in this study include: CD71 (R17217),Mac1 (M1/70), Gr1 (RB6-8C5), B220 (RA3-6B2), IgM (eB121-15F9), CD3 (145-2C11), and c-kit (2B8) from eBioscience; CD19 (1D3), CD4 (H29.19), CD5 (53-7.3), CD8 (53.6.7), CD16/32 (2.4G2,), CD34 (RAM34), CD115 (AFS98) from BD Pharmingen; TER119, Sca1 (D7), CD150 (TC15-12F12.2), CD105(MJ7/18), CD127/IL-7Rα (A7R34), and CD41 (MWReg30) from Biolegend. For analysis of CMP/GMP/MEP, the lineage panel included B220, CD3, CD4, CD8, Gr1, Ter119, CD19, IgM and CD127. For analysis of myeloerythroid progenitors, the lineage panel included B220, CD4, CD8, Mac1 and Gr1. To sort MkP, Ter119 was also included within this lineage mixture. For LSK sorting, the lineage panel included: B220, CD3, CD4, CD5, CD8, Mac1, Gr1 and Ter119.

Hemoglobin electrophoresis

Hemoglobin electrophoresis was performed as described (Chapter 3). Briefly, peripheral blood was lysed and the hemoglobin in lysate was separated by a cellulose acetate plate (Helena Laboratories, Beaumont, TX) and stained with Ponceau S.

In vitro colony forming assays

For colony forming unit (CFU) assays, cells were plated in duplicate or triplicate in 35mm dishes in mouse methylcellulose complete medium (R&D systems, HSC007) or in cytokine-free methylcellulose medium (M3234, Stem Cell Technologies). Colonies were scored 7-10 days after plating. For serial replating assays, colonies were picked on day 8, pooled and washed in DMEM containing 10% serum. Cells were counted and then replated in fresh methylcellulose medium. For megakaryocyte (Mk) progenitor assays, Mega-CultC (04950, Stem Cell Technologies) was supplemented with recombinant mTPO (50ng/ml) and mIL3 (10ng/ml) from Peprotech. Cultures of $1x10^5$ unfractionated bone marrow cells were dehydrated, fixed, stained and CFU-Mk were scored according to the manufacturer's instructions.

Morphological analysis and immunofluorescence microscopy

Bone marrow was transferred onto slides by touching the longitudinally cut femoras to the slide, peripheral blood was smeared onto slides, and sorted cells or dispersed colonies were cytospun onto slides. After staining with May-Grunwald and Giemsa stains (Sigma Aldrich), slides were mounted with Permount (Vector Laboratories). For vWF staining of bone marrow, tibias were fixed, decalcified and cryopreserved as previously described (Goldman et al., 2009). Cryosections were stained with rabbit anti- human vWF (Dako;

1:400), goat anti-rabbit cyanine 3 (Millipore; 0.5ug/ml), 4',6-diamidino-2-phenylindole (DAPI) and then mounted with FluoromountG (SouthernBiotech).

Statistical Analysis

Data were analyzed using Microsoft Excel or Prism 6 (GraphPad Software). Unless indicated, a two tailed, unpaired Student's t-test was used for assessing statistical significance. A p-value of <0.05 was considered significant.

Results

Deletion of *Rcor1* in adult hematopoietic cells results in a rapidly lethal anemia and abnormal leukocytes in the peripheral blood.

To assess Rcor1 function in the adult hematopoiesis, I generated mice carrying *Mx1-Cre* transgene and a single functional *Rcor1* allele in which exon 4 was flanked by loxP sites (*Mx1-Cre; Rcor1*$^{flox/-}$). Administration of polyinosinic:polycytidylic acid (poly(I:C) was used to induce Cre expression in interferon-responsive cells (Kuhn et al., 1995), and two weeks following Cre induction, genotype analysis confirmed the absence of the *Rcor1*^{flox} allele in the bone marrow (Figure 4.1B). Hereafter, we refer to these poly(I:C) induced Rcor1-deficient mice as *Rcor1*$^{-/-}$. Age-matched *Rcor1*$^{+/-}$ and *Mx1-Cre; Rcor1*$^{+/flox}$ mice were used as controls for these studies (Figure 4.1A), as both are heterozygous for *Rcor1 (Rcor1*$^{+/-}$*)* in BM cells after Cre induction (Figure 4.1B).

Whereas control mice remained healthy, the majority of *Rcor1*$^{-/-}$ mice died within 3 weeks following poly(I:C) treatment (Figure 4.1C), a time course consistent with bone marrow failure. Analysis of the peripheral blood revealed a rapidly progressive anemia in

Rcor1$^{-/-}$ mice consistent with a complete block in red cell production. (Figure 4.1D). By contrast, platelet counts increased transiently following Cre induction and then returned to normal levels (Figure 4.1E). The total number of circulating white blood cells (WBC) was persistently elevated exclusively due to an increase in circulating myelomonocytic cells (Figure 4.1F). Moreover, infiltrates of myelomonocytic cells were observed in the liver (Figure 4.1G).

The *Mx1* promoter is known to be active in some non-hematopoietic tissues, including the liver and bone marrow stroma (Park et al., 2012). To determine if restricting the loss of Rcor1 expression to hematopoietic cells will fully recapitulate these erythroid and myelomonocytic lineage abnormalities, chimeric mice in which *Mx1-Cre; Rcor1*$^{flox/-}$ cells contributed to >90% of hematopoietic cells were generated by the transplantation of unfractionated BM (Figure 4.2A). Two weeks following Cre induction, the BM-restricted knockout mice demonstrated anemia and an increase in circulating myelomoncoytic cells, but no significant change in circulating platelet counts (Figure 4.2B). This anemia rapidly progressed, and the mice were moribund within 3 weeks of induction. Taken together, these data demonstrate that Rcor1 expression is required in a hematopoietic cell-intrinsic manner to maintain the steady state production of cells of both the myeloid and erythroid lineages.

Rcor1 is required for the maturation of committed erythroid cells.

Rcor1$^{-/-}$ mice displayed splenomegaly suggesting anemia-induced extramedullary hematopoiesis (Figure 4.3A). Despite having elevated WBCs, the mutant mice had 32% fewer nucleated cells within their long bones than controls (Figure 4.3B). To begin to

determine which stages of adult erythroid cell maturation were affected by the loss of Rcor1, erythroid maturation was assessed by flow cytometry analysis of CD71 and Ter119 (Socolovsky et al., 2001). Whereas this antibody combination clearly distinguished proerythroblasts ($CD71^{hi}Ter119^{lo}$), maturing erythroblasts ($CD71^{hi/int}$ $Ter119^{hi}$) and reticulocytes ($CD71^{-}Ter119^{hi}$) in control cells, a highly aberrant expression pattern in the *Rcor1*$^{-/-}$ mice precluded the identification of normal erythroid maturation stages (Figure 4.3C).

To determine whether erythroid commitment was altered in Rcor1-deficient mice, phenotypically defined erythroid progenitors described by Pronk and colleagues were evaluated (Pronk et al., 2007). This analysis revealed a marked accumulation of $CD105^{+}$,$CD150^{-}$ cells (CFU-E) and $CD105^{+}$,$CD150^{+}$ cells (Pre-CFU-E) within the Lin^{-} $Sca1^{-}Kit^{+}$ ($LS^{neg}K$) myeloerythroid progenitor compartment (Figure 4.3D-E). To functionally test these erythroid progenitor cells, *Rcor1*$^{-/-}$ $LS^{neg}K$ cells were plated in a methylcellulose assay supplemented with EPO, SCF, IL-3 and IL-6. A 90% reduction in BFU-E colony forming activity (Figure 4.3F) indicated that in the absence of Rcor1, erythroid maturation is blocked downstream of phenotypically defined CFU-E.

To determine whether a normal hematopoietic microenvironment can alleviate the block in erythropoietic maturation, bone marrow (BM) isolated from CD45.2 *Rcor1*$^{-/-}$ mice with the Hbbd beta hemoglobin haplotype was infused into sublethally irradiated wild type CD45.1 host mice with the Hbbs beta hemoglobin haplotype (Figure 4.3G). Donor cell engraftment was monitored 2-9 weeks post-transplant, and all recipient mice appeared healthy and had normal RBC parameters (data not shown). Although >50% of

circulating leukocytes were derived from *Rcor1*$^{-/-}$ cells (Figure 4.3H), no *Rcor1*$^{-/-}$ donor-derived hemoglobin was detected in the peripheral blood (Figure 4.3I). These data demonstrate a cell-autonomous requirement for Rcor1 in the maturation of committed adult erythroid progenitor cells into mature red blood cells.

Thrombopoiesis is not Rcor1 dependent

The knockdown of Rcor1 expression has been reported to block megakaryocyte maturation in a megakaryoblast leukemia cell line (Saleque et al., 2007) and in cultured mouse primary fetal liver hematopoietic cells (Upadhyay et al., 2014). Based on these findings, we expected the *Rcor1*$^{-/-}$ mice to display defects in thrombopoiesis; however, circulating platelet counts were actually transiently elevated and never fell below normal levels (Figure 4.1E). Mature megakaryocytes with a normal morphology and vWF expression pattern were detected were present in *Rcor1*$^{-/-}$ BM (Figure 4.4A-B). Although the frequency of megakaryocyte progenitors (MkP: Lin^{-}, Scal-1^{-}, c-kit^{+}, CD150^{+}, CD41^{+}) (Pronk et al., 2007) was variable in the mutant mice, it was not statistically significant different from controls (Figure 4.4C-D). In culture conditions supporting megakaryocyte differentiation, *Rcor1*$^{-/-}$ cells produced acetylcholinesterase^{+} (AchE^{+}) CFU-Mk at a similar frequency to controls, although the Mk colonies were reduced in size (Figure 4.4E-F). To exclude the possibility that *Rcor1*$^{flox/-}$ megakaryocytes persist in poly(I:C) treated *Mx1-Cre Rcor1*$^{flox/-}$ mice due to incomplete Cre-mediated recombination, we isolated MkP progenitors and performed PCR genotyping. In two independent experiments, only the *Rcor1*$^{-}$ allele was detected, indicating complete ablation of *Rcor1* in the megakaryocytic lineage (Figure 4.4G). Based on these findings, we conclude that

Rcor1 is not essential for megakaryocyte maturation and the maintenance of normal platelet counts.

Absence of mature neutrophils and increased monopoiesis in Rcor1-deficient mice

To assess myeloid cells in the *Rcor1*$^{-/-}$ mice, May-Grunwald Giemsa stained PB smears and bone marrow touch preparations were examined. Whereas mature granulocytes were almost completely absent, immature myelomonocytic cells, monocytes and eosinophils were readily detectable (Figure 4.5A-B). Cell sorting combined with morphological analyses was performed to further assess myelomonocytic lineage differentiation. Consistent with the absence of mature granulocytes, the *Rcor1*$^{-/-}$ mice displayed dramatically decreeased Mac1^{+}Gr1^{hi} cells within the BM, spleen and PB (Figure 4.5C-D). Analysis of the remaining Mac1^{+}Gr1^{hi} cells in the mutant BM revealed the presence of both eosinophils and monocytes (Figure 4.5E-F).

More than 50% of the mutant BM had a Mac1^{+}Gr1^{low} phenotype compared to only ~10% in control mice (Figure 4.5C-D). Expansion of Mac1^{+}Gr^{low} cells and loss of Mac1^{+}Gr1^{hi} cells were also observed in *Mx1-Cre Rcor1*$^{flox/-}$ BM chimeric mice after Cre induction indicating a hematopoietic cell-autonomous defect (Figure 4.1H and data not shown). Normally, the Mac1^{+}Gr1^{low} cell population is primarily comprised of maturing granulocytes, though some monocytes are present (Figure 4.5E) (Hestdal et al., 1991; Walkley et al., 2002). By contrast, the Mac1^{+}Gr1^{low} cell population from *Rcor1*$^{-/-}$ BM almost exclusively contained monocytes although a few immature granulocytes were detected (Figure 4.5F). Both CD48 and Gr-1 expression were evaluated , as a

combination of these markers distinguishes 5 functionally and developmentally distinct subpopulations of myelomonocytic cells,(Vassen et al., 2012) namely: maturing granulocytes ($CD48^{lo}Gr1^{hi}$, R1), monocytes ($CD48^{hi}Gr1^{int}$; R2), precursor cells with both monocytic and granulocytic potential ($CD48^{hi}Gr1^{lo}$, R3) and granulocyte-committed precursors ($CD48^{lo}Gr1^{lo}$, R4; $CD48^{lo}Gr1^{int}$, R5). In the *Rcor1*$^{-/-}$ mice, although the maturing granulocytic cell population (R1) was nearly absent, granulocyte-committed precursor populations (R4, R5) were detected at normal frequency, indicating that neutrophil differentiation but not specification is Rcor1-dependent. The frequency of monocytic cells (R2) and mixed potential cells (R3) were increased 15-fold and 2.3 fold, respectively (Figure 4.5G-H). Supportive of our finding of expanded monopoiesis, most of the $Mac1^{+}$ cells in the Rcor1-deficient mice also co-expressed the receptor for CSF-1 (CD115; Figure 4.5I).

To test whether the defect is a cell autonomous defect, CD45.2 positive control and mutant whole bone marrow cells were transplanted into CD45.1 positive wild type host (Figure 4.6A). After transplant, even when donor cell engraftment level was low, mutant donor cells displayed the identical myelomonocytic differentiation defects, including decrease of $Mac1^{+}Gr1^{hi}$ mature granulocytes and increase of immature $Mac1^{+}Gr1^{low}$ population (Figure 4.6B). Also CD48-Gr1 staining recapitulated the loss of the R1 population and expanded R2 population (Figure 4.6C-D). The results taken together indicate that the block in neutrophil differentiation and excessive monocyte production are truly hematopoietic-cell autonomous defects. Although in some mice, the *Rcor1*$^{-/-}$

myeloid cells slowly accumulated in the recipient bone marrow, progression to leukemia was not observed.

Monocytosis in *Rcor1*$^{-/-}$ mice is driven primarily by the expansion of differentiating cells.

To begin to determine the mechanism of monocytic expansion in the *Rcor1*$^{-/-}$ mice, the frequency of both phenotypically and functionally-defined myelomonocytic progenitor cells was assessed. Although the size of the LS^{neg}K myeloerythroid progenitor compartment was increased 14-fold in the *Rcor1*$^{-/-}$ BM (Figure 4.7A), distinct populations of common myeloid progenitors (CMP) and granulocyte/monocyte progenitors (GMP)(Akashi et al., 2000) could not be easily identified due to aberrant cell surface marker expression (Figure 4.7B). Further fractionation of LS^{neg}K cells with an alternative combination of markers (Pronk et al., 2007) revealed that most of the LS^{neg}K cell subset in the *Rcor1*$^{-/-}$ mice was comprised of phenotypically defined erythroid progenitors (Figure 4.3D-E). The only expanded myeloid progenitor population detected was the CD41^{-}CD150^{-}CD16/32^{+} GMP, which was only 1.6 fold higher than controls. These phenotypic GMPs inappropriately expressed CD105 (Figure 4.7C-E). The other myeloid progenitor population, pre-GM (GMP precursors), were reduced in frequency by 66% (Figure 4.3D and Figure 4.7E).

To functionally assess myeloid cell progenitor frequency in *Rcor1*$^{-/-}$ mice, the myeloid colony forming activity of unfractionated BM and sorted LS^{neg}K cells was evaluated. *Rcor1*$^{-/-}$ BM formed significantly more myeloid colonies than control BM on a per cell basis, indicative of increased progenitor cell activity (Figure 4.7F). Specifically,

colony forming activity for monocytes/macrophages (CFU-M) was 16-fold higher in *Rcor1*$^{-/-}$ BM. Although mutant LS^{neg}K cells were also CFU-M biased, they formed 50% fewer myeloid CFU than their normal counter parts (Figure 4.7G), produced no detectable granulocytic colonies (CFU-G) and showed a 66% decrease in granulocyte/monocyte/macrophage colonies (CFU-GM). Thus, a significant amount of CFU activity in the *Rcor1*$^{-/-}$ WBM must have arisen outside of the LS^{neg}K cell subset (Figure 4.7A). Consistent with this finding, lineage marker expressing (Lin+) cells isolated from *Rcor1*$^{-/-}$ mice had 10-fold higher CFU activity than control Lin^{+} cells (data not shown).

As the Mac1^{+}Gr1^{low} cells comprised such a large proportion of the Lin^{+} BM cells in *Rcor1*$^{-/-}$ mice (Figure 4.5C), we directly tested their CFU activity. As expected, control Mac1^{+}Gr1^{low} cells had almost no detectable CFU potential and formed <1 colony per $5x10^3$ input cells. By contrast, mutant Mac1^{+}Gr1^{low} cells generated a mean of 92 CFU-M colonies per $5x10^3$ input cells (Figure 4.7H). Morphological analysis of the CFUs derived from the mutant Mac1^{+}Gr1^{low} cells confirmed their monocytic identity and also revealed that these cells were capable of differentiating into macrophages (Figure 4.7I). Remarkably, the Mac1^{+}Gr1^{lo} cells from Rcor1-deficient mice also possessed extensive serial replating activity and continually produced CFU-M for up to 5 passages in culture (Figure 4.7J). Interestingly, this robust CFU-M activity was completely dependent on the presence of cytokines, indicating these monocytic cells were not able to proliferate autonomously. Analysis of apoptosis in Mac1^{+}Gr1^{lo} BM cells directly isolated from *Rcor1*$^{-/-}$ mice revealed a 60% reduction in apoptotic cells compared to controls (Figure

4.7K). Together, these data indicate that the $Mac1^{+}Gr1^{lo}$ cell subset in the *Rcor1*$^{-/-}$ mice are cytokine-dependent, monocyte lineage cells that are resistant to apoptosis and possess extensive, abnormal self-renewal activity.

Discussion

In this study, we report the first *in vivo* functional analysis of the co-repressor Rcor1 in adult hematopoietic cell differentiation, and our findings are summarized in Figure 4.8. The Rcor1 knockout mice exhibited a subset of phenotypes consistent with certain clinical features of myelodysplastic syndrome (MDS) (Beachy and Aplan, 2010). Specifically, the differentiation of two major erythro-myelocytic lineages, erythrocytes and neutrophils, was completely blocked following Rcor1 deletion. The Rcor1-deficient mice also displayed features of myeloprolifeative neoplasms (MPN), namely a monocytic cell expansion that caused monocytosis and a monocytic liver infiltration. Importantly, Rcor1-deficient mice did not have any evidence of acute leukemia, and the enhanced survival and proliferation of the Rcor1-deficient monocytic cells were completely cytokine-dependent. Moreover, engraftment of *Rcor1*$^{-/-}$ cells into wild type hosts was dependent upon preconditioning with irradiation. This combination of dyserythropoiesis, dysgranulopoiesis and monocytosis in the Rcor1-deficient mice fits well with the evolving diagnostic criteria for MDS/MPN (Orazi and Germing, 2008). Although we have not observed transformation to acute myeloid leukemia in recipient mice for more than a year following transplant, more time may be required to develop the necessary mutations.

The etiology of MDS is just beginning to be understood. Recent genome wide discovery studies have identified a set of novel disease alleles in patients with MDS including MDS/MPN. Among these are several genes with a known or putative role in the epigenetic regulation of gene expression including TET2, ASXL1, EZH2, and DNMT3a (Issa, 2013; Patnaik et al., 2014). These findings underscore the importance of epigenetic modifiers in the etiology of MDS. Although mutations in Rcor1 have not yet been reported in human disease, our results raise the possibility that disruption of Rcor1 expression and/or function may contribute to the progression of myelodysplasia. Studies evaluating Rcor1 mutations in patients with MDS, MDS/MPN and bone marrow failure syndromes are currently underway.

The Rcor1/Kdm1a complex was previously shown to be a cofactor for Gfi1 or Gfi1b mediated transcriptional repression in different hematopoietic cell lines (Saleque et al., 2007). A comparison of adult hematopoietic defects in our Rcor1 knockout model with those reported for Kdm1a, Gfi1 and Gfi1b knockout mice provides additional insights into the biological relevance of these biochemical interactions. For example, if Rcor1 works together with Kdm1a, Gfi11 or Gfi1b to regulate a specific hematopoietic lineage *in vivo*, then it would be predicted that the loss of any component of this complex would cause identical lineage-specific defects. Indeed, the erythroid defects observed in *Rcor1*$^{-/-}$ mice phenocopy those observed in both Kdm1a-deficient and Gfi1b-deficient mice (Foudi et al., 2014; Kerenyi et al., 2013). Likewise, the ablation of Kdm1a, Gfi1 or Rcor1 causes severe neutropenia (Hock et al., 2003; Karsunky et al., 2002; Kerenyi et al.,

2013). Thus, all available data support previous reports that Rcor1/Kdm1a and Gfi11 or Gfi1b complexes regulate erythroid and granulocytic maturation.

Interestingly, not all hematopoietic phenotypes in Rcor1- , Kdma1-, Gfi1- and Gfi1b-deficient mice are identical. One of the most discordant phenotypes among the mutant mice is within the megakaryocyte lineage. While loss of Kdm1a or Gfi1b causes severe thrombocytopenia (Foudi et al., 2014; Kerenyi et al., 2013), loss of Rcor1 causes a transient increase in circulating platelets. Moreover, although *Gfi1b*$^{-/-}$ cells derived from either fetal liver or adult BM cannot form AchE^{+} megakaryocytic colonies in culture (Foudi et al., 2014; Saleque et al., 2002), both *Rcor1*$^{-/-}$ BM and fetal liver cells (H.Y and D.G., unpublished findings) produce AchE^{+} CFU-Mk. Although the maintenance of thrombopoiesis in Rcor1-deficient mice may simply reflect the functional redundancy among Rcor family members (Yang et al., 2011), these findings also raise the possibility that Gfi1b may normally use a cofactor other than Rcor1 in promegakaryocytes. Given the fact that Rcor1 function is not compensated for in all hematopoietic lineages, our results suggest that the molecular mechanisms that are employed during lineage differentiation are significantly more complex than previously recognized.

In conclusion, we have shown that the maturation of both erythroid cells and neutrophils are critically dependent on the transcription co-repressor Rcor1. By contrast, monocytic cell survival and self-renewal is enhanced in the absence of Rcor1. These results provide new insights into the complexity of the transcription regulatory networks that regulate normal hematopoiesis. As *Rcor1*$^{-/-}$ mice develop a severe myelodysplasia, it will be important to determine whether loss of Rcor1 function or expression is

responsible for the pathogenesis in subsets of patients with bone failure syndromes and myelodysplasia

Acknowledgements

We thank Carly Hernandez, Kim Hamlin, Hyunjung Lee, Andrea Ansari and Travis Polston for technical support. The work was supported by NIH grants to WHF (HL069133, S10), GM (NS22518). HY was supported by an American Heart Association predoctoral fellowship. GM is an Investigator of the Howard Hughes Medical Institute.

Figures and legends

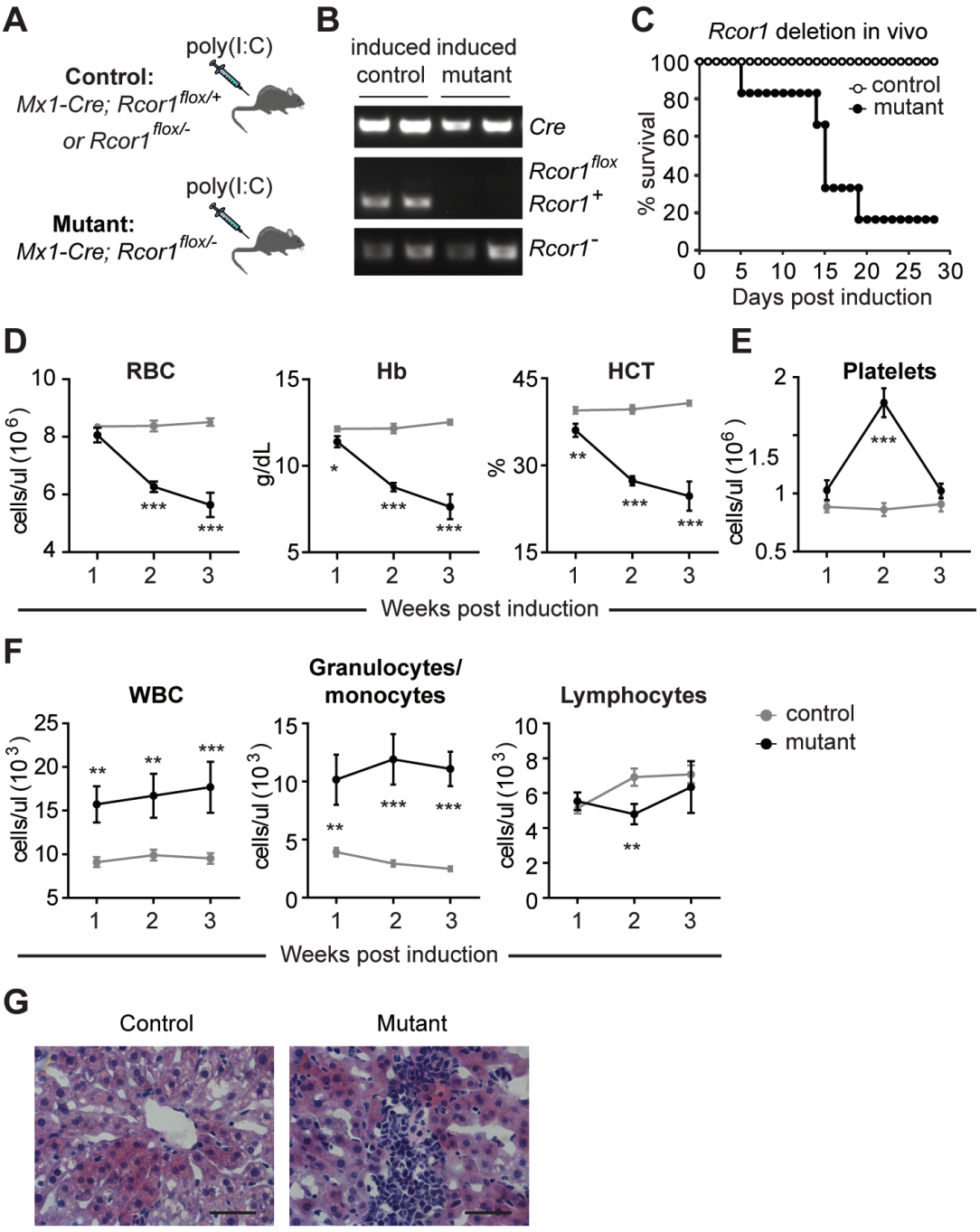

Figure 4.1 Loss of Rcor1 in adult mice causes a lethal anemia and expansion of myelomonocytic cells.

(A) Induction of Cre expression by injection of poly(I:C) in adult mice of the indicated genotypes. (B) PCR genotype analysis of bone marrow cells 2 weeks after Cre induction. Only the *Rcor1*$^{-}$ allele was detected in the mutant BM. (C) Survival analysis after *Rcor1* deletion. *Rcor1*$^{-/-}$ mice (N=6) typically died within 3 weeks of receiving poly(I:C), whereas all control mice (N=10) survived. (D) Circulating red blood cell (RBC) analysis. Progressive, severe reductions in RBC number, hemoglobin content (Hb) and hematocrit (HCT) were observed in *Rcor1*$^{-/-}$ mice. (E) Rcor1-deficient mice had transiently elevated platelet counts 2 weeks after Cre induction. (F) Circulating white blood cell (WBC) analysis. Leukocytosis in *Rcor1*$^{-/-}$ mice was driven by expansion of myelomonocytic cells. For (D-F) a minimum of 7 mice for each genotype was measured at each time point. The average ± the standard error of the mean (SEM) is shown, *$p<0.05$, **$p<0.01$, ***$p<0.001$. (G) Liver infiltration by myelomonocytic cells in *Rcor1*$^{-/-}$ mice. Images were acquired with a Zeiss Axiovert S-100, a Zeiss plan-neofluar 63X/1.25 oil lens and an AxioCam HRc camera. Scale bar: 50 microns.

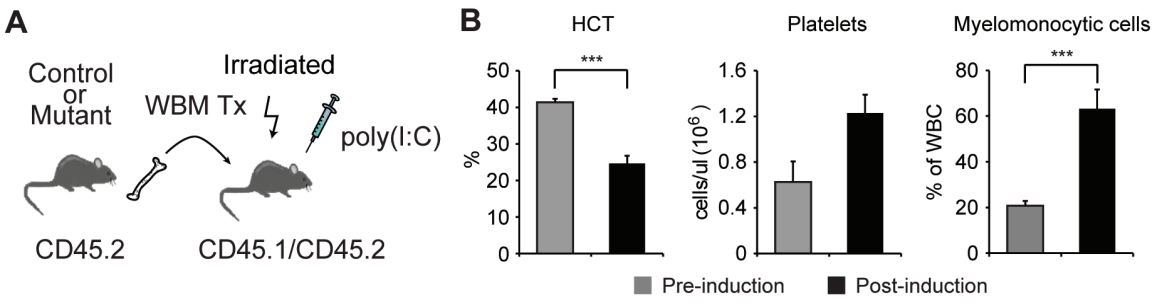

Figure 4.2 Maintaining the steady state production of erythroid and myeloid cells requires cell-intrinsic function of Rcor1.

(A) Generation of BM-chimeric mice in order to exclusively delete Rcor1 from hematopoietic cells. (B) Circulating blood analysis of BM- chimeric mice before and 2 weeks after Rcor1 deletion (N=3). The average ± the standard error of the mean (SEM) is shown, *p<0.05, **p<0.01, ***p<0.001. Paired, two-tailed Student's t-tests were used for statistical analysis.

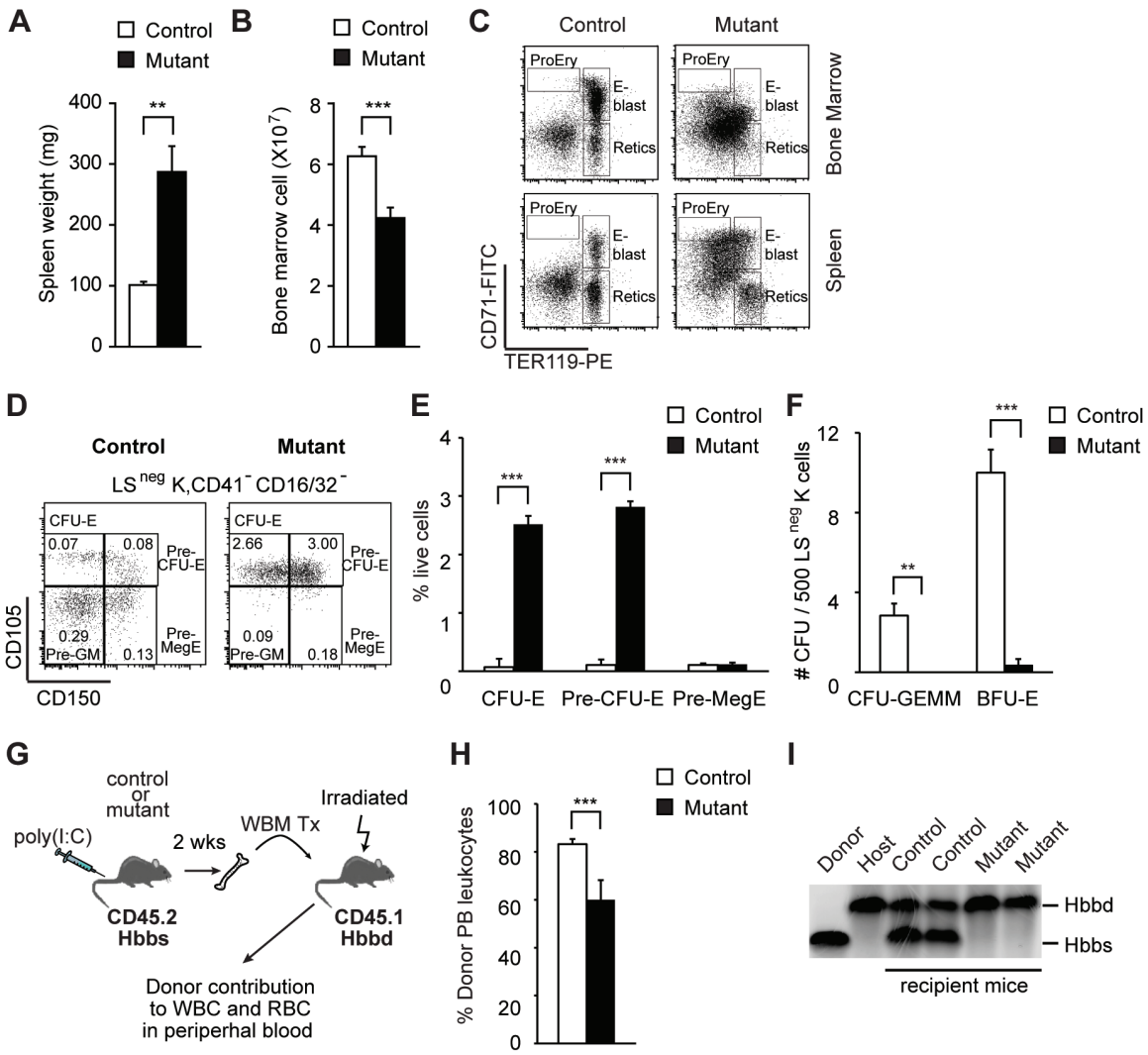

Figure 4.3 Lack of erythroid maturation in *Rcor1*$^{-/-}$ mice.

(A) Splenomegaly in Rcor1-deficient mice ($N_{control}$=8, N_{mutant}=10). (B) Decreased BM cellularity in *Rcor1*$^{-/-}$ mice ($N_{control}$=12, N_{mutant}=11). (C) Flow cytometry analysis of developing red cells in BM. Normal populations of maturing erythroid cells were not detected in mutant mice. ProEry: proerythroblasts; E-blast: erythroblasts; Retics: reticulocytes. (D) Flow cytometry analysis and (E) quantification of BM progenitors ($N_{control}$=3, N_{mutant}=3). Committed erythroid progenitors (CFU-E and Pre-CFU-E) were

significantly expanded in *Rcor1*$^{-/-}$ mice relative to controls, but bipotent erythroid and megakaryocyte progenitor (pre-MegEs) were not. Pre-GM: pre-granulocyte/macrophage progenitor (Pronk). The frequency of each population in total BM is indicated. (F) Lack of erythroid colony activity by myeloerythroid progenitors (Lin^{-}Sca1^{-}c-kit^{+}, LS^{neg}K) isolated from *Rcor1*$^{-/-}$ mice. Data from 3 independent experiments are shown. BFU-E: gurst forming unit-erythroid; CFU-GEMM: colony forming unit-granulocyte/erythrocyte/macrophage/megakaryocyte. (G) Transplantation schema for assessing the RBC potential of *Rcor1*$^{-/-}$ BM cells in a wild type environment. (H) PB donor cell analysis revealed a significant contribution of *Rcor1*$^{-/-}$ cells to circulating leukocytes in recipient mice ($N_{control}$=3, N_{mutant}=4). (I) RBC analysis of recipient mice ~4 weeks post-transplant. Hemoglobin derived from *Rcor1*$^{-/-}$ donor cells was below the level of detection (5%). The average ± the standard error of the mean (SEM) is shown, *p<0.05, **p<0.01, ***p<0.001.

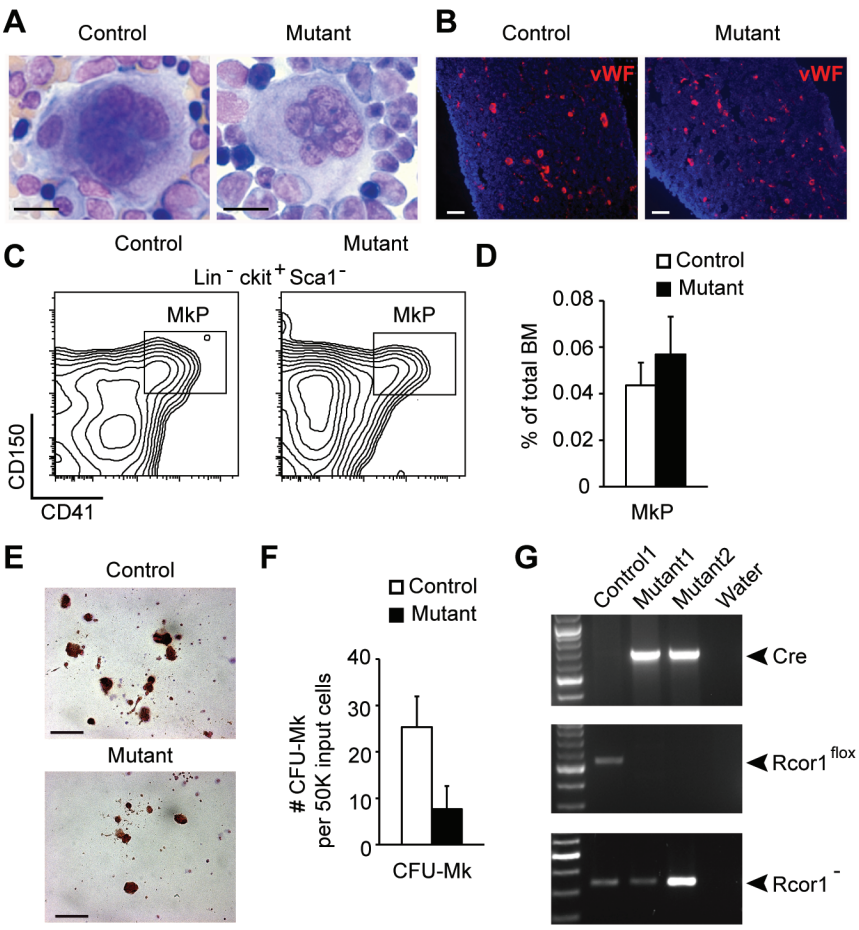

Figure 4.4 Rcor1 is dispensable for thrombopoiesis.

(A) May-Grunwald Giemsa stained bone marrow touch preparations and (B) vWF immunostaining of tibia sections revealed normal megakaryocyte morphology in *Rcor1-/-* mice. (C) Flow cytometry analysis of megakaryocyte progenitors (MkP). (D) MkP frequency was not significantly altered in Rcor1-deficient mice (Ncontrol=3, Nmutant=5). (E) Example of an acetylcholinesterase+ CFU-Mk derived from control and mutant BM cells. (F) CFU-Mk activity by Rcor1-deficient BM was not statistically different than control BM (Ncontrol=3, Nmutant=3). (G) Genotyping of FACS sorted MkPs after induction. Scale Bars: (A-B) 20 microns; (F) 100 microns. The average ± SEM is shown.

***p<0.001. Imaging was performed with a Zeiss Axiovert S-100, an AxioCam HRc camera and a Zeiss plan-neofluar 20X/0.50 lens.

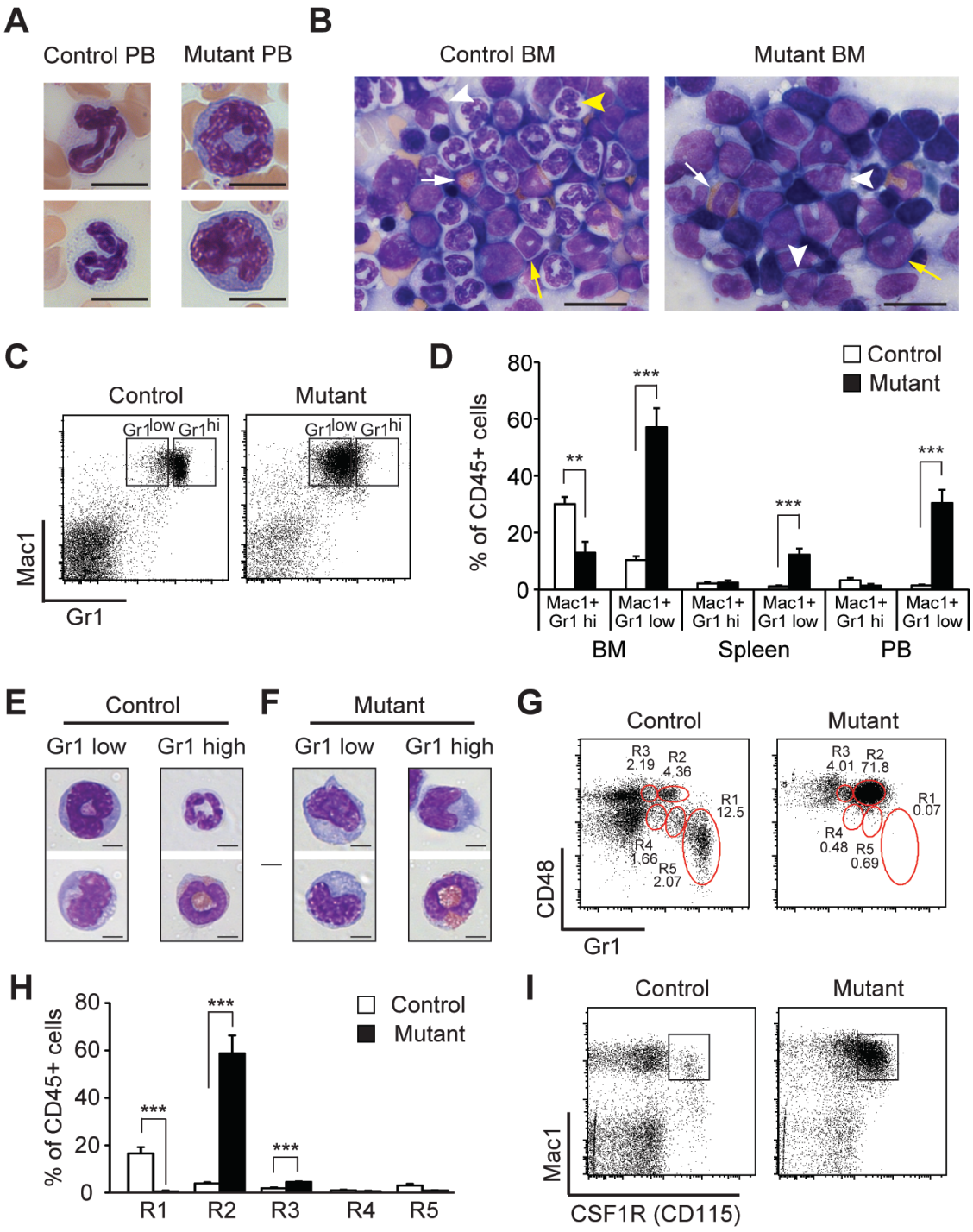

Figure 4.5 Loss of neutrophils and increased monocytes in Rcor1-deficient mice.

May-Grunwald Giemsa stained (A) PB smears or (B) BM touch preparations. Circulating mature neutrophils were not found in mutant mice. Likewise, mature neutrophils in the BM (yellow arrow head) were absent from *Rcor1*$^{-/-}$ mice. Monocytes (white arrow head), eosinophils (white arrow), and some immature neutrophils (yellow arrow) were present. (C) Mac1 and Gr1 expression on bone marrow cells. (D) A significant reduction in the proportion of Mac1^{+}Gr1^{hi} cells and a significant increase in the proportion of Mac1^{+}Gr1^{low} cells were observed in Rcor1-deficient BM, Spleen and PB ($N_{control}$=9, N_{mutant}=9). (E-F) Morphology of sorted myelomonocytic cells from control (E) and Rcor1-deficient (F) BM. (G) Characterization of myelomonocytic cells mice based on CD48 and Gr1 expression. (H) Although Rcor1-deficient mice lacked granulocytes (R1), they retained granulocytic precursor cells (R4, R5) and had significantly increased monocytic (R2) and bipotential (R3) cell populations relative to control mice ($N_{control}$=4, N_{mutant}=4). (I) Most *Rcor1*$^{-/-}$ Mac1^{+} cells co-expressed the monocytic marker CSF-1R. The average ± SEM is shown, *p<0.05, **p<0.01, ***p<0.001. Images were acquired with a Zeiss Axiovert S-100, a Zeiss plan-neofluar 63X/1.25 oil lens and an AxioCam HRc camera. Scale bars: 10 microns (A), 20 microns (B) and 5 microns (E-F).

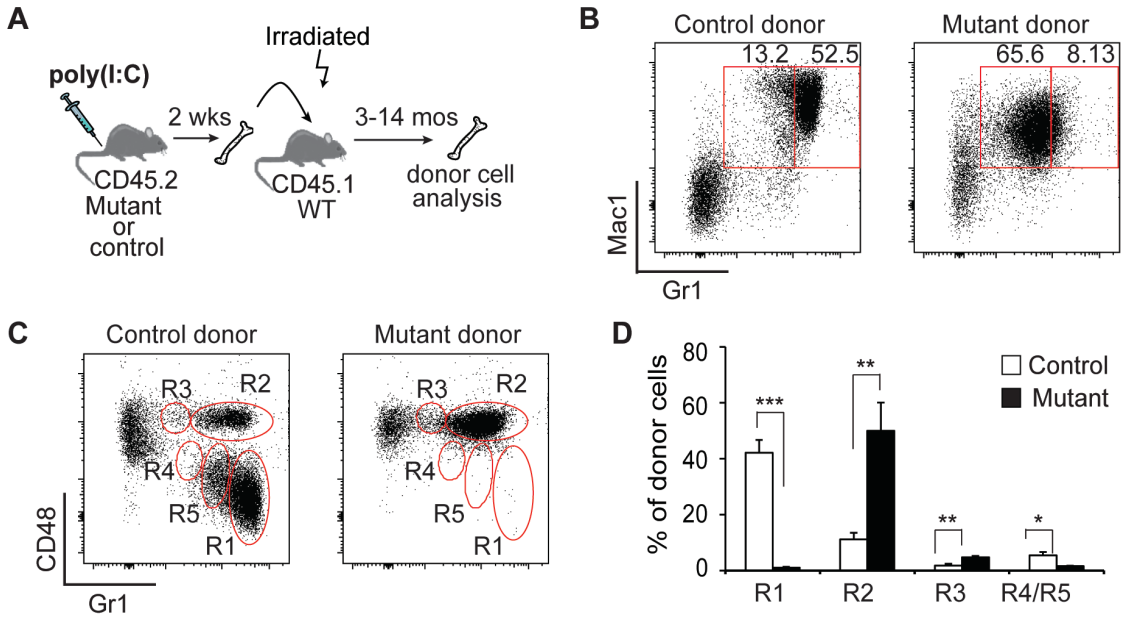

Figure 4.6 Knocking out of Rcor1 leads to loss of neutrophils and increase of monocytes.

(A) Cells after induction are transplanted into wild type host mice to test their myeloid different ion potential. (B-C) Analysis of control and mutant donor cell contribution to myelomonocytic populations after transplant into wild type hosts. Mutant cells fail to produce mature granulocytes ($Mac1^{+}Gr1^{hi}$ in B or R1 in C) and produce large monocytic cell populations ($Mac1^{+}Gr1^{lo}$ in B and R2 in C). (D) Quantification of mutant donor cells differentiation after transplant into a wild-type environment ($N_{control}=5$, $N_{mutant}=5$). The average ± SEM is shown, *p<0.05, **p<0.01, ***p<0.001.

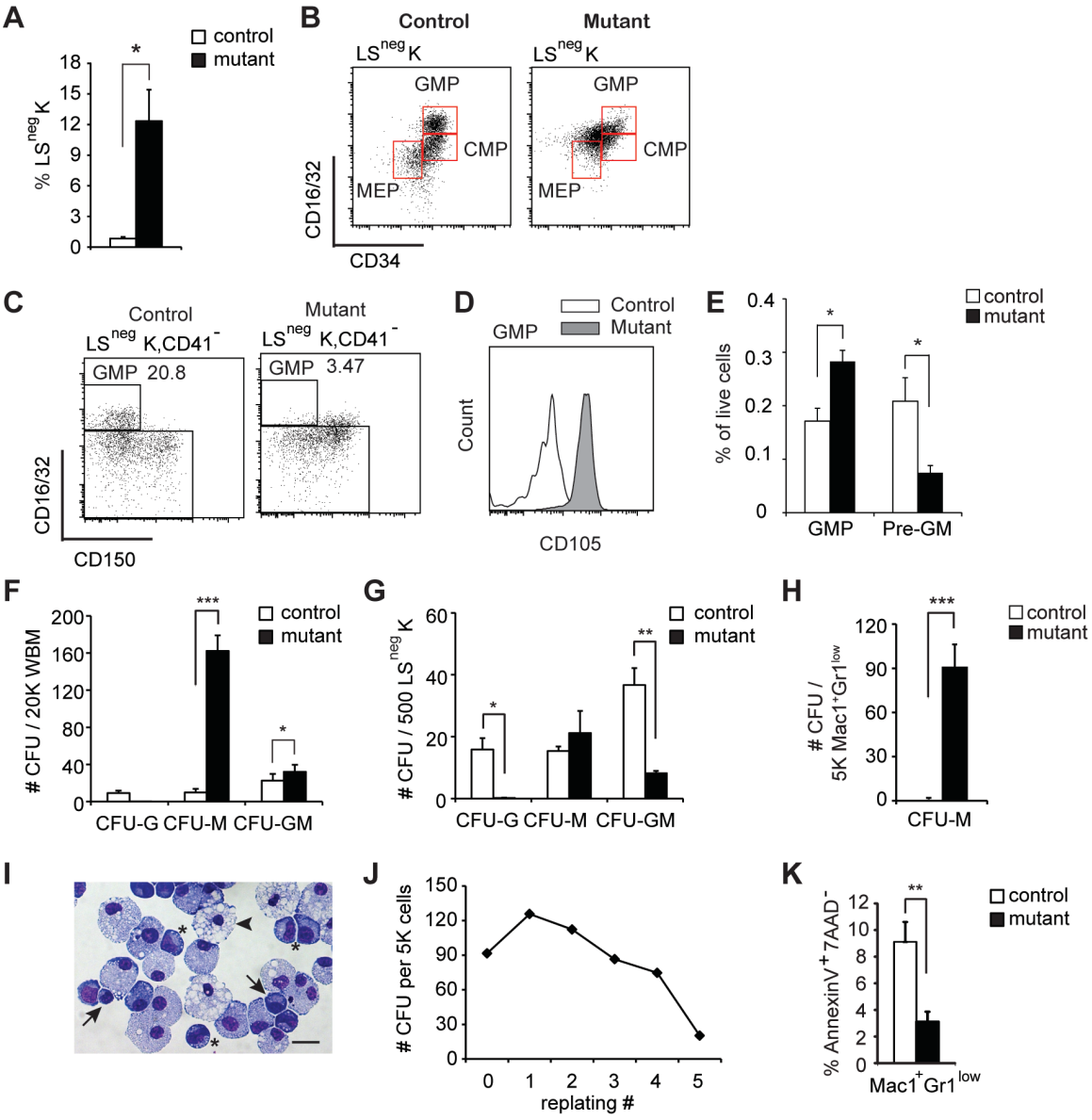

Figure 4.7 Abnormal myeloid progenitor cell activity in Rcor1-deficient monocytic cells

(A) Expansion of Lin$^-$Sca1$^-$ckit$^+$ (LS^{neg}K) myeloerythroid progenitor cells in the bone marrow of *Rcor1*$^{-/-}$ mice ($N_{control}$=4, N_{mutant}=5). (B) Aberrant CMP/GMP/MEP progenitor staining profile in mutant mice. (C) GMP progenitor analysis from control and mutant

BM. The frequency of GMP in parental gate is indicated. (D) Mutant GMP cells also express CD105. (E) The frequency of GMP and Pre-GM in total BM ($N_{control}$=3, N_{mutant}=3). (F-G) Comparison of myelomonocytic progenitor activity in: (F) unfractionated bone marrow (WBM); (G) sorted $LS^{neg}K$ cells ; (H) sorted $Mac1^{+}Gr1^{low}$ cells from mutant and control mice. Pooled results from 3 independent experiments are shown. (I) CFU derived from *Rcor1*$^{-/-}$ $Mac1^{+}Gr1^{low}$ cells contain maturing monocytes (asterisks), macrophages (arrow head) and immature cells similar to the $Mac1^{+}Gr1^{low}$ cells isolated from mutant mice used to seed the culture (arrow; also see Figure 4.5F). (J) CFU activity following serial replating every 8 days. $Mac1^{+}Gr1^{low}$ cells from mutants produced similar levels of CFU-activity through 4 serial replatings. (K) Decreased apoptosis in mutant $Mac1^{+}$ $Gr1^{low}$ cells in *Rcor1*$^{-/-}$ BM ($N_{control}$=4, N_{mutant}=5). The average ± SEM is shown, *p<0.05, **p<0.01, ***p<0.001. Imaging was performed with a Zeiss Axiovert S-100, an AxioCam HRc camera and a Zeiss plan-neofluar 40x/1.30 lens. Scale bar: 10 microns.

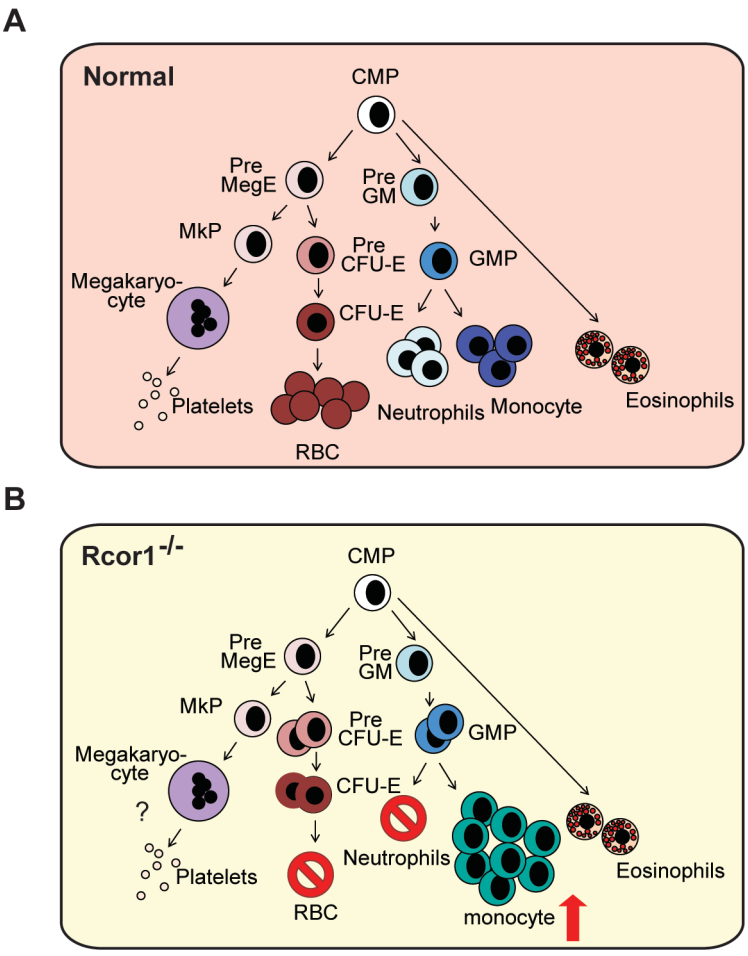

Figure 4.8 Summary of *Rcor1*$^{-/-}$ phenotype

(A) Normal differentiation of myeloerythroid lineages. (B) In *Rcor1*$^{-/-}$ mice, red blood cell and neutrophil differentiation are blocked downstream of committed progenitors in each lineage. Abnormal monocytes accumulate in the bone marrow, and some populations of phenotypic myeloerythroid progenitors are also increased. Megakaryocyte and platelet production are largely normal, but their functional status remains to be determined. CMP, common myeloid progenitor; GMP, granulocyte-macrophage progenitor.

CHAPTER 5: Concluding remarks and further direction

The main goal of my thesis work was to gain an understanding of the *in vivo* function of the transcription co-repressor Rcor1. Through characterization of three different Rcor1 knockout mouse models, we demonstrated that Rcor1 plays essential roles in the differentiation of multiple hematopoietic lineages (chapters 3 and 4), but is dispensable in nervous system development (chapter 2). Detailed analysis of fetal liver erythroid differentiation confirmed that Rcor1's function is to repress gene expression. Specifically, Rcor1 contributes to the establishment and maintenance of erythroid identity by repressing the expression of myeloid lineage genes as well as genes enriched in hematopoietic stem and progenitor cells (chapter 2). In this final section, I will place my results in the context of the field at large and propose the next steps that might be taken to advance this work.

Unraveling transcription networks

Transcription factors and their cofactors are important regulators of gene expression. Through different combination of these factors, thousands of gene expression patterns can be established by a limited number of transcription regulators. Previously, biochemical studies have revealed physical interactions among some transcriptional regulators, which laid a basic foundation for understanding their transcription networks. The development of genetically modified mice and the recent advance of large-scale, parallel sequencing techniques provide additional methods to further understand the importance of these interactions *in vivo*. Specifically, genetically modified mouse models allow us to re-evaluate the significance of physical interactions between factors based on the similarity of their biological functions *in vivo*. Parallel sequencing will allow us to

determine on a genome-wide level whether certain interactions exist on gene promoters. Our studies of the Rcor1 knockout mouse models provided new insights in to the transcriptional regulation network involved in Rcor1.

Rcor1 was first identified as a co-repressor for the neuronal repressor, REST (Andres et al., 1999). If interaction with Rcor1 is critical for REST's *in vivo* function, then we would expect that phenotypes in the Rcor1 knockout mice would be highly similar to that of REST knockout mice. REST knockout mice have small brain size with increased DNA damage and cell death (Mandel unpublished data), but we did not observe any obvious nervous system defects in Rcor1 null mice. These results indicate that a more complex regulatory network operates in neuronal cells *in vivo*. One reason for this may be that REST recruits HDACs to neuronal genes via another co-repressor, mSin3. Previous studies demonstrated that the Sin3/HDAC complex is sufficient to repress neuronal genes in transient assays (Grimes et al., 2000). Another reason could be that Rcor1 and Rcor2, another Rcor family member, are both expressed in the embryonic nervous system (Fig. 1D). Thus,Rcor2 may compensate for Rcor1 for neuronal gene repression. To tease apart this complicated network, transcriptome analyses can be done with control brain tissue and brain tissue without REST, Rcor1, Rcor2, or Sin3a.

In contrast, knocking out of Rcor1 phenocopied the erythroid differentiation defects due to loss of Gfi1b and myeloid differentiation defects due to loss of Gfi1 (Saleque et al., 2002; Upadhyay et al., 2014), confirming the importance of their physical interactions. However, detailed phenotype comparison indicates that in megakaryocyte lineage, Rcor1 may not be required for Gfi1b function. While Gfi1b knockout causes block of

megakaryocytes formation and dramatic decrease of platelets (Upadhyay et al., 2014), Rcor1 knockout did not block megakaryocyte differentiation and platelet generation increased transiently. These phenotypic differences suggest that Gfi1b use a different transcription cofactor in megakaryocyte lineage. All results taken together suggest that biochemical interaction data have to be combined with *in vivo* functional studies to fully understand the importance of transcription regulation mechanisms.

To really dissect a transcription network, protein interactions have to be studied on gene promoters. With the advance of next generation sequencing, it is now possible to do ChIP-seq analysis for transcription factors and cofactors and to map their binding sites in an unbiased manner. However, the currently available Rcor1 antibody generates high background noise (data not shown), preventing confident identification of Rcor1 binding sites. Therefore, it is important to develop new reagents, such as generating new anti-Rcor1 antibodies or generating tagged Rcor1 transgenic mice, to determine Rcor1 binding sites throughout the genome. Comparing Rcor1 binding sites to binding sites of its interacting transcription factors will provide more insights in how these proteins are collaborating and how their target genes are regulated.

How does Gfi1b/Rcor1/LSD1 function fit into the overall transcriptional regulation of erythropoiesis?

Erythroid differentiation is one of the best studied developmental events. Transcription regulation in this lineage has been largely focused on Gata1 and its interacting proteins. Two lines of evidence support that Gata1 has a central role in erythroid lineage gene

regulation. On one hand, Gata1 is required for normal erythropoiesis, as evidenced by failure of RBC differentiation in Gata1 knockout mice (Fujiwara et al., 1996; Pevny et al., 1995; Pevny et al., 1991). On the other hand, Gata1 also has an instructive role in red blood cell differentiation. For example, ectopic Gata1 expression in highly purified murine progenitor cells "instructed" their differentiation toward the erythroid and megakaryocytic lineages that Gata1 normally regulates (Heyworth et al., 2002; Iwasaki et al., 2003). No other transcription factor has been shown to have both functions in the RBC lineage.

Studies of molecular mechanisms of Gata1 in gene regulation demonstrated that it not only up-regulates the erythroid transcription program, but also suppresses early hematopoietic progenitor multipotentiality (through repression of Gata-2 expression) and alternative hematopoietic cell fate (through repression of the critical myeloid transcription factor Pu.1). Gata1's ability to up-regulate gene expression is synergized through a so-called pentameric complex, which includes SCL/Tal-1, LMO2, Ldb1, E2A and Gata1. These factors bind to composite E-box/GATA-1 DNA motifs that are spaced 9-11 nucleotides apart. Such motifs are present in many erythroid genes and in the regulatory elements of key transcription factor genes. Numerous lines of evidence suggested that Gata1 interactions with the FOG1/NuRD complex to repress gene expression (Hong et al., 2005; Tsang et al., 1997).

In this thesis, we demonstrated that Rcor1 is an essential regulator of both embryonic and adult erythropoiesis. The erythroid phenotype in Rcor1 deficient cells is very similar to the phenotypes in Gfi1b or LSD1 deficient cells. Given the previously demonstrated

physical interactions between Gfi1b, Rcor1 and LSD1, it is very likely that Gfi1b/Rcor1/LSD1 forms a complex and function together during erythroid differentiation (Saleque et al., 2007). This raises an interesting question that how this complex fit into the erythroid regulatory network centered around Gata1.

When comparing the phenotypes of Gfi1b or Rcor1 knockout mice to that of Gata1 knockout mice, we found that they have some similarities. For example, both *Gata1*$^{-/-}$ and *Rcor1*$^{-/-}$ erythroid cells fail to undergo erythroid maturation, are blocked at the proerythroblast stage (Pevny et al., 1995), and aberrantly differentiate into cells of the myeloid and mast cell lineages (Kitajima et al., 2006). The Gata1/FOG1 repressor complex has been proposed to suppress genes required to maintain the earlier multipotential progenitor state (eg, Gata2) and alternative hematopoietic lineage genes (eg, MBP) (Rodriguez et al., 2005). Thus, strong similarities exist in the function of these two repressor complexes.

One possibility for these phenotypic similarities may be that Gata1/FOG1 and Gfi1b/Rcor1 are in the same functional complex. However, no biochemical studies support this. Interestingly, while a small portion of Gfi1b can be pulled down by Gata1, Fog1 and Gfi1b cannot be pulled down by each other in erythroid progenitors (Rodriguez et al., 2005). These results suggest that while a small portion of Gfi1b may be function through Gata1, the two repression complexes, Gata1/FOG1 and Gfi1b/Rcor1 likely bind to different sites and/or regulate different genes. The functional independence of these two erythroid repressor complexes is suggested by the fact that genome-wide analysis has not identified statistically significant enrichment of Gfi1b-binding motifs in the vicinity

of Gata1 binding sites (Yu et al., 2009). Furthermore, when we compared 269 Gata1-repressed genes (Yu et al., 2009) with 760 Rcor1-repressed genes from our study, we found only 30 overlapping genes, supporting the view that Gata1 and Rcor1/Gfi1b largely regulate different groups of genes. However, all these studies are not performed in the same type of cells or tissues. It will be important to map Gfi1b and Gata1 binding sites in the same type of erythroid progenitors and make a head to head comparison.

Does Rcor1 have a role in the pathogenesis of MDS?

Myelodysplastic syndrome is a group of disorders characterized by increased stem cell proliferation coupled with aberrant differentiation resulting in a high rate of apoptosis and eventual symptoms related to bone marrow failure. The actual defect in MDS appears more traceable to abnormal differentiation. While abnormal proliferation of progenitors can happen, they may be compensatory proliferation triggered by defects in differentiation (Issa, 2013). Knocking out of Rcor1 in the hematopoietic system leads to a block of differentiation in both erythroid and myeloid lineages. While erythroid and myeloid progenitors were expanded in the Rcor1 null bone marrow, there was no increase of blast cells in the peripheral blood. Therefore, the overall *Rcor1*$^{-/-}$ phenotype mimics MDS in human patients.

As a clinically varied disease, it is not surprising that the molecular pathogenesis of MDS is quite heterogeneous. With the advance of novel genomic sequencing technologies, up to 80% of MDS patients have been identified with somatically acquired genetic abnormalities. Among all the mutations detected in MDS patients, a large group of

mutations were identified in genes encoding epigenetic modifiers. For example, mutations have been identified in DNA methylation controllers, such as DNA methyltransderase 3A (DNMT3A) and tet methylcytosine dioxygenase 2 (Tet2), a DNA demethylase. In addition, mutations have been found in histone modifiers, such as enhancer of zeste homologue 2 (EZH2), a methyltransferase that catalyzes H3K27, and sex combs-like 1 (ASXL1), another polycomb group proteins that regulates H3K27. Some mutations in metabolic enzymes such as isocitrate dehydrogenase 1 (IDH) and IDH2 can affect the function of both DNA demethylases TET2 and histone demethylases KDM4C, and they can be seen in some MDS cases (Issa, 2013; Shih et al., 2012). There is an emerging idea that MDS can be viewed as a prototypical epigenetic disease, not only because so many mutants in epigenetic modifiers have been identified, but also because MDS have shown significant sensitivity to drugs that modify the epigenome. These include DNA methylation inhibitors, 5-azacytidine (azacitidine) and 5-aza-2'-deoxycytidine (decitabine) (Issa and Kantarjian, 2009), and several histone deacetylase inhibitors (HDACis), including vorinostat (SAHA), LBH589, depsipeptide, MGCD-0103, and several others have shown to have clinical activity in trials involving MDS (Wei et al., 2011).

At the present time, there is no direct evidence suggesting that Rcor1 is involved in human MDS. However, our data and others' data have demonstrated that knocking out of CoREST or LSD1 perturbs differentiation of erythroid-megakaryocytic lineage as well as granulocytic cells, phenotypically similar to MDS. Interestingly, specific HOX genes, such as HOXA9 and HOXA7, are linked to the genesis of the malignant haematopoietic

stem cells underlying AML and MDS, either through reciprocal translocations (e.g. NUP98-HOXA9) or by overexpression (Heinrichs et al., 2005). We and others have observed Hoxa9 gene overexpression increase LSD1 null (Kerenyi et al., 2013) and Rcor1 null mice (data not shown). It would be important to revisit sequencing data from MDS samples to determine if Rcor1 is mutated in any samples. In addition to that, it would be interesting to investigate the Rcor1 expression levels in MDS samples, as deregulated Rcor1 expression could contribute to the progress of MDS.

References

Akashi, K., Traver, D., Miyamoto, T., and Weissman, I.L. (2000). A clonogenic common myeloid progenitor that gives rise to all myeloid lineages. Nature *404*, 193-197.

Andres, M.E., Burger, C., Peral-Rubio, M.J., Battaglioli, E., Anderson, M.E., Grimes, J., Dallman, J., Ballas, N., and Mandel, G. (1999). CoREST: a functional corepressor required for regulation of neural-specific gene expression. Proceedings of the National Academy of Sciences of the United States of America *96*, 9873-9878.

Athanasiou, M., Mavrothalassitis, G., Sun-Hoffman, L., and Blair, D.G. (2000). FLI-1 is a suppressor of erythroid differentiation in human hematopoietic cells. Leukemia *14*, 439-445.

Auffray, C., Sieweke, M.H., and Geissmann, F. (2009). Blood monocytes: development, heterogeneity, and relationship with dendritic cells. Annual review of immunology *27*, 669-692.

Azcoitia, V., Aracil, M., Martinez, A.C., and Torres, M. (2005). The homeodomain protein Meis1 is essential for definitive hematopoiesis and vascular patterning in the mouse embryo. Developmental biology *280*, 307-320.

Bailey, K.R., Rustay, N.R., and Crawley, J.N. (2006). Behavioral phenotyping of transgenic and knockout mice: practical concerns and potential pitfalls. ILAR journal / National Research Council, Institute of Laboratory Animal Resources *47*, 124-131.

Ballas, N., Battaglioli, E., Atouf, F., Andres, M.E., Chenoweth, J., Anderson, M.E., Burger, C., Moniwa, M., Davie, J.R., Bowers, W.J*., et al.* (2001). Regulation of neuronal traits by a novel transcriptional complex. Neuron *31*, 353-365.

Ballas, N., Grunseich, C., Lu, D.D., Speh, J.C., and Mandel, G. (2005). REST and its corepressors mediate plasticity of neuronal gene chromatin throughout neurogenesis. Cell *121*, 645-657.

Beachy, S.H., and Aplan, P.D. (2010). Mouse models of myelodysplastic syndromes. Hematology/oncology clinics of North America *24*, 361-375.

Boyer, L.A., Latek, R.R., and Peterson, C.L. (2004). The SANT domain: a unique histone-tail-binding module? Nature reviews Molecular cell biology *5*, 158-163.

Briegel, K., Lim, K.C., Plank, C., Beug, H., Engel, J.D., and Zenke, M. (1993). Ectopic expression of a conditional GATA-2/estrogen receptor chimera arrests erythroid differentiation in a hormone-dependent manner. Genes & development *7*, 1097-1109.

Cai, M., Langer, E.M., Gill, J.G., Satpathy, A.T., Albring, J.C., Kc, W., Murphy, T.L., and Murphy, K.M. (2012). Dual actions of Meis1 inhibit erythroid progenitor development and sustain general hematopoietic cell proliferation. Blood *120*, 335-346.

Calderone, A., Jover, T., Noh, K.M., Tanaka, H., Yokota, H., Lin, Y., Grooms, S.Y., Regis, R., Bennett, M.V., and Zukin, R.S. (2003). Ischemic insults derepress the gene silencer REST in neurons destined to die. The Journal of neuroscience : the official journal of the Society for Neuroscience *23*, 2112-2121.

Cammenga, J., Niebuhr, B., Horn, S., Bergholz, U., Putz, G., Buchholz, F., Lohler, J., and Stocking, C. (2007). RUNX1 DNA-binding mutants, associated with minimally differentiated acute myelogenous leukemia, disrupt myeloid differentiation. Cancer research *67*, 537-545.

Ceballos-Chavez, M., Rivero, S., Garcia-Gutierrez, P., Rodriguez-Paredes, M., Garcia-Dominguez, M., Bhattacharya, S., and Reyes, J.C. (2012). Control of neuronal differentiation by sumoylation of BRAF35, a subunit of the LSD1-CoREST histone demethylase complex. Proceedings of the National Academy of Sciences of the United States of America *109*, 8085-8090.

Chambers, S.M., Boles, N.C., Lin, K.Y., Tierney, M.P., Bowman, T.V., Bradfute, S.B., Chen, A.J., Merchant, A.A., Sirin, O., Weksberg, D.C*., et al.* (2007). Hematopoietic fingerprints: an expression database of stem cells and their progeny. Cell stem cell *1*, 578-591.

Chen, W.G., Chang, Q., Lin, Y., Meissner, A., West, A.E., Griffith, E.C., Jaenisch, R., and Greenberg, M.E. (2003). Derepression of BDNF transcription involves calcium-dependent phosphorylation of MeCP2. Science *302*, 885-889.

Cheng, J., Baumhueter, S., Cacalano, G., Carver-Moore, K., Thibodeaux, H., Thomas, R., Broxmeyer, H.E., Cooper, S., Hague, N., Moore, M*., et al.* (1996a). Hematopoietic defects in mice lacking the sialomucin CD34. Blood *87*, 479-490.

Cheng, T., Shen, H., Giokas, D., Gere, J., Tenen, D.G., and Scadden, D.T. (1996b). Temporal mapping of gene expression levels during the differentiation of individual primary hematopoietic cells. Proceedings of the National Academy of Sciences of the United States of America *93*, 13158-13163.

Chowdhury, A.H., Ramroop, J.R., Upadhyay, G., Sengupta, A., Andrzejczyk, A., and Saleque, S. (2013). Differential transcriptional regulation of meis1 by Gfi1b and its co-factors LSD1 and CoREST. PloS one *8*, e53666.

Cowger, J.J., Zhao, Q., Isovic, M., and Torchia, J. (2007). Biochemical characterization of the zinc-finger protein 217 transcriptional repressor complex: identification of a ZNF217 consensus recognition sequence. Oncogene *26*, 3378-3386.

Cunliffe, V.T. (2008). Eloquent silence: developmental functions of Class I histone deacetylases. Current opinion in genetics & development *18*, 404-410.

D'Andrea, R.J., Harrison-Findik, D., Butcher, C.M., Finnie, J., Blumbergs, P., Bartley, P., McCormack, M., Jones, K., Rowland, R., Gonda, T.J.*, et al.* (1998). Dysregulated hematopoiesis and a progressive neurological disorder induced by expression of an activated form of the human common beta chain in transgenic mice. The Journal of clinical investigation *102*, 1951-1960.

Davis, R.L., Weintraub, H., and Lassar, A.B. (1987). Expression of a single transfected cDNA converts fibroblasts to myoblasts. Cell *51*, 987-1000.

DeKoter, R.P., and Singh, H. (2000). Regulation of B lymphocyte and macrophage development by graded expression of PU.1. Science *288*, 1439-1441.

Dore, L.C., and Crispino, J.D. (2011). Transcription factor networks in erythroid cell and megakaryocyte development. Blood *118*, 231-239.

Dzierzak, E., and Philipsen, S. (2013). Erythropoiesis: development and differentiation. Cold Spring Harbor perspectives in medicine *3*, a011601.

Elagib, K.E., Racke, F.K., Mogass, M., Khetawat, R., Delehanty, L.L., and Goldfarb, A.N. (2003). RUNX1 and GATA-1 coexpression and cooperation in megakaryocytic differentiation. Blood *101*, 4333-4341.

Esteghamat, F., van Dijk, T.B., Braun, H., Dekker, S., van der Linden, R., Hou, J., Fanis, P., Demmers, J., van, I.W., Ozgur, Z.*, et al.* (2011). The DNA binding factor Hmg20b is a repressor of erythroid differentiation. Haematologica *96*, 1252-1260.

Ficara, F., Murphy, M.J., Lin, M., and Cleary, M.L. (2008). Pbx1 regulates self-renewal of long-term hematopoietic stem cells by maintaining their quiescence. Cell stem cell *2*, 484-496.

Fiskus, W., Sharma, S., Shah, B., Portier, B.P., Devaraj, S.G., Liu, K., Iyer, S.P., Bearss, D., and Bhalla, K.N. (2014). Highly effective combination of LSD1 (KDM1A) antagonist and pan-histone deacetylase inhibitor against human AML cells. Leukemia.

Foudi, A., Kramer, D.J., Qin, J., Ye, D., Behlich, A.S., Mordecai, S., Preffer, F.I., Amzallag, A., Ramaswamy, S., Hochedlinger, K.*, et al.* (2014). Distinct, strict requirements for Gfi-1b in adult bone marrow red cell and platelet generation. The Journal of experimental medicine *211*, 909-927.

Friedman, A.D. (2007). Transcriptional control of granulocyte and monocyte development. Oncogene *26*, 6816-6828.

Fuentes, P., Canovas, J., Berndt, F.A., Noctor, S.C., and Kukuljan, M. (2012). CoREST/LSD1 control the development of pyramidal cortical neurons. Cerebral cortex *22*, 1431-1441.

Fujiwara, Y., Browne, C.P., Cunniff, K., Goff, S.C., and Orkin, S.H. (1996). Arrested development of embryonic red cell precursors in mouse embryos lacking transcription factor GATA-1. Proceedings of the National Academy of Sciences of the United States of America *93*, 12355-12358.

Fukuchi, Y., Shibata, F., Ito, M., Goto-Koshino, Y., Sotomaru, Y., Ito, M., Kitamura, T., and Nakajima, H. (2006). Comprehensive analysis of myeloid lineage conversion using mice expressing an inducible form of C/EBP alpha. The EMBO journal *25*, 3398-3410.

Gao, Z., Ure, K., Ding, P., Nashaat, M., Yuan, L., Ma, J., Hammer, R.E., and Hsieh, J. (2011). The master negative regulator REST/NRSF controls adult neurogenesis by restraining the neurogenic program in quiescent stem cells. The Journal of neuroscience : the official journal of the Society for Neuroscience *31*, 9772-9786.

Garcia-Ramirez, M., Rocchini, C., and Ausio, J. (1995). Modulation of chromatin folding by histone acetylation. The Journal of biological chemistry *270*, 17923-17928.

Goldman, D.C., Bailey, A.S., Pfaffle, D.L., Al Masri, A., Christian, J.L., and Fleming, W.H. (2009). BMP4 regulates the hematopoietic stem cell niche. Blood *114*, 4393-4401.

Grimes, J.A., Nielsen, S.J., Battaglioli, E., Miska, E.A., Speh, J.C., Berry, D.L., Atouf, F., Holdener, B.C., Mandel, G., and Kouzarides, T. (2000). The co-repressor mSin3A is a functional component of the REST-CoREST repressor complex. The Journal of biological chemistry *275*, 9461-9467.

Grune, T., Brzeski, J., Eberharter, A., Clapier, C.R., Corona, D.F., Becker, P.B., and Muller, C.W. (2003). Crystal structure and functional analysis of a nucleosome recognition module of the remodeling factor ISWI. Molecular cell *12*, 449-460.

Guan, J.S., Haggarty, S.J., Giacometti, E., Dannenberg, J.H., Joseph, N., Gao, J., Nieland, T.J., Zhou, Y., Wang, X., Mazitschek, R.*, et al.* (2009). HDAC2 negatively regulates memory formation and synaptic plasticity. Nature *459*, 55-60.

Hakimi, M.A., Bochar, D.A., Chenoweth, J., Lane, W.S., Mandel, G., and Shiekhattar, R. (2002). A core-BRAF35 complex containing histone deacetylase mediates repression of neuronal-specific genes. Proceedings of the National Academy of Sciences of the United States of America *99*, 7420-7425.

Hall, M.A., Slater, N.J., Begley, C.G., Salmon, J.M., Van Stekelenburg, L.J., McCormack, M.P., Jane, S.M., and Curtis, D.J. (2005). Functional but abnormal adult erythropoiesis in the absence of the stem cell leukemia gene. Molecular and cellular biology *25*, 6355-6362.

Harris, W.J., Huang, X., Lynch, J.T., Spencer, G.J., Hitchin, J.R., Li, Y., Ciceri, F., Blaser, J.G., Greystoke, B.F., Jordan, A.M.*, et al.* (2012). The histone demethylase KDM1A sustains the oncogenic potential of MLL-AF9 leukemia stem cells. Cancer cell *21*, 473-487.

Hart, A., Melet, F., Grossfeld, P., Chien, K., Jones, C., Tunnacliffe, A., Favier, R., and Bernstein, A. (2000). Fli-1 is required for murine vascular and megakaryocytic development and is hemizygously deleted in patients with thrombocytopenia. Immunity *13*, 167-177.

Hayakawa, T., and Nakayama, J. (2011). Physiological roles of class I HDAC complex and histone demethylase. Journal of biomedicine & biotechnology *2011*, 129383.

Heavey, B., Charalambous, C., Cobaleda, C., and Busslinger, M. (2003). Myeloid lineage switch of Pax5 mutant but not wild-type B cell progenitors by C/EBPalpha and GATA factors. The EMBO journal *22*, 3887-3897.

Heinrichs, S., Berman, J.N., Ortiz, T.M., Kornblau, S.M., Neuberg, D.S., Estey, E.H., and Look, A.T. (2005). CD34+ cell selection is required to assess HOXA9 expression levels in patients with myelodysplastic syndrome. British journal of haematology *130*, 83-86.

Hestdal, K., Ruscetti, F.W., Ihle, J.N., Jacobsen, S.E., Dubois, C.M., Kopp, W.C., Longo, D.L., and Keller, J.R. (1991). Characterization and regulation of RB6-8C5 antigen expression on murine bone marrow cells. Journal of immunology *147*, 22-28.

Heyworth, C., Pearson, S., May, G., and Enver, T. (2002). Transcription factor-mediated lineage switching reveals plasticity in primary committed progenitor cells. The EMBO journal *21*, 3770-3781.

Hisakawa, H., Sugiyama, D., Nishijima, I., Xu, M.J., Wu, H., Nakao, K., Watanabe, S., Katsuki, M., Asano, S., Arai, K.*, et al.* (2001). Human granulocyte-macrophage colony-stimulating factor (hGM-CSF) stimulates primitive and definitive erythropoiesis in mouse embryos expressing hGM-CSF receptors but not erythropoietin receptors. Blood *98*, 3618-3625.

Hock, H., Hamblen, M.J., Rooke, H.M., Schindler, J.W., Saleque, S., Fujiwara, Y., and Orkin, S.H. (2004). Gfi-1 restricts proliferation and preserves functional integrity of haematopoietic stem cells. Nature *431*, 1002-1007.

Hock, H., Hamblen, M.J., Rooke, H.M., Traver, D., Bronson, R.T., Cameron, S., and Orkin, S.H. (2003). Intrinsic requirement for zinc finger transcription factor Gfi-1 in neutrophil differentiation. Immunity *18*, 109-120.

Hong, W., Nakazawa, M., Chen, Y.Y., Kori, R., Vakoc, C.R., Rakowski, C., and Blobel, G.A. (2005). FOG-1 recruits the NuRD repressor complex to mediate transcriptional repression by GATA-1. The EMBO journal *24*, 2367-2378.

Hsu, C.L., King-Fleischman, A.G., Lai, A.Y., Matsumoto, Y., Weissman, I.L., and Kondo, M. (2006). Antagonistic effect of CCAAT enhancer-binding protein-alpha and Pax5 in myeloid or lymphoid lineage choice in common lymphoid progenitors. Proceedings of the National Academy of Sciences of the United States of America *103*, 672-677.

Hu, X., Li, X., Valverde, K., Fu, X., Noguchi, C., Qiu, Y., and Huang, S. (2009). LSD1-mediated epigenetic modification is required for TAL1 function and hematopoiesis. Proceedings of the National Academy of Sciences of the United States of America *106*, 10141-10146.

Huang, S., and Brandt, S.J. (2000). mSin3A regulates murine erythroleukemia cell differentiation through association with the TAL1 (or SCL) transcription factor. Molecular and cellular biology *20*, 2248-2259.

Huang, S., Qiu, Y., Shi, Y., Xu, Z., and Brandt, S.J. (2000). P/CAF-mediated acetylation regulates the function of the basic helix-loop-helix transcription factor TAL1/SCL. The EMBO journal *19*, 6792-6803.

Huang, S., Qiu, Y., Stein, R.W., and Brandt, S.J. (1999). p300 functions as a transcriptional coactivator for the TAL1/SCL oncoprotein. Oncogene *18*, 4958-4967.

Huber, R., Pietsch, D., Gunther, J., Welz, B., Vogt, N., and Brand, K. (2014). Regulation of monocyte differentiation by specific signaling modules and associated transcription factor networks. Cellular and molecular life sciences : CMLS *71*, 63-92.

Humphrey, G.W., Wang, Y., Russanova, V.R., Hirai, T., Qin, J., Nakatani, Y., and Howard, B.H. (2001). Stable histone deacetylase complexes distinguished by the presence of SANT domain proteins CoREST/kiaa0071 and Mta-L1. The Journal of biological chemistry *276*, 6817-6824.

Ikonomi, P., Rivera, C.E., Riordan, M., Washington, G., Schechter, A.N., and Noguchi, C.T. (2000). Overexpression of GATA-2 inhibits erythroid and promotes megakaryocyte differentiation. Experimental hematology *28*, 1423-1431.

Issa, J.P. (2013). The myelodysplastic syndrome as a prototypical epigenetic disease. Blood *121*, 3811-3817.

Issa, J.P., and Kantarjian, H.M. (2009). Targeting DNA methylation. Clinical cancer research : an official journal of the American Association for Cancer Research *15*, 3938-3946.

Iwasaki, H., Mizuno, S., Wells, R.A., Cantor, A.B., Watanabe, S., and Akashi, K. (2003). GATA-1 converts lymphoid and myelomonocytic progenitors into the megakaryocyte/erythrocyte lineages. Immunity *19*, 451-462.

Josling, G.A., Selvarajah, S.A., Petter, M., and Duffy, M.F. (2012). The role of bromodomain proteins in regulating gene expression. Genes *3*, 320-343.

Karsunky, H., Zeng, H., Schmidt, T., Zevnik, B., Kluge, R., Schmid, K.W., Duhrsen, U., and Moroy, T. (2002). Inflammatory reactions and severe neutropenia in mice lacking the transcriptional repressor Gfi1. Nature genetics *30*, 295-300.

Kassouf, M.T., Hughes, J.R., Taylor, S., McGowan, S.J., Soneji, S., Green, A.L., Vyas, P., and Porcher, C. (2010). Genome-wide identification of TAL1's functional targets: insights into its mechanisms of action in primary erythroid cells. Genome research *20*, 1064-1083.

Kelly, T.K., De Carvalho, D.D., and Jones, P.A. (2010). Epigenetic modifications as therapeutic targets. Nature biotechnology *28*, 1069-1078.

Kerenyi, M.A., Shao, Z., Hsu, Y.J., Guo, G., Luc, S., O'Brien, K., Fujiwara, Y., Peng, C., Nguyen, M., and Orkin, S.H. (2013). Histone demethylase Lsd1 represses hematopoietic stem and progenitor cell signatures during blood cell maturation. eLife *2*, e00633.

Khandanpour, C., Sharif-Askari, E., Vassen, L., Gaudreau, M.C., Zhu, J., Paul, W.E., Okayama, T., Kosan, C., and Moroy, T. (2010). Evidence that growth factor independence 1b regulates dormancy and peripheral blood mobilization of hematopoietic stem cells. Blood *116*, 5149-5161.

Kiefer, C.M., Hou, C., Little, J.A., and Dean, A. (2008). Epigenetics of beta-globin gene regulation. Mutation research *647*, 68-76.

Kitajima, K., Zheng, J., Yen, H., Sugiyama, D., and Nakano, T. (2006). Multipotential differentiation ability of GATA-1-null erythroid-committed cells. Genes & development *20*, 654-659.

Korutla, L., Degnan, R., Wang, P., and Mackler, S.A. (2007). NAC1, a cocaine-regulated POZ/BTB protein interacts with CoREST. Journal of neurochemistry *101*, 611-618.

Krivtsov, A.V., Twomey, D., Feng, Z., Stubbs, M.C., Wang, Y., Faber, J., Levine, J.E., Wang, J., Hahn, W.C., Gilliland, D.G.*, et al.* (2006). Transformation from committed progenitor to leukaemia stem cell initiated by MLL-AF9. Nature *442*, 818-822.

Kuhn, R., Schwenk, F., Aguet, M., and Rajewsky, K. (1995). Inducible gene targeting in mice. Science *269*, 1427-1429.

Kulessa, H., Frampton, J., and Graf, T. (1995). GATA-1 reprograms avian myelomonocytic cell lines into eosinophils, thromboblasts, and erythroblasts. Genes & development *9*, 1250-1262.

Kundu, M., and Liu, P.P. (2003). Cbf beta is involved in maturation of all lineages of hematopoietic cells during embryogenesis except erythroid. Blood cells, molecules & diseases *30*, 164-169.

Lagger, G., O'Carroll, D., Rembold, M., Khier, H., Tischler, J., Weitzer, G., Schuettengruber, B., Hauser, C., Brunmeir, R., Jenuwein, T.*, et al.* (2002). Essential function of histone deacetylase 1 in proliferation control and CDK inhibitor repression. The EMBO journal *21*, 2672-2681.

Laiosa, C.V., Stadtfeld, M., Xie, H., de Andres-Aguayo, L., and Graf, T. (2006). Reprogramming of committed T cell progenitors to macrophages and dendritic cells by C/EBP alpha and PU.1 transcription factors. Immunity *25*, 731-744.

Lan, F., Collins, R.E., De Cegli, R., Alpatov, R., Horton, J.R., Shi, X., Gozani, O., Cheng, X., and Shi, Y. (2007). Recognition of unmethylated histone H3 lysine 4 links BHC80 to LSD1-mediated gene repression. Nature *448*, 718-722.

Laslo, P., Spooner, C.J., Warmflash, A., Lancki, D.W., Lee, H.J., Sciammas, R., Gantner, B.N., Dinner, A.R., and Singh, H. (2006). Multilineage transcriptional priming and determination of alternate hematopoietic cell fates. Cell *126*, 755-766.

Latchman, D.S. (1997). Transcription factors: an overview. The international journal of biochemistry & cell biology *29*, 1305-1312.

Lee, M.G., Wynder, C., Cooch, N., and Shiekhattar, R. (2005). An essential role for CoREST in nucleosomal histone 3 lysine 4 demethylation. Nature *437*, 432-435.

Lee, T.I., and Young, R.A. (2000). Transcription of eukaryotic protein-coding genes. Annual review of genetics *34*, 77-137.

Leeanansaksiri, W., Wang, H., Gooya, J.M., Renn, K., Abshari, M., Tsai, S., and Keller, J.R. (2005). IL-3 induces inhibitor of DNA-binding protein-1 in hemopoietic progenitor cells and promotes myeloid cell development. Journal of immunology *174*, 7014-7021.

Levine, M., and Tjian, R. (2003). Transcription regulation and animal diversity. Nature *424*, 147-151.

Li, B., Bailey, A.S., Jiang, S., Liu, B., Goldman, D.C., and Fleming, W.H. (2010). Endothelial cells mediate the regeneration of hematopoietic stem cells. Stem cell research *4*, 17-24.

Lister, J., Forrester, W.C., and Baron, M.H. (1995). Inhibition of an erythroid differentiation switch by the helix-loop-helix protein Id1. The Journal of biological chemistry *270*, 17939-17946.

Liu, P., Keller, J.R., Ortiz, M., Tessarollo, L., Rachel, R.A., Nakamura, T., Jenkins, N.A., and Copeland, N.G. (2003). Bcl11a is essential for normal lymphoid development. Nature immunology *4*, 525-532.

Lodish, H., Flygare, J., and Chou, S. (2010). From stem cell to erythroblast: regulation of red cell production at multiple levels by multiple hormones. IUBMB life *62*, 492-496.

Lorsbach, R.B., Moore, J., Ang, S.O., Sun, W., Lenny, N., and Downing, J.R. (2004). Role of RUNX1 in adult hematopoiesis: analysis of RUNX1-IRES-GFP knock-in mice reveals differential lineage expression. Blood *103*, 2522-2529.

Lu, T., Aron, L., Zullo, J., Pan, Y., Kim, H., Chen, Y., Yang, T.H., Kim, H.M., Drake, D., Liu, X.S.*, et al.* (2014). REST and stress resistance in ageing and Alzheimer's disease. Nature *507*, 448-454.

Lux, C.T., Yoshimoto, M., McGrath, K., Conway, S.J., Palis, J., and Yoder, M.C. (2008). All primitive and definitive hematopoietic progenitor cells emerging before E10 in the mouse embryo are products of the yolk sac. Blood *111*, 3435-3438.

Machlus, K.R., and Italiano, J.E., Jr. (2013). The incredible journey: From megakaryocyte development to platelet formation. The Journal of cell biology *201*, 785-796.

Mackler, S.A., Korutla, L., Cha, X.Y., Koebbe, M.J., Fournier, K.M., Bowers, M.S., and Kalivas, P.W. (2000). NAC-1 is a brain POZ/BTB protein that can prevent cocaine-induced sensitization in the rat. The Journal of neuroscience : the official journal of the Society for Neuroscience *20*, 6210-6217.

Mandel, G., Fiondella, C.G., Covey, M.V., Lu, D.D., Loturco, J.J., and Ballas, N. (2011). Repressor element 1 silencing transcription factor (REST) controls radial migration and temporal neuronal specification during neocortical development. Proceedings of the National Academy of Sciences of the United States of America *108*, 16789-16794.

Maren, S. (2001). Neurobiology of Pavlovian fear conditioning. Annual review of neuroscience *24*, 897-931.

Marmorstein, L.Y., Kinev, A.V., Chan, G.K., Bochar, D.A., Beniya, H., Epstein, J.A., Yen, T.J., and Shiekhattar, R. (2001). A human BRCA2 complex containing a structural DNA binding component influences cell cycle progression. Cell *104*, 247-257.

McCormack, M.P., and Gonda, T.J. (1997). Expression of activated mutants of the human interleukin-3/interleukin-5/granulocyte-macrophage colony-stimulating factor receptor common beta subunit in primary hematopoietic cells induces factor-independent proliferation and differentiation. Blood *90*, 1471-1481.

McGarry, M.P., Protheroe, C.A., and Lee, J.J. (2010). Mouse hematology : a laboratory manual (Cold Spring Harbor, N.Y.: Cold Spring Harbor Laboratory Press).

McIvor, Z., Hein, S., Fiegler, H., Schroeder, T., Stocking, C., Just, U., and Cross, M. (2003). Transient expression of PU.1 commits multipotent progenitors to a myeloid fate whereas continued expression favors macrophage over granulocyte differentiation. Experimental hematology *31*, 39-47.

Medvedovic, J., Ebert, A., Tagoh, H., and Busslinger, M. (2011). Pax5: a master regulator of B cell development and leukemogenesis. Advances in immunology *111*, 179-206.

Metzger, E., Wissmann, M., Yin, N., Muller, J.M., Schneider, R., Peters, A.H., Gunther, T., Buettner, R., and Schule, R. (2005). LSD1 demethylates repressive histone marks to promote androgen-receptor-dependent transcription. Nature *437*, 436-439.

Mosammaparast, N., and Shi, Y. (2010). Reversal of histone methylation: biochemical and molecular mechanisms of histone demethylases. Annual review of biochemistry *79*, 155-179.

Nakeff, A., and Maat, B. (1974). Separation of megakaryocytes from mouse bone marrow by velocity sedimentation. Blood *43*, 591-595.

Nakorn, T.N., Miyamoto, T., and Weissman, I.L. (2003). Characterization of mouse clonogenic megakaryocyte progenitors. Proceedings of the National Academy of Sciences of the United States of America *100*, 205-210.

Nichogiannopoulou, A., Trevisan, M., Neben, S., Friedrich, C., and Georgopoulos, K. (1999). Defects in hemopoietic stem cell activity in Ikaros mutant mice. The Journal of experimental medicine *190*, 1201-1214.

Nuez, B., Michalovich, D., Bygrave, A., Ploemacher, R., and Grosveld, F. (1995). Defective haematopoiesis in fetal liver resulting from inactivation of the EKLF gene. Nature *375*, 316-318.

Okuda, T., van Deursen, J., Hiebert, S.W., Grosveld, G., and Downing, J.R. (1996). AML1, the target of multiple chromosomal translocations in human leukemia, is essential for normal fetal liver hematopoiesis. Cell *84*, 321-330.

Olins, D.E., and Olins, A.L. (2003). Chromatin history: our view from the bridge. Nature reviews Molecular cell biology *4*, 809-814.

Orazi, A., and Germing, U. (2008). The myelodysplastic/myeloproliferative neoplasms: myeloproliferative diseases with dysplastic features. Leukemia *22*, 1308-1319.

Orkin, S.H., and Zon, L.I. (2008a). Hematopoiesis: an evolving paradigm for stem cell biology. Cell *132*, 631-644.

Orkin, S.H., and Zon, L.I. (2008b). SnapShot: hematopoiesis. Cell *132*, 712.

Otto, S.J., McCorkle, S.R., Hover, J., Conaco, C., Han, J.J., Impey, S., Yochum, G.S., Dunn, J.J., Goodman, R.H., and Mandel, G. (2007). A new binding motif for the transcriptional repressor REST uncovers large gene networks devoted to neuronal functions. The Journal of neuroscience : the official journal of the Society for Neuroscience *27*, 6729-6739.

Park, D., Spencer, J.A., Koh, B.I., Kobayashi, T., Fujisaki, J., Clemens, T.L., Lin, C.P., Kronenberg, H.M., and Scadden, D.T. (2012). Endogenous bone marrow MSCs are dynamic, fate-restricted participants in bone maintenance and regeneration. Cell stem cell *10*, 259-272.

Patnaik, M.M., Parikh, S.A., Hanson, C.A., and Tefferi, A. (2014). Chronic myelomonocytic leukaemia: a concise clinical and pathophysiological review. British journal of haematology *165*, 273-286.

Paul, R., Schuetze, S., Kozak, S.L., Kozak, C.A., and Kabat, D. (1991). The Sfpi-1 proviral integration site of Friend erythroleukemia encodes the ets-related transcription factor Pu.1. Journal of virology *65*, 464-467.

Peixoto, L., and Abel, T. (2013). The role of histone acetylation in memory formation and cognitive impairments. Neuropsychopharmacology : official publication of the American College of Neuropsychopharmacology *38*, 62-76.

Perkins, A.C., Sharpe, A.H., and Orkin, S.H. (1995). Lethal beta-thalassaemia in mice lacking the erythroid CACCC-transcription factor EKLF. Nature *375*, 318-322.

Perry, C., and Soreq, H. (2002). Transcriptional regulation of erythropoiesis. Fine tuning of combinatorial multi-domain elements. European journal of biochemistry / FEBS *269*, 3607-3618.

Persons, D.A., Allay, J.A., Allay, E.R., Ashmun, R.A., Orlic, D., Jane, S.M., Cunningham, J.M., and Nienhuis, A.W. (1999). Enforced expression of the GATA-2 transcription factor blocks normal hematopoiesis. Blood *93*, 488-499.

Pevny, L., Lin, C.S., D'Agati, V., Simon, M.C., Orkin, S.H., and Costantini, F. (1995). Development of hematopoietic cells lacking transcription factor GATA-1. Development *121*, 163-172.

Pevny, L., Simon, M.C., Robertson, E., Klein, W.H., Tsai, S.F., D'Agati, V., Orkin, S.H., and Costantini, F. (1991). Erythroid differentiation in chimaeric mice blocked by a targeted mutation in the gene for transcription factor GATA-1. Nature *349*, 257-260.

Porcher, C., Swat, W., Rockwell, K., Fujiwara, Y., Alt, F.W., and Orkin, S.H. (1996). The T cell leukemia oncoprotein SCL/tal-1 is essential for development of all hematopoietic lineages. Cell *86*, 47-57.

Pronk, C.J., Rossi, D.J., Mansson, R., Attema, J.L., Norddahl, G.L., Chan, C.K., Sigvardsson, M., Weissman, I.L., and Bryder, D. (2007). Elucidation of the phenotypic, functional, and molecular topography of a myeloerythroid progenitor cell hierarchy. Cell stem cell *1*, 428-442.

Randrianarison-Huetz, V., Laurent, B., Bardet, V., Blobe, G.C., Huetz, F., and Dumenil, D. (2010). Gfi-1B controls human erythroid and megakaryocytic differentiation by regulating TGF-beta signaling at the bipotent erythro-megakaryocytic progenitor stage. Blood *115*, 2784-2795.

Rekhtman, N., Radparvar, F., Evans, T., and Skoultchi, A.I. (1999). Direct interaction of hematopoietic transcription factors PU.1 and GATA-1: functional antagonism in erythroid cells. Genes & development *13*, 1398-1411.

Robertson, S.M., Kennedy, M., Shannon, J.M., and Keller, G. (2000). A transitional stage in the commitment of mesoderm to hematopoiesis requiring the transcription factor SCL/tal-1. Development *127*, 2447-2459.

Rodriguez, P., Bonte, E., Krijgsveld, J., Kolodziej, K.E., Guyot, B., Heck, A.J., Vyas, P., de Boer, E., Grosveld, F., and Strouboulis, J. (2005). GATA-1 forms distinct activating and repressive complexes in erythroid cells. The EMBO journal *24*, 2354-2366.

Rosmarin, A.G., Yang, Z., and Resendes, K.K. (2005). Transcriptional regulation in myelopoiesis: Hematopoietic fate choice, myeloid differentiation, and leukemogenesis. Experimental hematology *33*, 131-143.

Saijo, K., Winner, B., Carson, C.T., Collier, J.G., Boyer, L., Rosenfeld, M.G., Gage, F.H., and Glass, C.K. (2009). A Nurr1/CoREST pathway in microglia and astrocytes protects dopaminergic neurons from inflammation-induced death. Cell *137*, 47-59.

Saleque, S., Cameron, S., and Orkin, S.H. (2002). The zinc-finger proto-oncogene Gfi-1b is essential for development of the erythroid and megakaryocytic lineages. Genes & development *16*, 301-306.

Saleque, S., Kim, J., Rooke, H.M., and Orkin, S.H. (2007). Epigenetic regulation of hematopoietic differentiation by Gfi-1 and Gfi-1b is mediated by the cofactors CoREST and LSD1. Molecular cell *27*, 562-572.

Sanchez, M.J., Bockamp, E.O., Miller, J., Gambardella, L., and Green, A.R. (2001). Selective rescue of early haematopoietic progenitors in Scl(-/-) mice by expressing Scl under the control of a stem cell enhancer. Development *128*, 4815-4827.

Sanders, S.L., Portoso, M., Mata, J., Bahler, J., Allshire, R.C., and Kouzarides, T. (2004). Methylation of histone H4 lysine 20 controls recruitment of Crb2 to sites of DNA damage. Cell *119*, 603-614.

Sankaran, V.G., Menne, T.F., Xu, J., Akie, T.E., Lettre, G., Van Handel, B., Mikkola, H.K., Hirschhorn, J.N., Cantor, A.B., and Orkin, S.H. (2008). Human fetal hemoglobin expression is regulated by the developmental stage-specific repressor BCL11A. Science *322*, 1839-1842.

Sankaran, V.G., Xu, J., and Orkin, S.H. (2010). Advances in the understanding of haemoglobin switching. British journal of haematology *149*, 181-194.

Satake, S., Hirai, H., Hayashi, Y., Shime, N., Tamura, A., Yao, H., Yoshioka, S., Miura, Y., Inaba, T., Fujita, N.*, et al.* (2012). C/EBPbeta is involved in the amplification of early granulocyte precursors during candidemia-induced "emergency" granulopoiesis. Journal of immunology *189*, 4546-4555.

Sauvageau, G., Thorsteinsdottir, U., Eaves, C.J., Lawrence, H.J., Largman, C., Lansdorp, P.M., and Humphries, R.K. (1995). Overexpression of HOXB4 in hematopoietic cells causes the selective expansion of more primitive populations in vitro and in vivo. Genes & development *9*, 1753-1765.

Schenk, T., Chen, W.C., Gollner, S., Howell, L., Jin, L., Hebestreit, K., Klein, H.U., Popescu, A.C., Burnett, A., Mills, K.*, et al.* (2012). Inhibition of the LSD1 (KDM1A) demethylase reactivates the all-trans-retinoic acid differentiation pathway in acute myeloid leukemia. Nature medicine *18*, 605-611.

Schoch, H., and Abel, T. (2014). Transcriptional co-repressors and memory storage. Neuropharmacology *80*, 53-60.

Schoenherr, C.J., Paquette, A.J., and Anderson, D.J. (1996). Identification of potential target genes for the neuron-restrictive silencer factor. Proceedings of the National Academy of Sciences of the United States of America *93*, 9881-9886.

Schroeder, T. (2010). Hematopoietic stem cell heterogeneity: subtypes, not unpredictable behavior. Cell stem cell *6*, 203-207.

Shi, Y., Chichung Lie, D., Taupin, P., Nakashima, K., Ray, J., Yu, R.T., Gage, F.H., and Evans, R.M. (2004a). Expression and function of orphan nuclear receptor TLX in adult neural stem cells. Nature *427*, 78-83.

Shi, Y., Lan, F., Matson, C., Mulligan, P., Whetstine, J.R., Cole, P.A., Casero, R.A., and Shi, Y. (2004b). Histone demethylation mediated by the nuclear amine oxidase homolog LSD1. Cell *119*, 941-953.

Shi, Y.J., Matson, C., Lan, F., Iwase, S., Baba, T., and Shi, Y. (2005). Regulation of LSD1 histone demethylase activity by its associated factors. Molecular cell *19*, 857-864.

Shih, A.H., Abdel-Wahab, O., Patel, J.P., and Levine, R.L. (2012). The role of mutations in epigenetic regulators in myeloid malignancies. Nature reviews Cancer *12*, 599-612.

Shuga, J., Zhang, J., Samson, L.D., Lodish, H.F., and Griffith, L.G. (2007). In vitro erythropoiesis from bone marrow-derived progenitors provides a physiological assay for toxic and mutagenic compounds. Proceedings of the National Academy of Sciences of the United States of America *104*, 8737-8742.

Socolovsky, M., Nam, H., Fleming, M.D., Haase, V.H., Brugnara, C., and Lodish, H.F. (2001). Ineffective erythropoiesis in Stat5a(-/-)5b(-/-) mice due to decreased survival of early erythroblasts. Blood *98*, 3261-3273.

Spooner, C.J., Cheng, J.X., Pujadas, E., Laslo, P., and Singh, H. (2009). A recurrent network involving the transcription factors PU.1 and Gfi1 orchestrates innate and adaptive immune cell fates. Immunity *31*, 576-586.

Spyropoulos, D.D., Pharr, P.N., Lavenburg, K.R., Jackers, P., Papas, T.S., Ogawa, M., and Watson, D.K. (2000). Hemorrhage, impaired hematopoiesis, and lethality in mouse embryos carrying a targeted disruption of the Fli1 transcription factor. Molecular and cellular biology *20*, 5643-5652.

Stafford, J.M., and Lattal, K.M. (2009). Direct comparisons of the size and persistence of anisomycin-induced consolidation and reconsolidation deficits. Learning & memory *16*, 494-503.

Stafford, J.M., Raybuck, J.D., Ryabinin, A.E., and Lattal, K.M. (2012). Increasing histone acetylation in the hippocampus-infralimbic network enhances fear extinction. Biological psychiatry *72*, 25-33.

Starck, J., Cohet, N., Gonnet, C., Sarrazin, S., Doubeikovskaia, Z., Doubeikovski, A., Verger, A., Duterque-Coquillaud, M., and Morle, F. (2003). Functional cross-antagonism between transcription factors FLI-1 and EKLF. Molecular and cellular biology *23*, 1390-1402.

Strahl, B.D., Ohba, R., Cook, R.G., and Allis, C.D. (1999). Methylation of histone H3 at lysine 4 is highly conserved and correlates with transcriptionally active nuclei in Tetrahymena. Proceedings of the National Academy of Sciences of the United States of America *96*, 14967-14972.

Subramanian, A., Tamayo, P., Mootha, V.K., Mukherjee, S., Ebert, B.L., Gillette, M.A., Paulovich, A., Pomeroy, S.L., Golub, T.R., Lander, E.S.*, et al.* (2005). Gene set enrichment analysis: a knowledge-based approach for interpreting genome-wide expression profiles. Proceedings of the National Academy of Sciences of the United States of America *102*, 15545-15550.

Suh, H.C., Gooya, J., Renn, K., Friedman, A.D., Johnson, P.F., and Keller, J.R. (2006). C/EBPalpha determines hematopoietic cell fate in multipotential progenitor cells by inhibiting erythroid differentiation and inducing myeloid differentiation. Blood *107*, 4308-4316.

Takahashi, K., and Yamanaka, S. (2006). Induction of pluripotent stem cells from mouse embryonic and adult fibroblast cultures by defined factors. Cell *126*, 663-676.

Tallquist, M.D., and Soriano, P. (2000). Epiblast-restricted Cre expression in MORE mice: a tool to distinguish embryonic vs. extra-embryonic gene function. Genesis *26*, 113-115.

Tapscott, S.J. (2005). The circuitry of a master switch: Myod and the regulation of skeletal muscle gene transcription. Development *132*, 2685-2695.

Traver, D., Miyamoto, T., Christensen, J., Iwasaki-Arai, J., Akashi, K., and Weissman, I.L. (2001). Fetal liver myelopoiesis occurs through distinct, prospectively isolatable progenitor subsets. Blood *98*, 627-635.

Tsai, F.Y., Keller, G., Kuo, F.C., Weiss, M., Chen, J., Rosenblatt, M., Alt, F.W., and Orkin, S.H. (1994). An early haematopoietic defect in mice lacking the transcription factor GATA-2. Nature *371*, 221-226.

Tsang, A.P., Visvader, J.E., Turner, C.A., Fujiwara, Y., Yu, C., Weiss, M.J., Crossley, M., and Orkin, S.H. (1997). FOG, a multitype zinc finger protein, acts as a cofactor for transcription factor GATA-1 in erythroid and megakaryocytic differentiation. Cell *90*, 109-119.

Tsiftsoglou, A.S., Vizirianakis, I.S., and Strouboulis, J. (2009). Erythropoiesis: model systems, molecular regulators, and developmental programs. IUBMB life *61*, 800-830.

Upadhyay, G., Chowdhury, A.H., Vaidyanathan, B., Kim, D., and Saleque, S. (2014). Antagonistic actions of Rcor proteins regulate LSD1 activity and cellular differentiation. Proceedings of the National Academy of Sciences of the United States of America.

van der Meer, L.T., Jansen, J.H., and van der Reijden, B.A. (2010). Gfi1 and Gfi1b: key regulators of hematopoiesis. Leukemia *24*, 1834-1843.

van Dijk, T.B., Baltus, B., Caldenhoven, E., Handa, H., Raaijmakers, J.A., Lammers, J.W., Koenderman, L., and de Groot, R.P. (1998). Cloning and characterization of the human interleukin-3 (IL-3)/IL-5/ granulocyte-macrophage colony-stimulating factor receptor betac gene: regulation by Ets family members. Blood *92*, 3636-3646.

van Dijk, T.B., Baltus, B., Raaijmakers, J.A., Lammers, J.W., Koenderman, L., and de Groot, R.P. (1999). A composite C/EBP binding site is essential for the activity of the promoter of the IL-3/IL-5/granulocyte-macrophage colony-stimulating factor receptor beta c gene. Journal of immunology *163*, 2674-2680.

Vassen, L., Duhrsen, U., Kosan, C., Zeng, H., and Moroy, T. (2012). Growth factor independence 1 (Gfi1) regulates cell-fate decision of a bipotential granulocytic-monocytic precursor defined by expression of Gfi1 and CD48. American journal of blood research *2*, 228-242.

Visvader, J.E., Elefanty, A.G., Strasser, A., and Adams, J.M. (1992). GATA-1 but not SCL induces megakaryocytic differentiation in an early myeloid line. The EMBO journal *11*, 4557-4564.

Walkley, C.R., Yuan, Y.D., Chandraratna, R.A., and McArthur, G.A. (2002). Retinoic acid receptor antagonism in vivo expands the numbers of precursor cells during granulopoiesis. Leukemia *16*, 1763-1772.

Wang, J., Scully, K., Zhu, X., Cai, L., Zhang, J., Prefontaine, G.G., Krones, A., Ohgi, K.A., Zhu, P., Garcia-Bassets, I.*, et al.* (2007). Opposing LSD1 complexes function in developmental gene activation and repression programmes. Nature *446*, 882-887.

Weaver, R.F. (2002). Molecular biology, 2nd edn (Boston: McGraw-Hill).

Wei, Y., Ganan-Gomez, I., Salazar-Dimicoli, S., McCay, S.L., and Garcia-Manero, G. (2011). Histone methylation in myelodysplastic syndromes. Epigenomics *3*, 193-205.

Wen, Q., Goldenson, B., and Crispino, J.D. (2011). Normal and malignant megakaryopoiesis. Expert reviews in molecular medicine *13*, e32.

Wernig, G., Kharas, M.G., Okabe, R., Moore, S.A., Leeman, D.S., Cullen, D.E., Gozo, M., McDowell, E.P., Levine, R.L., Doukas, J.*, et al.* (2008). Efficacy of TG101348, a selective JAK2 inhibitor, in treatment of a murine model of JAK2V617F-induced polycythemia vera. Cancer cell *13*, 311-320.

Whetstine, J.R., Nottke, A., Lan, F., Huarte, M., Smolikov, S., Chen, Z., Spooner, E., Li, E., Zhang, G., Colaiacovo, M.*, et al.* (2006). Reversal of histone lysine trimethylation by the JMJD2 family of histone demethylases. Cell *125*, 467-481.

Wilson, N.K., Foster, S.D., Wang, X., Knezevic, K., Schutte, J., Kaimakis, P., Chilarska, P.M., Kinston, S., Ouwehand, W.H., Dzierzak, E.*, et al.* (2010). Combinatorial transcriptional control in blood stem/progenitor cells: genome-wide analysis of ten major transcriptional regulators. Cell stem cell *7*, 532-544.

Wong, P., Hattangadi, S.M., Cheng, A.W., Frampton, G.M., Young, R.A., and Lodish, H.F. (2011). Gene induction and repression during terminal erythropoiesis are mediated by distinct epigenetic changes. Blood *118*, e128-138.

Xie, H., Ye, M., Feng, R., and Graf, T. (2004). Stepwise reprogramming of B cells into macrophages. Cell *117*, 663-676.

Xu, J., Bauer, D.E., Kerenyi, M.A., Vo, T.D., Hou, S., Hsu, Y.J., Yao, H., Trowbridge, J.J., Mandel, G., and Orkin, S.H. (2013). Corepressor-dependent silencing of fetal hemoglobin expression by BCL11A. Proceedings of the National Academy of Sciences of the United States of America *110*, 6518-6523.

Xu, J., Peng, C., Sankaran, V.G., Shao, Z., Esrick, E.B., Chong, B.G., Ippolito, G.C., Fujiwara, Y., Ebert, B.L., Tucker, P.W., *et al.* (2011). Correction of sickle cell disease in adult mice by interference with fetal hemoglobin silencing. Science *334*, 993-996.

Yamada, Y., Warren, A.J., Dobson, C., Forster, A., Pannell, R., and Rabbitts, T.H. (1998). The T cell leukemia LIM protein Lmo2 is necessary for adult mouse hematopoiesis. Proceedings of the National Academy of Sciences of the United States of America *95*, 3890-3895.

Yamamura, K., Ohishi, K., Katayama, N., Yu, Z., Kato, K., Masuya, M., Fujieda, A., Sugimoto, Y., Miyata, E., Shibasaki, T., *et al.* (2006). Pleiotropic role of histone deacetylases in the regulation of human adult erythropoiesis. British journal of haematology *135*, 242-253.

Yang, M., Gocke, C.B., Luo, X., Borek, D., Tomchick, D.R., Machius, M., Otwinowski, Z., and Yu, H. (2006). Structural basis for CoREST-dependent demethylation of nucleosomes by the human LSD1 histone demethylase. Molecular cell *23*, 377-387.

Yang, P., Wang, Y., Chen, J., Li, H., Kang, L., Zhang, Y., Chen, S., Zhu, B., and Gao, S. (2011). RCOR2 is a subunit of the LSD1 complex that regulates ESC property and substitutes for SOX2 in reprogramming somatic cells to pluripotency. Stem cells *29*, 791-801.

Yao, H., Goldman, D.C., Nechiporuk, T., Kawane, S., McWeeney, S.K., Tyner, J.W., Fan, G., Kerenyi, M.A., Orkin, S.H., Fleming, W.H., *et al.* (2014). Corepressor Rcor1 is essential for murine erythropoiesis. Blood *123*, 3175-3184.

Yokoyama, A., Takezawa, S., Schule, R., Kitagawa, H., and Kato, S. (2008). Transrepressive function of TLX requires the histone demethylase LSD1. Molecular and cellular biology *28*, 3995-4003.

You, A., Tong, J.K., Grozinger, C.M., and Schreiber, S.L. (2001). CoREST is an integral component of the CoREST- human histone deacetylase complex. Proceedings of the National Academy of Sciences of the United States of America *98*, 1454-1458.

Yu, M., Riva, L., Xie, H., Schindler, Y., Moran, T.B., Cheng, Y., Yu, D., Hardison, R., Weiss, M.J., Orkin, S.H., *et al.* (2009). Insights into GATA-1-mediated gene activation versus repression via genome-wide chromatin occupancy analysis. Molecular cell *36*, 682-695.

Zhang, J., Socolovsky, M., Gross, A.W., and Lodish, H.F. (2003). Role of Ras signaling in erythroid differentiation of mouse fetal liver cells: functional analysis by a flow cytometry-based novel culture system. Blood *102*, 3938-3946.

Zhang, P., Iwasaki-Arai, J., Iwasaki, H., Fenyus, M.L., Dayaram, T., Owens, B.M., Shigematsu, H., Levantini, E., Huettner, C.S., Lekstrom-Himes, J.A., *et al.* (2004).

Enhancement of hematopoietic stem cell repopulating capacity and self-renewal in the absence of the transcription factor C/EBP alpha. Immunity *21*, 853-863.

Zhu, J., and Emerson, S.G. (2002). Hematopoietic cytokines, transcription factors and lineage commitment. Oncogene *21*, 3295-3313.

Zimmerman, L., Parr, B., Lendahl, U., Cunningham, M., McKay, R., Gavin, B., Mann, J., Vassileva, G., and McMahon, A. (1994). Independent regulatory elements in the nestin gene direct transgene expression to neural stem cells or muscle precursors. Neuron *12*, 11-24.